THE EUROPEAN
PHYSICAL JOURNAL C

Search for electroweak production of charginos and sleptons decaying into final states with two leptons and missing transverse momentum in $\sqrt{s} = 13$ TeV pp collisions using the ATLAS detector

ATLAS Collaboration[⋆]

CERN, 1211 Geneva 23, Switzerland

Abstract A search for the electroweak production of charginos and sleptons decaying into final states with two electrons or muons is presented. The analysis is based on 139 fb^{-1} of proton–proton collisions recorded by the ATLAS detector at the Large Hadron Collider at $\sqrt{s} = 13$ TeV. Three R-parity-conserving scenarios where the lightest neutralino is the lightest supersymmetric particle are considered: the production of chargino pairs with decays via either W bosons or sleptons, and the direct production of slepton pairs. The analysis is optimised for the first of these scenarios, but the results are also interpreted in the others. No significant deviations from the Standard Model expectations are observed and limits at 95% confidence level are set on the masses of relevant supersymmetric particles in each of the scenarios. For a massless lightest neutralino, masses up to 420 GeV are excluded for the production of the lightest-chargino pairs assuming W-boson-mediated decays and up to 1 TeV for slepton-mediated decays, whereas for slepton-pair production masses up to 700 GeV are excluded assuming three generations of mass-degenerate sleptons.

Contents

⋆ e-mail: atlas.publications@cern.ch

1 Introduction

Weak-scale supersymmetry (SUSY) [1–7] is a theoretical extension to the Standard Model (SM) that, if realised in nature, would solve the hierarchy problem [8–11] through the introduction of a new fermion (boson) supersymmetric partner for each boson (fermion) in the SM. In SUSY models that conserve R-parity [12], SUSY particles (sparticles) must be produced in pairs. The lightest supersymmetric particle (LSP) is stable and weakly interacting, thus potentially providing a viable candidate for dark matter [13,14]. Due to its stability, any LSP produced at the Large Hadron Collider (LHC) would escape detection and give rise to momentum imbalance in the form of missing transverse momentum ($\mathbf{p}_{\mathrm{T}}^{\mathrm{miss}}$) in the final state, which can be used to discriminate SUSY signals from the SM background.

The superpartners of the SM Higgs boson and the electroweak gauge bosons, known as the higgsinos, winos and binos, are collectively labelled as electroweakinos. They mix to form chargino ($\tilde{\chi}_i^{\pm}$, $i = 1, 2$) and neutralino ($\tilde{\chi}_j^0$, $j = 1, 2, 3, 4$) mass eigenstates where the labels i and j refer to states of increasing mass.

Sparticle production cross-sections at the LHC are highly dependent on the sparticle masses as well as on the production mechanism. The coloured sparticles (squarks and gluinos) are strongly produced and have significantly larger production cross-sections than non-coloured sparticles of equal masses, such as the sleptons (superpartners of the SM leptons) and the electroweakinos. If gluinos and squarks were much heavier than low-mass electroweakinos, then SUSY production at the LHC would be dominated by direct electroweakino production. The latest ATLAS and CMS limits on squark and gluino production [15–23] extend well beyond the TeV scale, thus making electroweak production of sparticles a promising and important probe in searches for SUSY at the LHC.
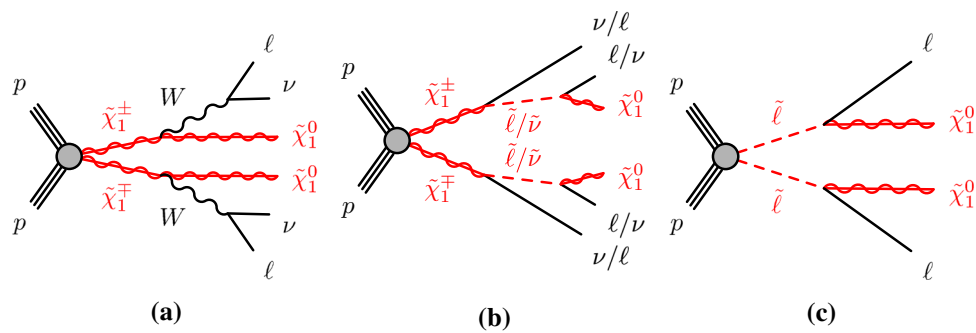
Springer

Fig. 1 Diagrams of the supersymmetric models considered, with two leptons and weakly interacting particles in the final state: **a** $\tilde{\chi}_1^+ \tilde{\chi}_1^-$ production with W-boson-mediated decays, **b** $\tilde{\chi}_1^+ \tilde{\chi}_1^-$ production with slepton/sneutrino-mediated-decays and **c** slepton pair production. In the model with intermediate sleptons, all three flavours ($\tilde{e}$, $\tilde{\mu}$, $\tilde{\tau}$) are included, while only $\tilde{e}$ and $\tilde{\mu}$ are included in the direct slepton model. In the final state, ℓ stands for an electron or muon, which can be produced directly or, in the case of **a** and **b** only, via a leptonically decaying τ-lepton with additional neutrinos

This paper presents a search for the electroweak production of charginos and sleptons decaying into final states with two charged leptons (electrons and/or muons) using 139 fb^{-1} of proton–proton collision data recorded by the ATLAS detector at the LHC at $\sqrt{s} = 13$ TeV. The analysis is optimised to target the direct production of $\tilde{\chi}_1^+ \tilde{\chi}_1^-$, where each chargino decays into the LSP $\tilde{\chi}_1^0$ and an on-shell W boson. Signal events are characterised by the presence of exactly two isolated leptons (e, μ) with opposite electric charge, and significant $\mathbf{p}_T^{\text{miss}}$ (the magnitude of which is referred to as E_T^{miss}), expected from neutrinos and LSPs in the final states. The same analysis strategy is also applied to two other searches. One of them is the search for the direct production of $\tilde{\chi}_1^+ \tilde{\chi}_1^-$, where each chargino decays into a slepton (charged slepton $\tilde{\ell}$ or sneutrino $\tilde{\nu}$) via the emission of a lepton (neutrino ν or charged lepton ℓ) and the slepton itself decays into a lepton and the LSP. The other one is the search for the direct pair production of sleptons where each slepton decays into a lepton and the LSP.

The search described here significantly extends the areas of the parameter space beyond those excluded by previous searches by ATLAS [24,25] and CMS [26–31] in the same channels.

After a description of the considered SUSY scenarios in Sect. 2 and of the ATLAS detector in Sect. 3, the data and simulated Monte Carlo (MC) samples used in the analysis are detailed in Sect. 4. Sections 5 and 6 present the event reconstruction and the search strategy. The SM background estimation and the systematic uncertainties are discussed in Sects. 7 and 8, respectively. Finally, the results and their interpretations are reported in Sect. 9. Section 10 summarises the conclusions.

2 SUSY scenarios

The design of the analysis and the interpretation of results are based on simplified models [32], where the masses of relevant sparticles (in this case the $\tilde{\chi}_1^\pm$, $\tilde{\ell}$, $\tilde{\nu}$ and $\tilde{\chi}_1^0$) are the only free parameters. The $\tilde{\chi}_1^\pm$ is assumed to be pure wino and two possible decay modes are considered. The first is a decay into the $\tilde{\chi}_1^0$ via emission of a W boson, which may decay into an electron or muon plus neutrino(s) either directly or through the emission of a leptonically decaying τ-lepton (Fig. 1a). The second decay mode proceeds via a slepton–neutrino/sneutrino–lepton pair (Fig. 1b). In this case it is assumed that the scalar partners of the left-handed charged leptons and neutrinos are also light and thus accessible in the sparticle decay chains. It is also assumed they are mass-degenerate, and their masses are chosen to be midway between the mass of the chargino and that of the $\tilde{\chi}_1^0$, which is pure bino. Equal branching ratios for the three slepton flavours are assumed and charginos decay into charged sleptons or sneutrinos with a branching ratio of 50% to each. Lepton flavour is conserved in all models. In models with direct $\tilde{\ell}\tilde{\ell}$ production (Fig. 1c), each slepton decays into a lepton and a $\tilde{\chi}_1^0$ with a 100% branching ratio. Only $\tilde{e}$ and $\tilde{\mu}$ are considered in these models, and different assumptions about the masses of the superpartners of the left-handed and right-handed charged leptons, $\tilde{e}_L$, $\tilde{e}_R$, $\tilde{\mu}_L$ and $\tilde{\mu}_R$, are considered.

3 ATLAS detector

The ATLAS detector [33] at the LHC is a general-purpose detector with a forward–backward symmetric cylindrical geometry and an almost complete coverage in solid angle

around the collision point.[1] It consists of an inner tracking detector surrounded by a thin superconducting solenoid, electromagnetic and hadronic calorimeters, and a muon spectrometer incorporating three large superconducting toroid magnets.

The inner-detector (ID) system is immersed in a $2\,T$ axial magnetic field produced by the solenoid and provides charged-particle tracking in the range $|\eta| < 2.5$. It consists of a high-granularity silicon pixel detector, a silicon microstrip tracker and a transition radiation tracker, which enables radially extended track reconstruction up to $|\eta| = 2.0$. The transition radiation tracker also provides electron identification information. During the first LHC long shutdown, a new tracking layer, known as the Insertable B-Layer [34,35], was added with an average sensor radius of 33 mm from the beam pipe to improve tracking and b-tagging performance.

The calorimeter system covers the pseudorapidity range $|\eta| < 4.9$. Within the region $|\eta| < 3.2$, electromagnetic calorimetry is provided by barrel and endcap high-granularity lead/liquid-argon (LAr) sampling calorimeters. Hadronic calorimetry is provided by an iron/scintillator-tile sampling calorimeter for $|\eta| < 1.7$, and two copper/LAr hadronic endcap calorimeters. The solid angle coverage is completed with forward copper/LAr and tungsten/LAr calorimeter modules optimised for electromagnetic and hadronic measurements, respectively.

The muon spectrometer (MS) comprises separate trigger and high-precision tracking chambers measuring the deflection of muons in a magnetic field generated by superconducting air-core toroids. The precision chamber system covers the region $|\eta| < 2.7$ with three layers of monitored drift tubes, complemented by cathode strip chambers in the forward region, where the background is higher. The muon trigger system covers the range $|\eta| < 2.4$ with resistive plate chambers in the barrel, and thin gap chambers in the endcap regions.

A two-level trigger system is used to select events. There is a low-level hardware trigger implemented in custom electronics, which reduces the incoming data rate to a design value of 100 kHz using a subset of detector information, and a high-level software trigger that selects interesting final-state events with algorithms accessing the full detector information, and further reduces the rate to about 1 kHz [36].

---

[1] ATLAS uses a right-handed coordinate system with its origin at the nominal interaction point (IP) in the centre of the detector and the z-axis along the beam pipe. The x-axis points from the IP to the centre of the LHC ring, and the y-axis points upwards. Cylindrical coordinates (r, ϕ) are used in the transverse plane, ϕ being the azimuthal angle around the z-axis. The pseudorapidity is defined in terms of the polar angle θ as $\eta = -\ln\tan(\theta/2)$. Rapidity is defined as $y = 0.5\ln[(E + p_z)/(E - p_z)]$, where E and p_z denote the energy and the component of the particle momentum along the beam direction, respectively.

4 Data and simulated event samples

The analysis uses data collected by the ATLAS detector during pp collisions at a centre-of-mass energy of $\sqrt{s} = 13$ TeV from 2015 to 2018. The average number $\langle\mu\rangle$ of additional pp interactions per bunch crossing (pile-up) ranged from 14 in 2015 to about 38 in 2017–2018. After data-quality requirements, the data sample amounts to a total integrated luminosity of 139 fb^{-1}. The uncertainty in the combined 2015–2018 integrated luminosity is 1.7% [37], obtained using the LUCID-2 detector [38] for the primary luminosity measurements.

Candidate events were selected by a trigger that required at least two leptons (electrons and/or muons). The trigger-level thresholds for the transverse momentum, p_T, of the leptons involved in the trigger decision were different according to the data-taking periods. They were in the range 8–22 GeV for data collected in 2015 and 2016, and 8–24 GeV for data collected in 2017 and 2018. These thresholds are looser than those applied in the lepton offline selection to ensure that trigger efficiencies are constant in the relevant phase space.

Simulated event samples are used for the SM background estimate and to model the SUSY signal. The MC samples were processed through a full simulation of the ATLAS detector [39] based on GEANT 4 [40] or a fast simulation using a parameterisation of the ATLAS calorimeter response and GEANT 4 for the other components of the detector [39]. They were reconstructed with the same algorithms as those used for the data. To compensate for differences between data and simulation in the lepton reconstruction efficiency, energy scale, energy resolution and modelling of the trigger [41,42], and in the b-tagging efficiency [43], correction factors are derived from data and applied as weights to the simulated events.

All SM backgrounds used are listed in Table 1 along with the relevant parton distribution function (PDF) sets, the configuration of underlying-event and hadronisation parameters (tune), and the cross-section order in α_s used to normalise the event yields for these samples. Further information on the ATLAS simulations of $t\bar{t}$, single top (Wt), multiboson and boson plus jet processes can be found in the relevant public notes [44–47].

The SUSY signal samples were generated from leading-order (LO) matrix elements with up to two extra partons using MADGRAPH5_aMC@NLO 2.6.1 [48] interfaced to PYTHIA 8.186 [49], with the A14 tune [50], for the modelling of the SUSY decay chain, parton showering, hadronisation and the description of the underlying event. Parton luminosities were provided by the NNPDF2.3LO PDF set [51]. Jet–parton matching was performed following the CKKW-L prescription [52], with a matching scale set to one quarter of the mass of the pair-produced SUSY particles. Signal cross-sections were calculated to next-to-leading order (NLO) in

α_s adding the resummation of soft gluon emission at next-to-leading-logarithm accuracy (NLO+NLL) [53–59]. The nominal cross-sections and their uncertainties were taken from an envelope of cross-section predictions using different PDF sets and factorisation and renormalisation scales, as described in Ref. [60]. The cross-section for $\tilde{\chi}_1^+ \tilde{\chi}_1^-$ production, each with a mass of 400 GeV, is 58.6 ± 4.7 fb, while the cross-section for $\tilde{\ell}\tilde{\ell}$ production, each with a mass of 500 GeV, is 0.47 ± 0.03 fb for each generation of left-handed sleptons and 0.18 ± 0.01 fb for each generation of right-handed sleptons.

Inelastic pp interactions were generated and overlaid onto the hard-scattering process to simulate the effect of multiple proton–proton interactions occurring during the same (in-time) or a nearby (out-of-time) bunch crossing. These were produced using PYTHIA 8.186 and EvtGen [61] with the NNPDF2.3LO set of PDFs [51] and the A3 tune [62]. The MC samples were reweighted so that the distribution of the average number of interactions per bunch crossing reproduces the observed distribution in the data.

5 Object identification

Leptons selected for analysis are categorised as baseline or signal leptons according to various quality and kinematic selection criteria. Baseline objects are used in the calculation of missing transverse momentum, to resolve ambiguities between the analysis objects in the event and in the fake/non-prompt (FNP) lepton background estimation described in Sect. 7. Leptons used for the final event selection must satisfy more stringent signal requirements.

Baseline electron candidates are reconstructed using clusters of energy deposits in the electromagnetic calorimeter that are matched to an ID track. They are required to satisfy a *Loose* likelihood-based identification requirement [41], and to have $p_T > 10$ GeV and $|\eta| < 2.47$. They are also required to be within $|z_0 \sin\theta| = 0.5$ mm of the primary vertex,[2] where z_0 is the longitudinal impact parameter relative to the primary vertex. Signal electrons are required to satisfy a *Tight* identification requirement [41] and the track associated with the signal electron is required to have $|d_0|/\sigma(d_0) < 5$, where d_0 is the transverse impact parameter relative to the reconstructed primary vertex and $\sigma(d_0)$ is its error.

Baseline muon candidates are reconstructed in the pseudorapidity range $|\eta| < 2.7$ from MS tracks matching ID tracks. They are required to have $p_T > 10$ GeV, to be within $|z_0 \sin\theta| = 0.5$ mm of the primary vertex and to satisfy the *Medium* identification requirements defined in Ref. [42]. The

---

[2] The primary vertex is defined as the vertex with the highest scalar sum of the squared transverse momentum of associated tracks with $p_T > 500$ MeV.

Table 1 Simulated background event samples with the corresponding matrix element and parton shower (PS) generators, cross-section order in α_s used to normalise the event yield, underlying-event tune and the generator PDF sets used

Physics process	Generator	Parton shower	Normalisation	Tune	PDF (generator)	PDF (PS)
$t\bar{t}$	POWHEG-BOX v2 [63–66]	PYTHIA 8.230 [67]	NNLO+NNLL [68]	A14 [50]	NNPDF3.0NLO [69]	NNPDF2.3LO [51]
$t\bar{t}+V(V=W,Z)$	MADGRAPH5_aMC@NLO [48]	PYTHIA 8.210 [67]	NLO [48,70]	A14	NNPDF3.0NLO	NNPDF2.3LO
$t\bar{t}+WW$	MADGRAPH5_aMC@NLO	PYTHIA 8.186 [49]	NLO [48]	A14	NNPDF2.3LO	NNPDF2.3LO
$tZ, t\bar{t}t\bar{t}, t\bar{t}t$	MADGRAPH5_aMC@NLO	PYTHIA 8.230	NLO [48]	A14	NNPDF3.0NLO	NNPDF2.3LO
Single top (Wt)	POWHEG-BOX v2 [64,65,71]	PYTHIA 8.230	NLO+NNLL [72,73]	A14	NNPDF3.0NLO	NNPDF2.3LO
$Z/\gamma^*(\to ll)$+jets	SHERPA 2.2.1 [74–76]	SHERPA 2.2.1	NNLO [77]	SHERPA default [76]	NNPDF3.0NNLO [69]	NNPDF3.0NNLO [69]
WW, WZ, ZZ	POWHEG-BOX v2 [64,65,78,79]	PYTHIA 8.210	NLO [46,78,79]	AZNLO [80]	CT10 NLO [81]	CTEQ6L1 [82]
$VVV(V=W,Z)$	SHERPA 2.2.2 [46,74,75]	SHERPA 2.2.2	NLO [46,75]	SHERPA default [46]	NNPDF3.0NNLO	NNPDF3.0NNLO
Higgs boson	POWHEG-BOX v2 [64,65,83–86]	PYTHIA 8.186	NLO [87]	AZNLO	NNPDF3.0NLO[a]	CTEQ6L1

[a] The PDF4LHC15 set have been used for some Higgs production processes, as via gluon-gluon fusion, VBF and VH

Medium identification criterion defines requirements on the number of hits in the different ID and MS subsystems, and on the significance of the charge-to-momentum ratio q/p. Finally, the track associated with the signal muon must have $|d_0|/\sigma(d_0) < 3$.

Isolation criteria are applied to signal electrons and muons. The scalar sum of the p_T of tracks inside a variable-size cone around the lepton (excluding its own track), must be less than 15% of the lepton p_T. The track isolation cone size for electrons (muons) $\Delta R = \sqrt{(\Delta\eta)^2 + (\Delta\phi)^2}$ is given by the minimum of $\Delta R = 10\,\text{GeV}/p_T$ and $\Delta R = 0.2\,(0.3)$. In addition, for electrons (muons) the sum of the transverse energy of the calorimeter energy clusters in a cone of $\Delta R = 0.2$ around the lepton (excluding the energy from the lepton itself) must be less than 20% (30%) of the lepton p_T. For electrons with $p_T > 200$ GeV these isolation requirements are not applied, and instead an upper limit of $\max(0.015 \times p_T, 3.5\,\text{GeV})$ is placed on the transverse energy of the calorimeter energy clusters in a cone of $\Delta R = 0.2$ around the electron.

Jets are reconstructed from topological clusters of energy in the calorimeter [88] using the anti-k_t jet clustering algorithm [89] as implemented in the FastJet package [90], with a radius parameter $R = 0.4$. The reconstructed jets are then calibrated by the application of a jet energy scale derived from 13 TeV data and simulation [91]. Only jet candidates with $p_T > 20$ GeV and $|\eta| < 2.4$ are considered,[3] although jets with $|\eta| < 4.9$ are included in the missing transverse momentum calculation and are considered when applying the procedure to remove reconstruction ambiguities, which is described later in this section.

To reduce the effects of pile-up, for jets with $|\eta| \leq 2.5$ and $p_T < 120$ GeV a significant fraction of the tracks associated with each jet are required to have an origin compatible with the primary vertex, as defined by the jet vertex tagger [92]. This requirement reduces jets from pile-up to 1%, with an efficiency for pure hard-scatter jets of about 90%. For jets with $|\eta| > 2.5$ and $p_T < 60$ GeV, pile-up suppression is achieved through the forward jet vertex tagger [93], which exploits topological correlations between jet pairs. Finally, events containing a jet that does not satisfy the jet-quality requirements [94,95] are rejected to remove events impacted by detector noise and non-collision backgrounds.

The MV2C10 boosted decision tree algorithm [43] identifies jets containing b-hadrons ('b-jets') by using quantities such as the impact parameters of associated tracks, and well-reconstructed secondary vertices. A selection that provides 85% efficiency for tagging b-jets in simulated $t\bar{t}$ events is used. The corresponding rejection factors against jets originating from c-quarks, from τ-leptons, and from light quarks and gluons in the same sample at this working point are 2.7, 6.1 and 25, respectively.

---

[3] Hadronic τ-lepton decay products are treated as jets.

To avoid the double counting of analysis baseline objects, a procedure to remove reconstruction ambiguities is applied as follows:

- jet candidates within $\Delta R' = \sqrt{\Delta y^2 + \Delta\phi^2} = 0.2$ of an electron candidate are removed;
- jets with fewer than three tracks that lie within $\Delta R' = 0.4$ of a muon candidate are removed;
- electrons and muons within $\Delta R' = 0.4$ of the remaining jets are discarded, to reject leptons from the decay of b- or c-hadrons;
- electron candidates are rejected if they are found to share an ID track with a muon.

The missing transverse momentum ($\mathbf{p}_T^{\text{miss}}$), which has the magnitude E_T^{miss}, is defined as the negative vector sum of the transverse momenta of all identified physics objects (electrons, photons, muons and jets). Low-momentum tracks from the primary vertex that are not associated with reconstructed analysis objects (the 'soft term') are also included in the calculation, and the E_T^{miss} value is adjusted for the calibration of the selected physics objects [96]. Linked to the E_T^{miss} value is the 'object-based E_T^{miss} significance', referred to as E_T^{miss} significance in this paper, that helps to separate events with true E_T^{miss} (arising from weakly interacting particles) from those where it is consistent with particle mismeasurement, resolution or identification inefficiencies. On an event-by-event basis, given the full event composition, E_T^{miss} significance evaluates the p-value that the observed E_T^{miss} is consistent with the null hypothesis of zero real E_T^{miss}, as further detailed in Ref. [97].

6 Search strategy

Events are required to have exactly two oppositely charged signal leptons ℓ_1 and ℓ_2, both with $p_T > 25$ GeV. To remove contributions from low-mass resonances and to ensure good modelling of the SM background in all relevant regions, the invariant mass of the two leptons must be $m_{\ell_1\ell_2} > 100$ GeV. Events are further required to have no reconstructed b-jets, to suppress contributions from processes with top quarks. Selected events must also satisfy $E_T^{\text{miss}} > 110$ GeV and E_T^{miss} significance > 10.

The stransverse mass m_{T2} [98,99] is a kinematic variable used to bound the masses of a pair of particles that are assumed to have each decayed into one visible and one invisible particle. It is defined as

$$
m_{T2}(\mathbf{p}_{T,1}, \mathbf{p}_{T,2}, \mathbf{p}_T^{\text{miss}})
$$
$$
= \min_{\mathbf{q}_{T,1} + \mathbf{q}_{T,2} = \mathbf{p}_T^{\text{miss}}} \left\{ \max[m_T(\mathbf{p}_{T,1}, \mathbf{q}_{T,1}), m_T(\mathbf{p}_{T,2}, \mathbf{q}_{T,2})] \right\},
$$

where m_T indicates the transverse mass,[4] $\mathbf{p}_{T,1}$ and $\mathbf{p}_{T,2}$ are the transverse-momentum vectors of the two leptons, and $\mathbf{q}_{T,1}$ and $\mathbf{q}_{T,2}$ are vectors with $\mathbf{p}_T^{miss} = \mathbf{q}_{T,1} + \mathbf{q}_{T,2}$. The minimisation is performed over all the possible decompositions of $\mathbf{p}_T^{miss}$. For $t\bar{t}$ or WW decays, assuming an ideal detector with perfect momentum resolution, $m_{T2}(\mathbf{p}_{T,\ell_1}, \mathbf{p}_{T,\ell_2}, \mathbf{p}_T^{miss})$ has a kinematic endpoint at the mass of the W boson [99]. Signal models with significant mass splittings between the $\tilde{\chi}_1^{\pm}$ and the $\tilde{\chi}_1^0$ feature m_{T2} distributions that extend beyond the kinematic endpoint expected from the dominant SM backgrounds. Therefore, events are required to have high m_{T2} values.

Events are separated into 'same flavour' (SF) events, i.e. $e^{\pm}e^{\mp}$ and $\mu^{\pm}\mu^{\mp}$, and 'different flavour' (DF) events, i.e. $e^{\pm}\mu^{\mp}$, since the two classes of events have different background compositions. SF events are required to have a dilepton invariant mass far from the Z peak, $m_{\ell_1\ell_2} > 121.2$ GeV, to reduce diboson and Z+jets backgrounds.

Events are further classified by the multiplicity of non-b-tagged jets ($n_{\text{non-}b\text{-tagged jets}}$), i.e. the number of jets not identified as b-jets by the MV2C10 boosted decision tree algorithm. All events are required to have no more than one non-b-tagged jet. Following the classification of the events, two sets of signal regions (SRs) are defined: a set of exclusive, 'binned' SRs, to maximise model-dependent search sensitivity, and a set of 'inclusive' SRs, to be used for model-independent results. Among the second set of SRs two are fully inclusive, with a different lower bound on m_{T2} to target different chargino or slepton mass regions, while two have both lower and upper bounds on m_{T2} to target models with lower endpoints. The definitions of these regions are shown in Table 2. Each SR is identified by the lepton flavour combination (DF or SF), the number of non-b-tagged jets (0J,1J) and the range of the m_{T2} interval.

7 Background estimation and validation

The SM backgrounds can be classified into irreducible backgrounds, from processes with prompt leptons, and reducible backgrounds, which contain one or more FNP leptons. The main irreducible backgrounds come from SM diboson (WW, WZ, ZZ) and top-quark ($t\bar{t}$ and Wt) production. These are estimated from simulated events, normalised using a simultaneous likelihood fit to data (as described in Sect. 9) in dedicated control regions (CRs). The CRs are designed to be enriched in the particular background process under study while remaining kinematically similar to the SRs. The nor-

Table 2 The definitions of the binned and inclusive signal regions. Relevant kinematic variables are defined in the text. The bins labelled 'DF' or 'SF' refer to signal regions with different lepton flavour or same lepton flavour pair combinations, respectively, and the '0J' and '1J' labels refer to the multiplicity of non-b-tagged jets

Signal region (SR)	SR-DF-0J	SR-DF-1J	SR-SF-0J	SR-SF-1J
$n_{\text{non-}b\text{-tagged jets}}$	= 0	= 1	= 0	= 1
$m_{\ell_1\ell_2}$ [GeV]	\multicolumn{2}{	}{>100}	\multicolumn{2}{	}{>121.2}
E_T^{miss} [GeV]		>110		
E_T^{miss} significance		>10		
$n_{b\text{-tagged jets}}$		= 0		
Binned SRs				
m_{T2} [GeV]		$\in[100,105)$		
		$\in[105,110)$		
		$\in[110,120)$		
		$\in[120,140)$		
		$\in[140,160)$		
		$\in[160,180)$		
		$\in[180,220)$		
		$\in[220,260)$		
		$\in[260,\infty)$		
Inclusive SRs				
m_{T2} [GeV]		$\in[100,\infty)$		
		$\in[160,\infty)$		
		$\in[100,120)$		
		$\in[120,160)$		

malisations of the relevant backgrounds are then validated in a set of validation regions (VRs), which are not used to constrain the fit, but are used to verify that the data and predictions, in terms of the yields and of the shapes of the relevant kinematic distributions, agree within uncertainties in regions of the phase space kinematically close to the SRs. Three CRs are used, as defined in Table 3: CR-WW, targeting WW production; CR-VZ, targeting WZ and ZZ production, which are normalised by using a single parameter in the likelihood fit to the data; and CR-top, targeting $t\bar{t}$ and single-top-quark production, which are also normalised by using a single parameter in the likelihood fit to the data. A single normalisation parameter is used for $t\bar{t}$ and single-top-quark (Wt) production as the relative amounts of each process are consistent within uncertainties in the CR and SRs.

The definitions of the VRs are shown in Table 4. For the WW background two validation regions are considered (VR-WW-0J and VR-WW-1J), according to the multiplicity of non-b-tagged jets in the event. As contributions from top-quark backgrounds in VR-WW-0J and VR-WW-1J are not negligible, three VRs are defined for this background. VR-top-low requires a similar m_{T2} range as VR-WW-0J and VR-WW-1J, thus allowing the modelling of top-quark production at lower values of m_{T2} to be validated. VR-top-high requires $m_{T2} > 100$ GeV and provides validation in the high m_{T2} region where the SRs are also defined. Finally, VR-top-WW requires the same E_T^{miss}, E_T^{miss} significance and m_{T2} ranges as CR-WW and provides validation of the modelling of top-quark production in this region.

---

[4] The transverse mass is defined as $m_T = \sqrt{2 \times |\mathbf{p}_{T,1}| \times |\mathbf{p}_{T,2}| \times (1 - \cos(\Delta\phi))}$, where $\Delta\phi$ is the difference in azimuthal angle between the particles with transverse momenta $\mathbf{p}_{T,1}$ and $\mathbf{p}_{T,2}$.

To obtain CRs and VRs of reasonable purity in WW production, CR-WW, VR-WW-0J and VR-WW-1J all require lower m_{T2} values than the SRs. To validate the tails of the m_{T2} distribution, a method similar to the one described in Ref. [31] is used. Three-lepton events, purely from WZ production, are selected by requiring the absence of b-tagged jets and the presence of one same-flavour opposite-sign (SFOS) lepton pair with an invariant mass consistent with that of the Z boson ($|m_{\ell_1\ell_2} - m_Z| < 10$ GeV). To avoid overlaps with portions of the phase space relevant for other searches, three-lepton events are also required to satisfy $E_T^{miss} \in [40, 170]$ GeV. To emulate the signal regions, events are also required to have zero or one non-b-tagged jet. The transverse momentum of the lepton in the SFOS pair that has the same charge as the remaining lepton is added to the $\mathbf{p}_T^{miss}$ vector, to mimic a neutrino. The m_{T2} value can then be calculated using the remaining two leptons in the event. With this selection, there is a good agreement between the shapes of the m_{T2} distributions observed in data and simulation, and no additional systematic uncertainty is applied to the WW background at high m_{T2}.

Sub-dominant irreducible SM background contributions come from Drell–Yan, $t\bar{t} + V$ and Higgs boson production. These processes, jointly referred to as 'Other backgrounds' (or 'Others' in the Figures) are estimated directly from sim-ulation using the samples described in Sect. 4. The remaining background from FNP leptons is estimated from data using the matrix method (MM) [100]. This method considers two types of lepton identification criteria: 'signal' leptons, corresponding to leptons passing the full analysis selection, and 'baseline' leptons, as defined in Sect. 5. Probabilities for prompt leptons satisfying the baseline selection to also satisfy the signal selection are measured as a function of lepton p_T and η in dedicated regions enriched in Z boson processes. Similar probabilities for FNP leptons are measured in events dominated by leptons from the decays of heavy-flavour hadrons and from photon conversions. These probabilities are used in the MM to extract data-driven estimates for the FNP lepton background in the CRs, VRs, and

Table 3 Control region definitions for extracting normalisation factors for the dominant background processes. 'DF' or 'SF' refer to signal regions with different lepton flavour or same lepton flavour pair combinations, respectively

Region	CR-WW	CR-VZ	CR-top
Lepton flavour	DF	SF	DF
$n_{b\text{-tagged jets}}$	$= 0$	$= 0$	$= 1$
$n_{\text{non-}b\text{-tagged jets}}$	$= 0$	$= 0$	$= 0$
m_{T2} (GeV)	$\in [60, 65]$	> 120	> 80
E_T^{miss} (GeV)	$\in [60, 100]$	> 110	> 110
E_T^{miss} significance	$\in [5, 10]$	> 10	> 10
$m_{\ell_1\ell_2}$ (GeV)	> 100	$\in [61.2, 121.2]$	> 100

Table 5 Observed event yields and predicted background yields from the fit in the CRs. For backgrounds with a normalisation extracted from the fit, the yield expected from the simulation before the fit is also shown. 'Other backgrounds' include the non-dominant background sources, i.e. $t\bar{t}+V$, Higgs boson and Drell–Yan events. A '–' symbol indicates that the background contribution is negligible

Region	CR-WW	CR-VZ	CR-top
Observed events	962	811	321
Fitted backgrounds	962 ± 31	811 ± 28	321 ± 18
Fitted WW	670 ± 60	19.1 ± 1.9	5.5 ± 2.7
Fitted WZ	11.8 ± 0.7	188 ± 7	0.32 ± 0.15
Fitted ZZ	0.29 ± 0.06	577 ± 23	–
Fitted $t\bar{t}$	170 ± 50	1.8 ± 1.3	270 ± 16
Fitted single top	88 ± 8	0.65 ± 0.35	38.6 ± 2.6
Other backgrounds	0.17 ± 0.06	19 ± 7	2.21 ± 0.20
FNP leptons	21 ± 8	5^{+6}_{-5}	4.2 ± 2.2
Simulated WW	528	15.1	4.3
Simulated WZ	9.9	158	0.27
Simulated ZZ	0.24	487	–
Simulated $t\bar{t}$	210	2.2	327
Simulated single top	107	0.8	46.7

Table 4 Validation region definitions used to study the modelling of the SM backgrounds. 'DF' or 'SF' refer to regions with different lepton flavour or same lepton flavour pair combinations, respectively

Region	VR-WW-0J	VR-WW-1J	VR-VZ	VR-top-low	VR-top-high	VR-top-WW
Lepton flavour	DF	DF	SF	DF	DF	DF
$n_{b\text{-tagged jets}}$	$= 0$	$= 0$	$= 0$	$= 1$	$= 1$	$= 1$
$n_{\text{non-}b\text{-tagged jets}}$	$= 0$	$= 1$	$= 0$	$= 0$	$= 1$	$= 1$
m_{T2} (GeV)	$\in [65, 100]$	$\in [65, 100]$	$\in [100, 120]$	$\in [80, 100]$	> 100	$\in [60, 65]$
E_T^{miss} (GeV)	> 60	> 60	> 110	> 110	> 110	$\in [60, 100]$
E_T^{miss} significance	> 5	> 5	> 10	$\in [5, 10]$	> 10	$\in [5, 10]$
$m_{\ell_1\ell_2}$ (GeV)	> 100	> 100	$\in [61.2, 121.2]$	> 100	> 100	> 100

(a) m_{T2} distribution in CR-VZ

(b) m_{T2} distribution in CR-top
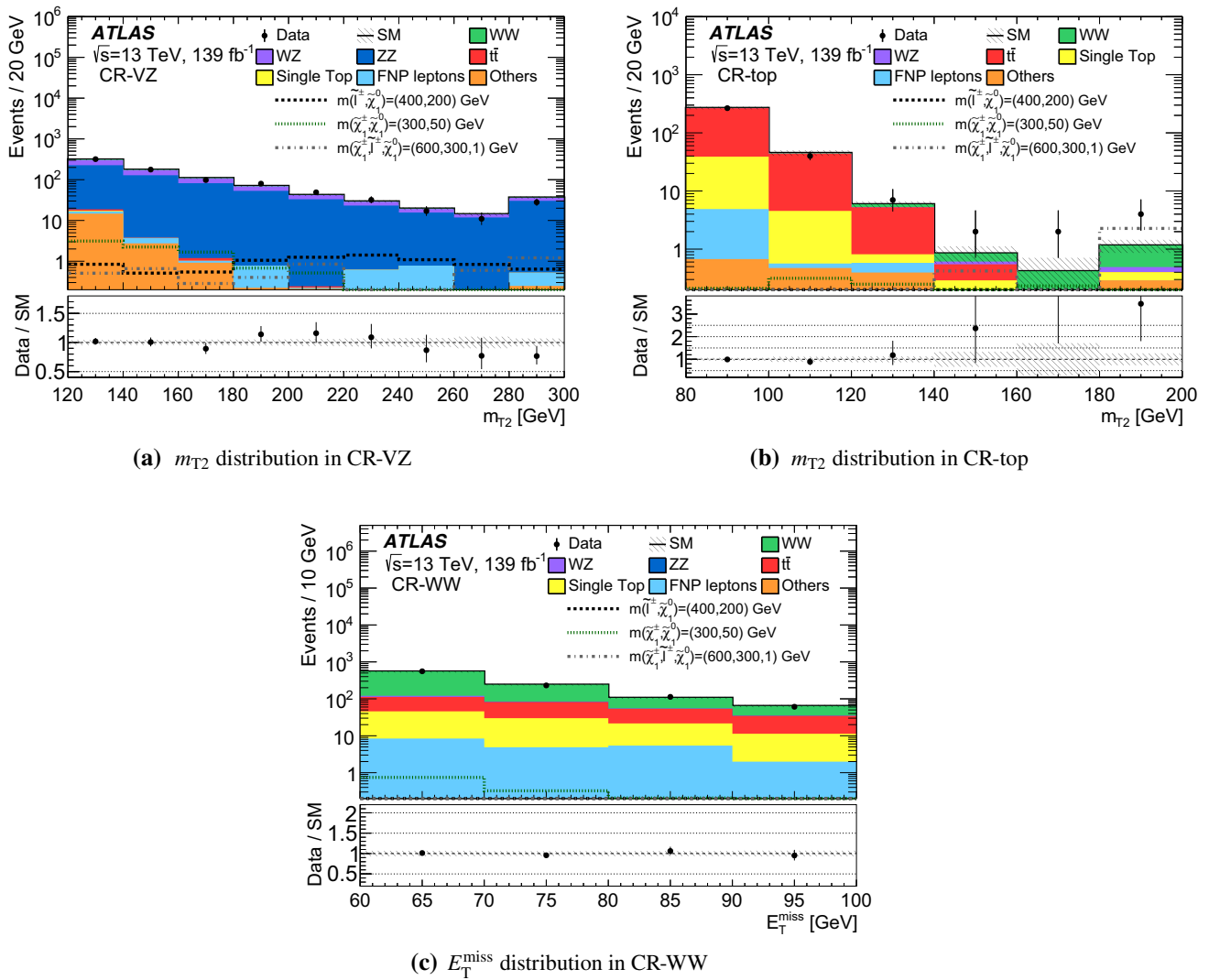

(c) E_T^{miss} distribution in CR-WW

Fig. 2 Distributions of m_{T2} in **a** CR-VZ and **b** CR-top and **c** E_T^{miss} in CR-WW for data and the estimated SM backgrounds. The normalisation factors extracted from the corresponding CRs are used to rescale the $t\bar{t}$, single-top-quark, WW, WZ and ZZ backgrounds. The FNP lepton background is calculated using the data-driven matrix method. Negligible background contributions are not included in the legends. The uncertainty band includes systematic and statistical errors from all sources and the final bin in each histogram includes the overflow. Distributions for three benchmark signal points are overlaid for comparison. The lower panels show the ratio of data to the SM background estimate

SRs, comparing the numbers of events containing a pair of baseline leptons in which one of the two leptons, both or none of them satisfy the signal selection in a given region. To avoid double counting between the simulated samples used for background estimation and the FNP lepton background estimate provided by the MM, all simulated events containing one or more FNP leptons are removed.

The number of observed events in each CR, as well as the predicted yield of each SM process, is shown in Table 5. For backgrounds whose normalisation is extracted from the likelihood fit, the yield expected from the simulation before the fit is also shown. After the fit, the central value of the total number of predicted events in each CR matches the data, as expected from the normalisation procedure. The nor-

malisation factors returned by the fit for the WW, $t\bar{t}$ and single-top-quark backgrounds, and WZ/ZZ backgrounds are 1.25 ± 0.11, 0.82 ± 0.06 and 1.18 ± 0.05 respectively, which for diboson backgrounds are applied to MC samples scaled to NLO cross-sections (as detailed in Table 1). The shapes of kinematic distributions are well reproduced by the simulation in each CR. The distributions of m_{T2} in CR-VZ and CR-top and of E_T^{miss} in CR-WW are shown in Fig. 2.

The number of observed events and the predicted background in each VR are shown in Table 6. For backgrounds with a normalisation extracted from the fit, the expected yield from simulated samples before the fit is also shown. Figure 3 shows a selection of kinematic distributions for data and the

Table 6 Observed event yields and predicted background yields in the VRs. For backgrounds with a normalisation extracted from the fit in the CRs, the yield expected from the simulation before the fit is also shown.

'Other backgrounds' include the non-dominant background sources, i.e. $t\bar{t} + V$, Higgs boson and Drell–Yan events. A '–' symbol indicates that the background contribution is negligible

Regions	VR-WW-0J	VR-WW-1J	VR-VZ	VR-top-low	VR-top-high	VR-top-WW
Observed events	2742	2671	464	190	50	953
Fitted backgrounds	2760 ± 120	2840 ± 250	420 ± 40	185 ± 17	53 ± 7	850 ± 80
Fitted WW	1550 ± 150	990 ± 120	17.6 ± 2.2	2.1 ± 0.7	2.6 ± 1.4	16.1 ± 2.5
Fitted WZ	34.2 ± 2.0	27.0 ± 2.3	99 ± 9	$0.05^{+0.17}_{-0.05}$	$0.2^{+0.6}_{-0.2}$	0.53 ± 0.13
Fitted ZZ	0.50 ± 0.06	0.39 ± 0.07	268 ± 25	–	–	$0.01^{+0.03}_{-0.01}$
Fitted $t\bar{t}$	790 ± 110	1400 ± 270	10.5 ± 3.2	157 ± 15	40 ± 7	650 ± 70
Fitted single top	336 ± 32	380 ± 40	2.2 ± 1.4	24.3 ± 2.6	4.6 ± 1.4	182 ± 15
Other backgrounds	0.92 ± 0.30	2.1 ± 0.5	21^{+27}_{-21}	0.28 ± 0.06	3.20 ± 0.20	0.39 ± 0.11
FNP leptons	44 ± 23	38 ± 21	$0.2^{+2.1}_{-0.2}$	2.3 ± 1.4	1.8 ± 0.5	–
Simulated WW	1230	790	14.0	1.6	2.0	12.8
Simulated WZ	28.8	22.8	84	0.04	0.1	0.45
Simulated ZZ	0.42	0.33	226	–	–	0.01
Simulated $t\bar{t}$	960	1700	13	190	49	790
Simulated single top	406	462	2.6	29.4	5.6	220

estimated SM background in the validation regions defined in Table 4. Good agreement is observed in all regions.

8 Systematic uncertainties

All relevant sources of experimental and theoretical systematic uncertainty affecting the SM background estimates and the signal predictions are included in the likelihood fit described in Sect. 9. The dominant sources of systematic uncertainty are related to theoretical uncertainties in the MC modelling, while the largest sources of experimental uncertainty are related to the jet energy scale (JES) and jet energy resolution (JER). The statistical uncertainty in the simulated event samples is also accounted for. Since the normalisation of the predictions for the dominant background processes is extracted from dedicated control regions, the systematic uncertainties only affect the extrapolation to the signal regions in these cases.

The JES and JER uncertainties are considered as a function of jet p_T and η, the pile-up conditions and the flavour composition of the selected jet sample. They are derived using a combination of data and simulation, through measurements of the transverse momentum balance between a jet and a reference object in dijet, Z+jets and γ+jets events [91]. An additional uncertainty in $\mathbf{p}_T^{miss}$ comes from the soft-term resolution and scale [96]. Uncertainties in the scale factors applied to the simulated samples to account for differences between data and simulation in the b-jet identification efficiency are also included. The remaining experimental systematic uncertainties, such as those in the lepton reconstruc-

tion efficiency, lepton energy scale and lepton energy resolution and differences between the trigger efficiencies in data and simulation are included and are found to be a few per mille in all channels. The reweighting procedure (pile-up reweighting) applied to simulation to match the distribution of the number of interactions per bunch crossing observed in data results in a negligible contribution to the total systematic uncertainty.

Several sources of theoretical uncertainty in the modelling of the dominant backgrounds are considered. Uncertainties in the MC modelling of diboson events are estimated by varying the PDF sets as well as the renormalisation and factorisation scales used to generate the samples. To account for effects due to the choice of generator, the nominal POWHEG- BOX diboson samples are compared with SHERPA diboson samples that have a different matrix element calculation and parton shower simulation.

For $t\bar{t}$ production, uncertainties in the parton shower simulation are estimated by comparing samples generated with POWHEG- BOX interfaced to either PYTHIA 8.186 or HERWIG 7.04 [101,102]. Another source of uncertainty comes from the modelling of initial- and final-state radiation, which is calculated by comparing the predictions of the nominal sample with two alternative samples generated with POWHEG- BOX interfaced to PYTHIA 8.186 but with the radiation settings varied [103]. The uncertainty associated with the choice of event generator is estimated by comparing the nominal samples with samples generated with aMC@NLO interfaced to PYTHIA 8.186 [104]. Finally, for single-top-quark production an uncertainty is assigned to the treatment of the interference between the Wt and $t\bar{t}$ samples. This is done by comparing
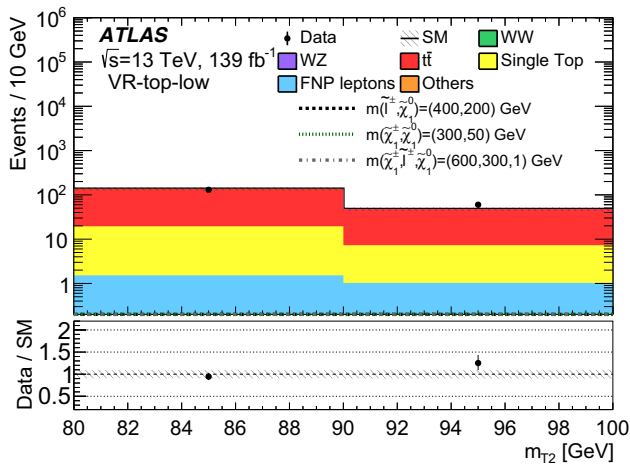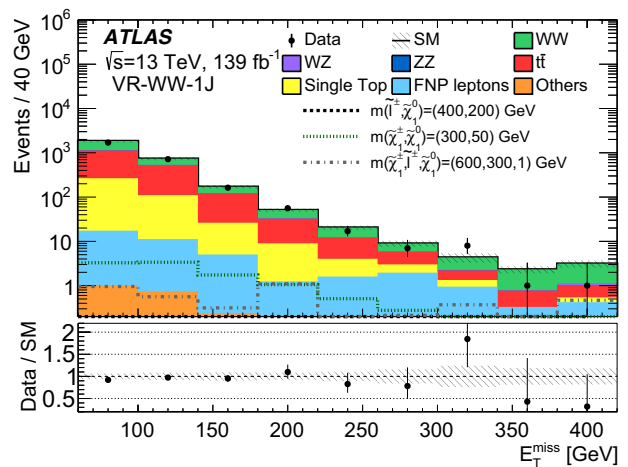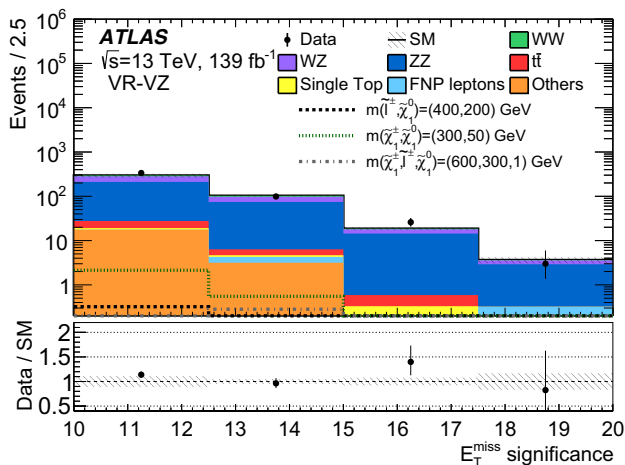
(a) m_{T2} distribution in VR-top-low
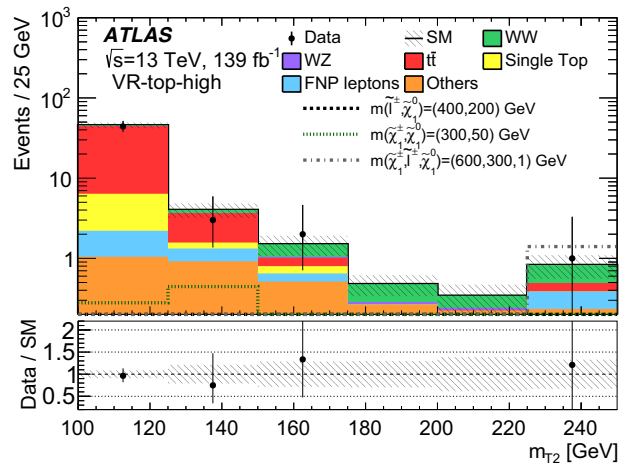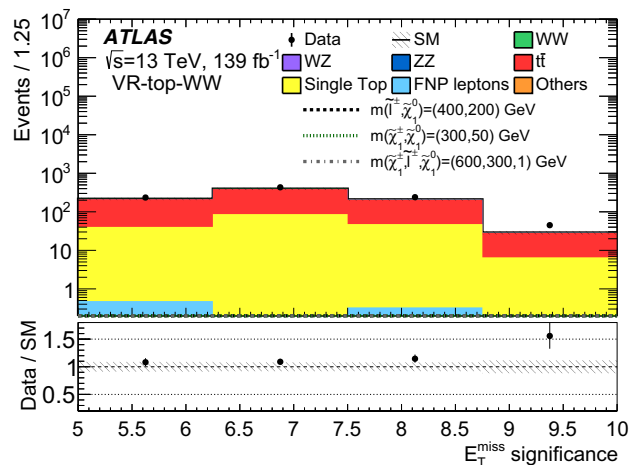

(b) m_{T2} distribution in VR-top-high
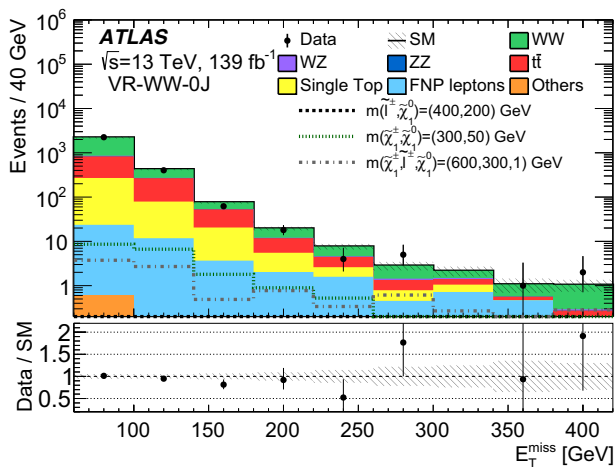
(c) E_T^{miss} distribution in VR-WW-0J

(d) E_T^{miss} distribution in VR-WW-1J

(e) E_T^{miss} significance distribution in VR-VZ

(f) E_T^{miss} significance distribution in VR-top-WW

Fig. 3 Distributions of m_{T2} in **a** VR-top-low and **b** VR-top-high, E_T^{miss} in **c** VR-WW-0J and **d** VR-WW-1J, and E_T^{miss} significance in **e** VR-VZ and **f** VR-top-WW, for data and the estimated SM backgrounds. The normalisation factors extracted from the corresponding CRs are used to rescale the $t\bar{t}$, single-top-quark, WW, WZ and ZZ backgrounds. The FNP lepton background is calculated using the data-driven matrix method. Negligible background contributions are not included in the legends. The uncertainty band includes systematic and statistical errors from all sources and the last bin includes the overflow. Distributions for three benchmark signal points are overlaid for comparison. The lower panels show the ratio of data to the SM background estimate

Table 7 Summary of the dominant systematic uncertainties in the background estimates in the inclusive SRs requiring $m_{T2} > 100$ GeV after performing the profile likelihood fit. The individual uncertainties can be correlated, and do not necessarily add in quadrature to the total background uncertainty. The percentages show the size of the uncertainty relative to the total expected background. 'Top theoretical uncertainties' refers to $t\bar{t}$ theoretical uncertainties and the uncertainty associated with Wt–$t\bar{t}$ interference added in quadrature

| Region m_{T2} (GeV)	SR-DF-0J $\in[100,\infty)$	SR-DF-1J $\in[100,\infty)$	SR-SF-0J $\in[100,\infty)$	SR-SF-1J $\in[100,\infty)$
Total background expectation	96	75	144	124
MC statistical uncertainties	3 %	3 %	2 %	3 %
WW normalisation	7 %	6 %	4 %	3 %
VZ normalisation	< 1 %	< 1 %	1 %	1 %
$t\bar{t}$ normalisation	1 %	2 %	< 1 %	1 %
Diboson theoretical uncertainties	7 %	7 %	4 %	3 %
Top theoretical uncertainties	7 %	8 %	3 %	6 %
E_T^{miss} modelling	1 %	1 %	< 1 %	2 %
Jet energy scale	2 %	3 %	2 %	2 %
Jet energy resolution	1 %	2 %	1 %	2 %
Pile-up reweighting	< 1 %	1 %	< 1 %	< 1 %
b-tagging	< 1 %	2 %	< 1 %	1 %
Lepton modelling	1 %	1 %	1 %	3 %
FNP leptons	1 %	1 %	1 %	1 %
Total systematic uncertainties	15 %	12 %	8 %	10 %
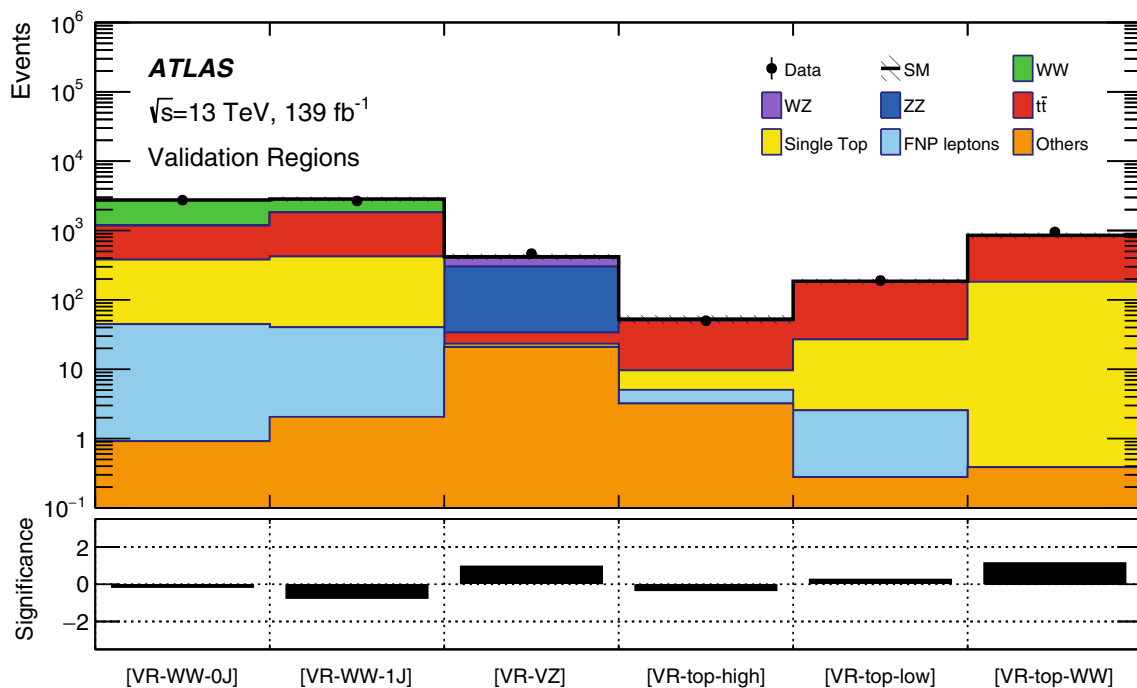
Fig. 4 The upper panel shows the observed number of events in each of the VRs defined in Table 4, together with the expected SM backgrounds obtained after the background-only fit in the CRs. The shaded band represents the total uncertainty in the expected SM background. The lower panel shows the significance as defined in Ref. [106]

the nominal sample generated using the diagram removal method with a sample generated using the diagram subtraction method [103].

There are several contributions to the uncertainty in the MM estimate of the FNP background. First, an uncertainty is included to account for the difference between the probability in simulation and the probability in data that prompt
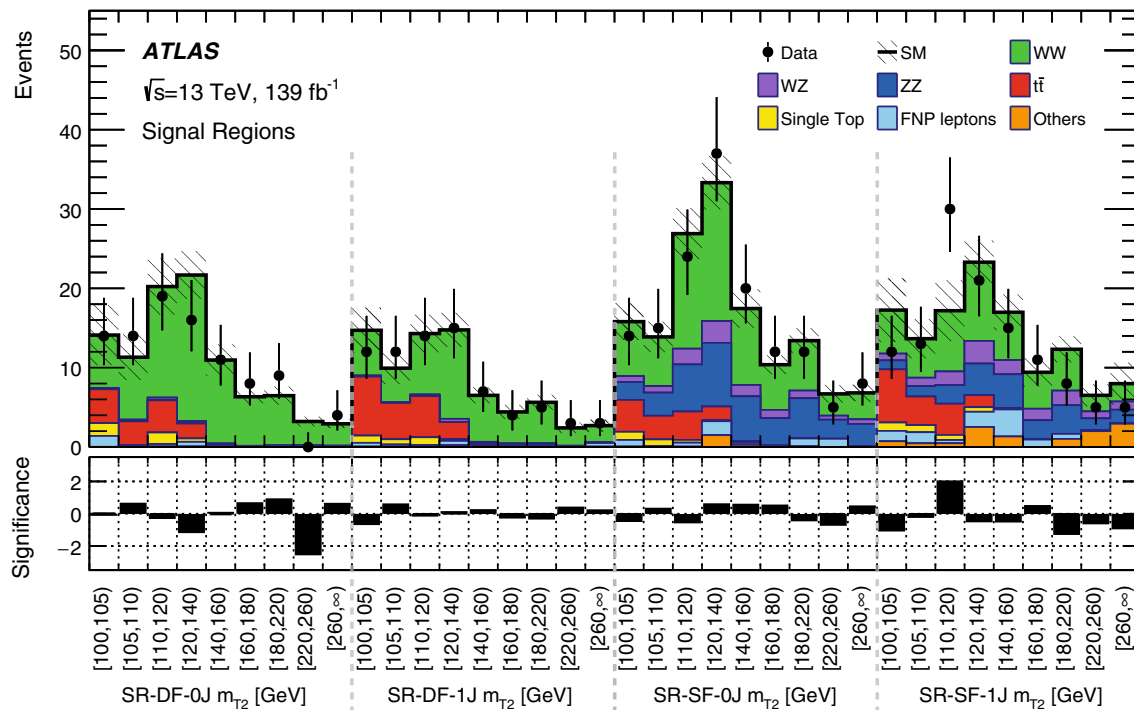
Fig. 5 The upper panel shows the observed number of events in each of the SRs defined in Table 2, together with the expected SM backgrounds obtained after the background-only fit in the CRs. The shaded band represents the total uncertainty in the expected SM background. The lower panel shows the significance as defined in Ref. [106]

leptons may satisfy the signal selection. Furthermore, uncertainties in the expected composition of the FNP leptons in the signal regions are included. Finally, two uncertainties associated with the control regions used to derive the probabilities for baseline leptons to satisfy the signal requirements are considered. The first accounts for limited numbers of events in these regions and the second for the subtraction of prompt-lepton contamination.

Systematic uncertainties on the signal acceptance and shape due to scale and parton shower variations are found to be negligible. The systematic uncertainty on the signal cross section has been described in Sect. 4.

A summary of the impact of the systematic uncertainties on the background yields in the inclusive SRs with $m_{T2} >$ 100 GeV, after performing the likelihood fit, is shown in Table 7. For the binned SRs defined in Table 2, the impact of the uncertainties associated with the limited numbers of MC events is higher than for the inclusive SRs.

9 Results

The statistical interpretation of the final results is performed using the HistFitter framework [105]. A simultaneous likelihood fit is performed, which includes either just the CRs (in the case of the background-only fit) or the CRs and

one or more of the SRs (when calculating exclusion limits). The likelihood is a product of Poisson probability density functions describing the observed number of events in each CR/SR and Gaussian distributions that constrain the nuisance parameters associated with the systematic uncertainties. Systematic uncertainties that are correlated between different samples are accounted for in the fit configuration by using the same nuisance parameter. These include the diboson theory uncertainties, for which a combined nuisance parameter is used for the WW, WZ and ZZ backgrounds. The uncertainties are applied in each of the CRs and SRs and their effect is correlated for events across all regions in the fit. Poisson distributions are used for MC statistical uncertainties.

A background-only fit that uses data only in the CRs is performed to constrain the nuisance parameters of the likelihood function, which include the background normalisation factors and parameters associated with the systematic uncertainties. The results of the background-only fit are used to assess how well the data agree with the background estimates in the validation regions. Good agreement, within about one standard deviation for all VRs, is observed, as described in Sect. 7 and shown in Fig. 4.

The results of the background-only fit in the CRs together with the observed data in the binned SRs are shown in Fig. 5. The observed and predicted number of background events in the inclusive SRs are shown in Tables 8 and 9. Figure 6

Table 8 Observed event yields and predicted background yields from the fit for the DF inclusive SRs. The model-independent upper limits at 95% CL on the observed and expected numbers of beyond-the-SM events $S_{\mathrm{obs/exp}}^{0.95}$ and on the effective beyond-the-SM cross-section $\sigma_{\mathrm{obs}}^{0.95}$ are also shown. The $\pm 1\sigma$ variations on $S_{\mathrm{exp}}^{0.95}$ are also provided. The last row shows the p_0-value of the SM-only hypothesis. For SRs where the data yield is smaller than expected, the p_0-value is capped at 0.50. 'Other backgrounds' include the non-dominant background sources, i.e. $t\bar{t}+V$, Higgs boson and Drell–Yan events. A '–' symbol indicates that the background contribution is negligible

Region m_{T2} (GeV)	SR-DF-0J $\in[100,\infty)$	SR-DF-0J $\in[160,\infty)$	SR-DF-0J $\in[100,120)$	SR-DF-0J $\in[120,160)$
Observed events	95	21	47	27
Fitted backgrounds	96 ± 15	18.8 ± 2.4	45 ± 9	33 ± 5
Fitted WW	76 ± 10	18.2 ± 2.4	29 ± 4	29 ± 4
Fitted WZ	1.53 ± 0.17	0.40 ± 0.07	0.66 ± 0.11	0.47 ± 0.07
Fitted ZZ	$0.00^{+0.19}_{-0.00}$	0.14 ± 0.03	$0.06^{+0.23}_{-0.06}$	< 0.04
Fitted $t\bar{t}$	13 ± 7	–	11 ± 6	2.1 ± 1.2
Fitted single top	3.7 ± 2.0	–	3.3 ± 1.8	0.42 ± 0.25
Other backgrounds	0.24 ± 0.08	0.07 ± 0.02	0.08 ± 0.02	0.09 ± 0.05
FNP leptons	1.8 ± 0.6	–	1.4 ± 0.4	0.47 ± 0.17
$S_{\mathrm{obs}}^{0.95}$	34.1	12.7	23.8	11.8
$S_{\mathrm{exp}}^{0.95}$	$35.2^{+13.9}_{-10.0}$	$11.0^{+4.9}_{-3.2}$	$22.8^{+9.1}_{-6.5}$	$15.1^{+6.3}_{-4.5}$
$\sigma_{\mathrm{obs}}^{0.95}$ (fb)	0.24	0.09	0.17	0.08
p_0	0.50	0.33	0.44	0.50
Region m_{T2} (GeV)	SR-DF-1J $\in[100,\infty)$	SR-DF-1J $\in[160,\infty)$	SR-DF-1J $\in[100,120)$	SR-DF-1J $\in[120,160)$
Observed events	75	15	38	22
Fitted backgrounds	75 ± 9	15.1 ± 2.7	39 ± 6	21.3 ± 2.8
Fitted WW	48 ± 8	13.4 ± 2.6	17.7 ± 2.6	17.1 ± 2.8
Fitted WZ	1.54 ± 0.21	0.53 ± 0.12	0.43 ± 0.09	0.59 ± 0.11
Fitted ZZ	0.08 ± 0.01	$0.07^{+0.24}_{-0.07}$	< 0.04	0.01 ± 0.00
Fitted $t\bar{t}$	20 ± 7	0.09 ± 0.03	17 ± 6	2.4 ± 0.9
Fitted single top	2.8 ± 1.4	–	2.6 ± 1.3	0.21 ± 0.13
Other backgrounds	0.80 ± 0.13	0.25 ± 0.05	0.19 ± 0.10	0.34 ± 0.04
FNP leptons	2.2 ± 0.6	0.71 ± 0.16	0.87 ± 0.29	0.59 ± 0.16
$S_{\mathrm{obs}}^{0.95}$	25.1	10.2	16.8	12.3
$S_{\mathrm{exp}}^{0.95}$	$25.3^{+10.3}_{-7.2}$	$10.3^{+4.6}_{-3.0}$	$17.6^{+7.3}_{-5.1}$	$11.9^{+5.2}_{-3.3}$
$\sigma_{\mathrm{obs}}^{0.95}$ (fb)	0.18	0.07	0.12	0.09
p_0	0.50	0.50	0.50	0.45

shows the m_{T2} distribution for the data and the estimated SM backgrounds for events in the SRs.

No significant deviations from the SM expectations are observed in any of the SRs considered, as shown in Figs. 5 and 6. The $\mathrm{CL_s}$ prescription [107] is used to set model-independent upper limits at 95% confidence level (CL) on the visible signal cross-section $\sigma_{\mathrm{obs}}^{0.95}$, defined as the cross-section times acceptance times efficiency, of processes beyond the SM. They are derived in each inclusive SR by performing a fit that includes the observed yield in the SR as a constraint, and a signal yield in the SR as a free parameter of interest.

The observed ($S_{\mathrm{obs}}^{0.95}$) and expected ($S_{\mathrm{exp}}^{0.95}$) limits at 95% CL on the numbers of events from processes beyond the SM in the inclusive SRs defined in Sect. 6 are calculated. The p_0-values, which represent the probability of the SM background alone to fluctuate to the observed number of events or higher, are also provided and are capped at $p_0 = 0.50$. These results are presented in Tables 8 and 9 for the DF and SF inclusive SRs, respectively.

Exclusion limits at 95% CL are set on the masses of the chargino, neutralino and sleptons for the simplified models shown in Fig. 1. These also use the $\mathrm{CL_s}$ prescription and

Table 9 Observed event yields and predicted background yields from the fit for the SF inclusive SRs. The model-independent upper limits at 95% CL on the observed and expected numbers of beyond-the-SM events $S^{0.95}_{\mathrm{obs/exp}}$ and on the effective beyond-the-SM cross-section $\sigma^{0.95}_{\mathrm{obs}}$ are also shown. The $\pm 1\sigma$ variations on $S^{0.95}_{\mathrm{exp}}$ are also provided. The last row shows the p_0-value of the SM-only hypothesis. For SRs where the data yield is smaller than expected, the p_0-value is capped at 0.50. 'Other backgrounds' include the non-dominant background sources, i.e. $t\bar{t} + V$, Higgs boson and Drell–Yan events. A '–' symbol indicates that the background contribution is negligible

Region m_{T2} (GeV)	SR-SF-0J $\in[100,\infty)$	SR-SF-0J $\in[160,\infty)$	SR-SF-0J $\in[100,120)$	SR-SF-0J $\in[120,160)$
Observed events	147	37	53	57
Fitted backgrounds	144 ± 12	37.3 ± 3.0	56 ± 6	51 ± 5
Fitted WW	73 ± 8	18.1 ± 2.1	27.6 ± 3.0	27 ± 4
Fitted WZ	10.8 ± 0.8	3.08 ± 0.27	3.55 ± 0.29	4.2 ± 0.5
Fitted ZZ	38.6 ± 2.6	13.8 ± 1.0	11.1 ± 0.8	13.7 ± 1.5
Fitted $t\bar{t}$	13 ± 4	–	11 ± 4	1.9 ± 0.7
Fitted single top	2.4 ± 1.4	–	2.2 ± 1.3	0.15 ± 0.09
Other backgrounds	2.1 ± 1.5	$0.10^{+0.33}_{-0.10}$	$0.2^{+1.4}_{-0.2}$	1.76 ± 0.30
FNP leptons	5.4 ± 1.4	2.2 ± 0.4	1.1 ± 0.6	2.0 ± 0.5
$S^{0.95}_{\mathrm{obs}}$	35.5	14.3	17.8	23.5
$S^{0.95}_{\mathrm{exp}}$	$33.6^{+13.6}_{-9.3}$	$14.5^{+6.3}_{-4.2}$	$20.0^{+8.1}_{-5.6}$	$18.7^{+7.8}_{-5.3}$
$\sigma^{0.95}_{\mathrm{obs}}$ (fb)	0.25	0.10	0.13	0.17
p_0	0.44	0.50	0.50	0.25
Region m_{T2} (GeV)	SR-SF-1J $\in[100,\infty)$	SR-SF-1J $\in[160,\infty)$	SR-SF-1J $\in[100,120)$	SR-SF-1J $\in[120,160)$
Observed events	120	29	55	36
Fitted backgrounds	124 ± 12	36 ± 5	48 ± 8	40 ± 4
Fitted WW	48 ± 6	14.1 ± 2.1	18.1 ± 2.4	16.0 ± 2.2
Fitted WZ	13.4 ± 1.1	5.2 ± 0.6	3.62 ± 0.33	4.7 ± 0.5
Fitted ZZ	22.2 ± 1.8	9.1 ± 1.1	4.8 ± 0.5	8.2 ± 0.9
Fitted $t\bar{t}$	16 ± 8	$0.07^{+0.10}_{-0.07}$	14 ± 7	1.6 ± 0.8
Fitted single top	3.3 ± 1.7	–	2.6 ± 1.4	0.7 ± 0.4
Other backgrounds	11.1 ± 4.0	5.6 ± 2.1	$1.7^{+2.4}_{-1.7}$	3.8 ± 1.3
FNP leptons	10.3 ± 1.5	1.80 ± 0.34	3.1 ± 0.6	5.3 ± 0.7
$S^{0.95}_{\mathrm{obs}}$	30.6	11.2	27.3	12.6
$S^{0.95}_{\mathrm{exp}}$	$33.5^{+13.3}_{-9.3}$	$15.3^{+6.5}_{-4.5}$	$21.9^{+9.0}_{-6.2}$	$15.5^{+6.5}_{-4.2}$
$\sigma^{0.95}_{\mathrm{obs}}$ (fb)	0.22	0.08	0.19	0.09
p_0	0.50	0.50	0.26	0.50

include the exclusive SRs and the CRs in the simultaneous likelihood fit. For the models of chargino pair production the SF and DF SRs are included in the likelihood fit, whilst for direct slepton production only the SF SRs are included. The results are shown in Fig. 7. In the model of direct chargino pair production with decays via W bosons with a massless $\tilde{\chi}^0_1$, $\tilde{\chi}^\pm_1$ masses up to 420 GeV are excluded at 95% CL. In the model of direct chargino pair production with decays via sleptons or sneutrinos with a massless $\tilde{\chi}^0_1$, $\tilde{\chi}^\pm_1$ masses up to 1 TeV are excluded at 95% CL. Finally, in the model of direct slepton pair production with a massless $\tilde{\chi}^0_1$, slepton masses up to 700 GeV are excluded at 95% CL. For direct slepton production, exclusion limits are also set for selectrons and smuons separately by including only the di-electron and di-muon SF SRs in the likelihood fit respectively. These are shown in Fig. 8 for single slepton species $\tilde{e}_{\mathrm{R}}$, $\tilde{\mu}_{\mathrm{R}}$, $\tilde{e}_{\mathrm{L}}$, $\tilde{\mu}_{\mathrm{L}}$ along with combined limits for mass-degenerate $\tilde{e}_{\mathrm{L,R}}$ and $\tilde{\mu}_{\mathrm{L,R}}$. The observed limit for $\tilde{\ell}_{\mathrm{L}}$ is shown on the exclusion plot for chargino pair production with slepton-mediated decays in Fig. 7 for comparison. However since the sensitivity does not depend strongly on the slepton mass hypothesis for a broad range of slepton masses [24], these results are applicable for many models not excluded by the direct slepton limits. These
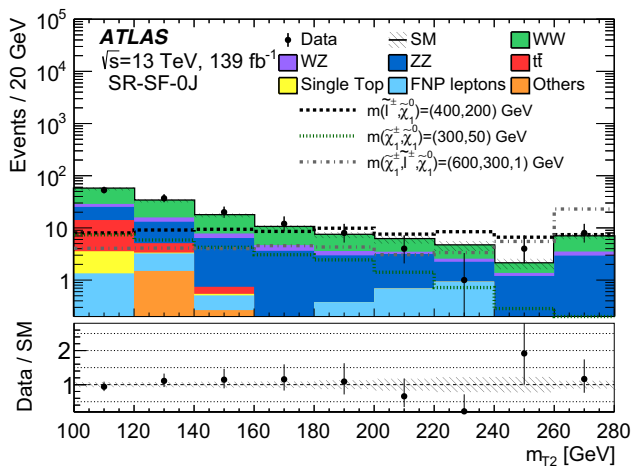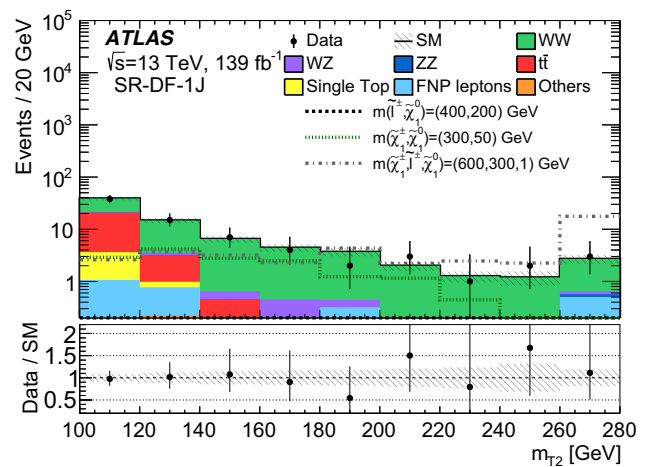
(a) m_{T2} distribution in SR-SF-0J
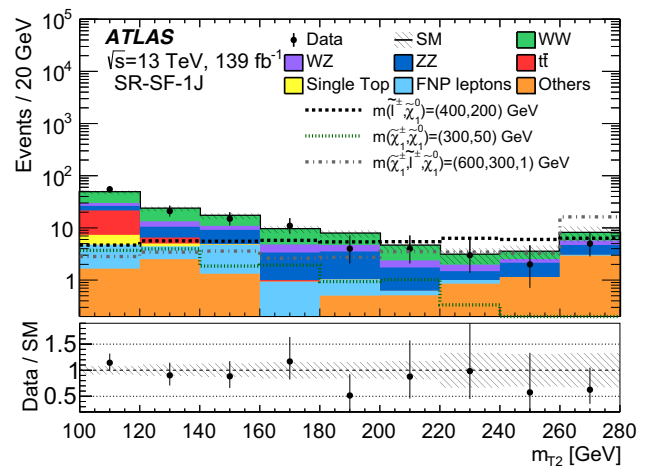
(b) m_{T2} distribution in SR-SF-1J
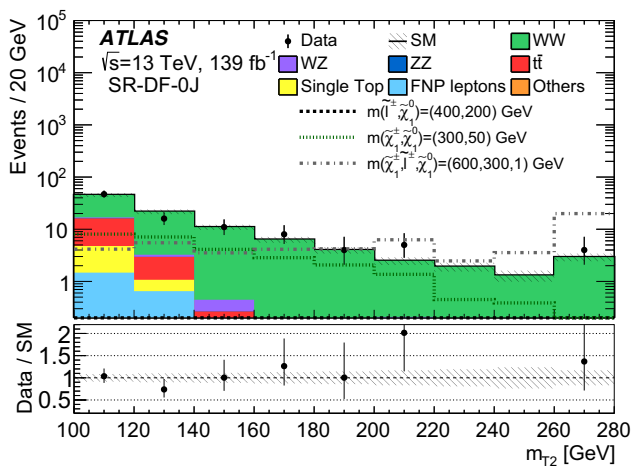
(c) m_{T2} distribution in SR-DF-0J

(d) m_{T2} distribution in SR-DF-1J

Fig. 6 Distributions of m_{T2} in **a** SR-SF-0J, **b** SR-SF-1J, **c** SR-DF-0J and **d** SR-DF-1J, for data and the estimated SM backgrounds. The normalisation factors extracted from the corresponding CRs are used to rescale the $t\bar{t}$, single-top-quark, WW, WZ and ZZ backgrounds. The FNP lepton background is calculated using the data-driven matrix method. Negligible background contributions are not included in the legends. The uncertainty band includes systematic and statistical errors from all sources and the last bin includes the overflow. Distributions for three benchmark signal points are overlaid for comparison. The lower panels show the ratio of data to the SM background estimate

results significantly extend the previous exclusion limits [24–29,31] for the same scenarios.

10 Conclusion

A search for the electroweak production of charginos and sleptons decaying into final states with exactly two oppositely charged leptons and missing transverse momentum is presented. The analysis uses 139 fb^{-1} of $\sqrt{s} = 13$ TeV proton–proton collisions recorded by the ATLAS detector at the LHC between 2015 and 2018. Three scenarios are considered: the production of lightest-chargino pairs, followed by their decays into final states with leptons and the light-

est neutralino via either W bosons or sleptons/sneutrinos, and direct production of slepton pairs, where each slepton decays directly into the lightest neutralino and a lepton and different assumptions about the masses of the superpartners of the left-handed and right-handed charged leptons, $\tilde{e}_L$, $\tilde{e}_R$, $\tilde{\mu}_L$ and $\tilde{\mu}_R$, are considered. No significant deviations from the Standard Model expectations are observed and limits at 95% CL are set on the masses of relevant supersymmetric particles in each of these scenarios. For a massless lightest neutralino, masses up to 420 GeV are excluded for the production of the lightest-chargino pairs assuming W-boson-mediated decays and up to 1 TeV for slepton-pair-mediated decays, whereas for slepton-pair production masses up to 700 GeV are excluded assuming three generations of mass-
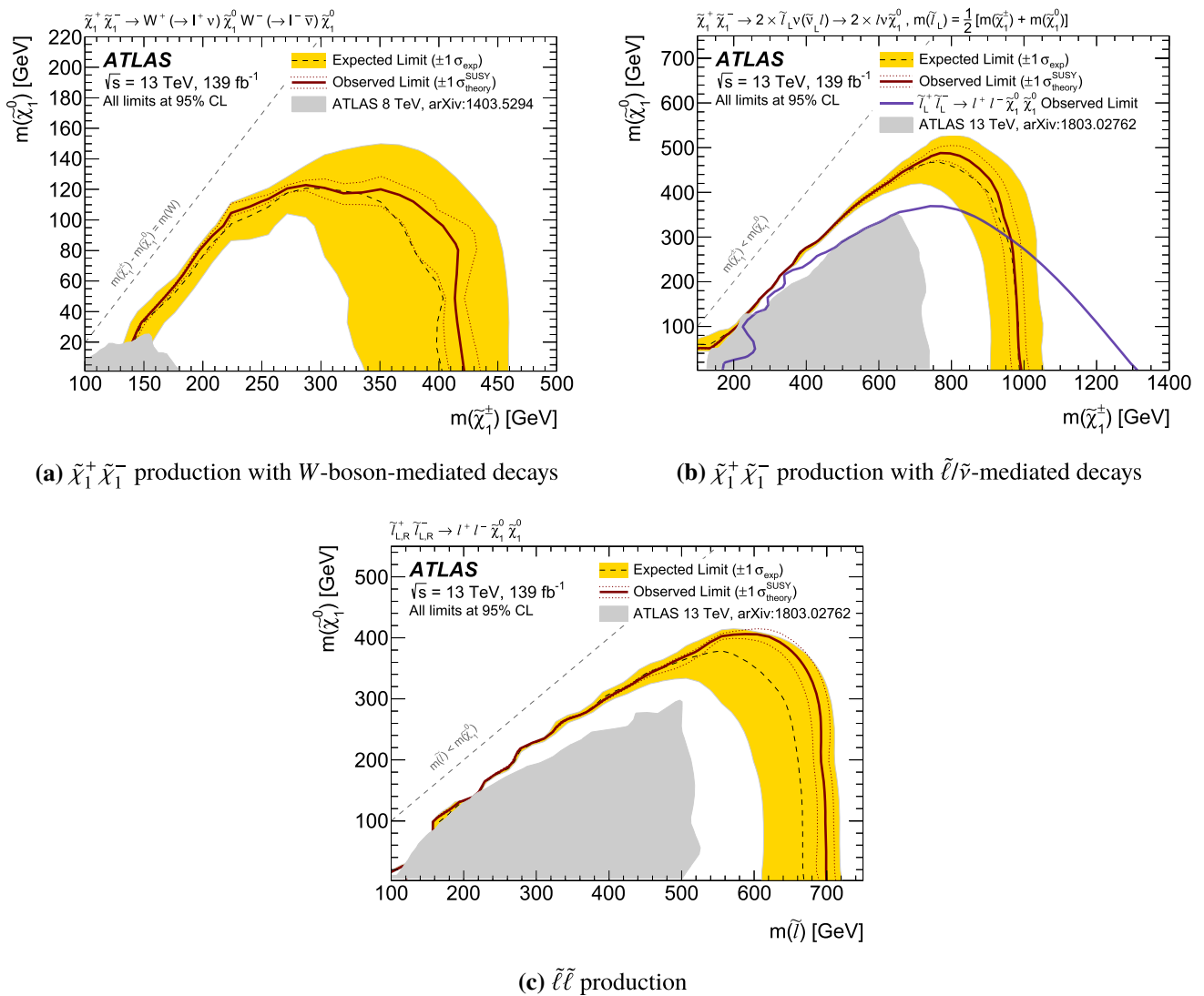
(a) $\tilde{\chi}_1^+ \tilde{\chi}_1^-$ production with W-boson-mediated decays

(b) $\tilde{\chi}_1^+ \tilde{\chi}_1^-$ production with $\tilde{\ell}/\tilde{\nu}$-mediated decays

(c) $\tilde{\ell}\tilde{\ell}$ production

Fig. 7 Observed and expected exclusion limits on SUSY simplified models for chargino-pair production with **a** W-boson-mediated decays and **b** slepton/sneutrino-mediated decays, and **c** for slepton-pair production. In **b** all three slepton flavours ($\tilde{e}$, $\tilde{\mu}$, $\tilde{\tau}$) are considered, while only $\tilde{e}$ and $\tilde{\mu}$ are considered in **c**. The observed (solid thick line) and expected (thin dashed line) exclusion contours are indicated. The upper shaded band corresponds to the $\pm 1\sigma$ variations in the expected limit, including all uncertainties except theoretical uncertainties in the signal cross-section. The dotted lines around the observed limit illustrate the change in the observed limit as the nominal signal cross-section is scaled up and down by the theoretical uncertainty. The blue line in **b** corresponds to the observed limit for $\tilde{\ell}_L$ projected into this model for the chosen slepton mass hypothesis (slepton masses midway between the mass of the chargino and that of the $\tilde{\chi}_1^0$). All limits are computed at 95% CL. The observed limits obtained by ATLAS in previous searches are also shown (lower shaded areas) [24,25]

degenerate sleptons. These results significantly extend the previous exclusion limits for the same scenarios.

(a) $\tilde{e}\tilde{e}$ production   **(b)** $\tilde{\mu}\tilde{\mu}$
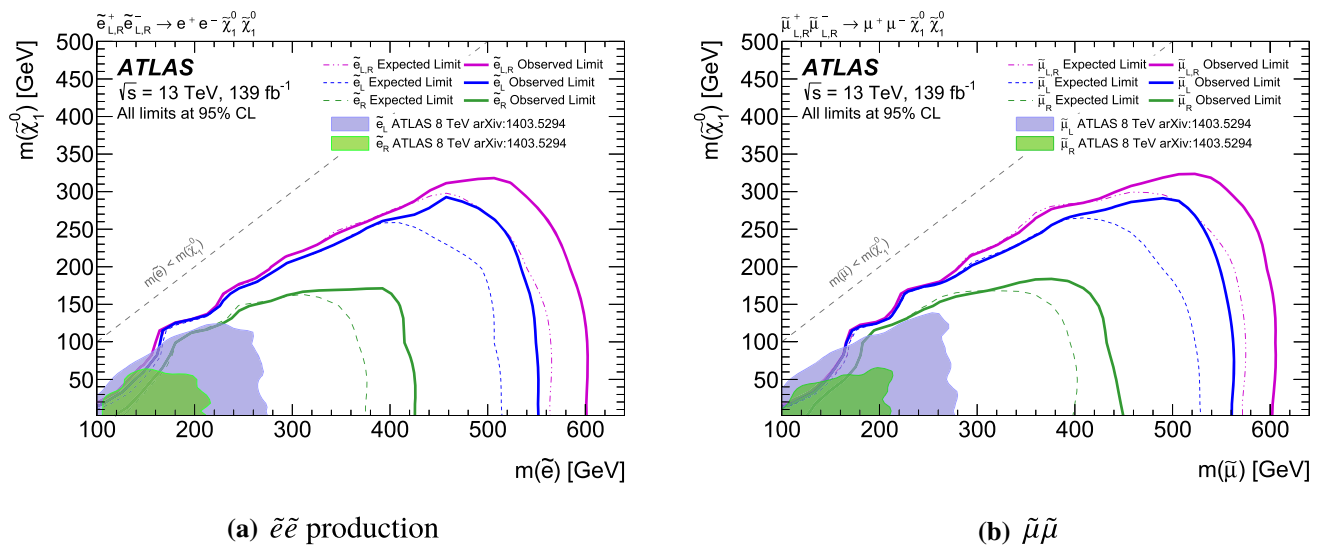
Fig. 8 Observed and expected exclusion limits on SUSY simplified models for **a** direct selectron production and **b** direct smuon production. In **a** the observed (solid thick lines) and expected (dashed lines) exclusion contours are indicated for combined $\tilde{e}_{L,R}$ and for $\tilde{e}_L$ and $\tilde{e}_R$. In **b** the observed (solid thick lines) and expected (dashed lines) exclusion contours are indicated for combined $\tilde{\mu}_{L,R}$ and for $\tilde{\mu}_L$ and $\tilde{\mu}_R$. All limits are computed at 95% CL. The observed limits obtained by ATLAS in previous searches are also shown in the shaded areas [25]

Data Availability Statement This manuscript has no associated data or the data will not be deposited. [Authors' comment: All ATLAS scientific output is published in journals, and preliminary results are made available in Conference Notes. All are openly available, without restriction on use by external parties beyond copyright law and the standard conditions agreed by CERN. Data associated with journal publications are also made available: tables and data from plots (e.g. cross section values, likelihood profiles, selection efficiencies, cross section limits, ...) are stored in appropriate repositories such as HEPDATA (http://hepdata.cedar.ac.uk/). ATLAS also strives to make additional material related to the paper available that allows a reinterpretation of the data in the context of new theoretical models. For example, an extended encapsulation of the analysis is often provided for measurements in the framework of RIVET (http://rivet.hepforge.org/). This information is taken from the ATLAS Data Access Policy, which is a public document that can be downloaded from http://opendata.cern.ch/record/413 [opendata.cern.ch].]

References

1. Y.A. Golfand, E.P. Likhtman, Extension of the algebra of Poincare group generators and violation of P invariance. JETP Lett. **13**, 323 (1971)
2. Y.A. Golfand, E.P. Likhtman, Extension of the algebra of Poincare group generators and violation of P invariance. Pisma Zh. Eksp. Teor. Fiz. **13**, 452 (1971)
3. D.V. Volkov, V.P. Akulov, Is the neutrino a goldstone particle? Phys. Lett. B **46**, 109 (1973)
4. J. Wess, B. Zumino, Supergauge transformations in four dimensions. Nucl. Phys. B **70**, 39 (1974)
5. J. Wess, B. Zumino, Supergauge invariant extension of quantum electrodynamics. Nucl. Phys. B **78**, 1 (1974)
6. S. Ferrara, B. Zumino, Supergauge invariant Yang–Mills theories. Nucl. Phys. B **79**, 413 (1974)
7. A. Salam, J.A. Strathdee, Super-symmetry and non-Abelian gauges. Phys. Lett. B **51**, 353 (1974)
8. N. Sakai, Naturalness in supersymmetric GUTS. Z. Phys. C **11**, 153 (1981)
9. S. Dimopoulos, S. Raby, F. Wilczek, Supersymmetry and the scale of unification. Phys. Rev. D **24**, 1681 (1981)
10. L.E. Ibanez, G.G. Ross, Low-energy predictions in supersymmetric grand unified theories. Phys. Lett. B **105**, 439 (1981)
11. S. Dimopoulos, H. Georgi, Softly broken supersymmetry and SU(5). Nucl. Phys. B **193**, 150 (1981)

12. G.R. Farrar, P. Fayet, Phenomenology of the production, decay, and detection of new hadronic states associated with supersymmetry. Phys. Lett. B **76**, 575 (1978)

13. H. Goldberg, Constraint on the photino mass from cosmology. Phys. Rev. Lett. **50**, 1419 (1983) [Erratum: Phys. Rev. Lett. **103**, 099905 (2009)]

14. J.R. Ellis, J.S. Hagelin, D.V. Nanopoulos, K.A. Olive, M. Srednicki, Supersymmetric relics from the big bang. Nucl. Phys. B **238**, 453 (1984)

15. ATLAS Collaboration, Search for squarks and gluinos in final states with jets and missing transverse momentum using 36 fb^{-1} of $\sqrt{s} = 13\,TeV$ pp collision data with the ATLAS detector. Phys. Rev. D **97**, 112001 (2018). arXiv:1712.02332 [hep-ph]

16. ATLAS Collaboration, Search for supersymmetry in final states with missing transverse momentum and multiple b-jets in proton–proton collisions at $\sqrt{s} = 13\,TeV$ with the ATLAS detector. JHEP **06**, 107 (2018). arXiv:1711.01901 [hep-ex]

17. ATLAS Collaboration, Search for new phenomena with large jet multiplicities and missing transverse momentum using large-radius jets and flavour-tagging at ATLAS in 13 TeV pp collisions. JHEP **12**, 034 (2017). arXiv:1708.02794 [hep-ex]

18. ATLAS Collaboration, Search for supersymmetry in final states with two same-sign or three leptons and jets using 36 fb^{-1} of $\sqrt{s} = 13\,TeV$ pp collision data with the ATLAS detector. JHEP **09**, 084 (2017). arXiv:1706.03731 [hep-ex]

19. CMS Collaboration, Search for supersymmetry in multijet events with missing transverse momentum in proton–proton collisions at 13 TeV. Phys. Rev. D **96**, 032003 (2017). arXiv:1704.07781 [hep-ex]

20. CMS Collaboration, Search for new phenomena with the M_{T2} variable in the all-hadronic final state produced in proton–proton collisions at $\sqrt{s} = 13\,TeV$. Eur. Phys. J. C **77**, 710 (2017). arXiv:1705.04650 [hep-ex]

21. CMS Collaboration, Search for supersymmetry in proton–proton collisions at 13 TeV using identified top quarks. Phys. Rev. D **97**, 012007 (2018). arXiv:1710.11188 [hep-ex]

22. CMS Collaboration, Search for natural and split supersymmetry in proton–proton collisions at $\sqrt{s} = 13\,TeV$ in final states with jets and missing transverse momentum. JHEP **05**, 025 (2018). arXiv:1802.02110 [hep-ex]

23. CMS Collaboration, Search for physics beyond the standard model in events with high-momentum Higgs bosons and missing transverse momentum in proton–proton collisions at 13 TeV. Phys. Rev. Lett. **120**, 241801 (2018). arXiv:1712.08501 [hep-ex]

24. ATLAS Collaboration, Search for direct production of charginos, neutralinos and sleptons in final states with two leptons and missing transverse momentum in pp collisions at $\sqrt{s} = 13\,TeV$ with the ATLAS detector. JHEP **05**, 071 (2014). arXiv:1403.5294 [hep-ex]

25. ATLAS Collaboration, Search for electroweak production of supersymmetric particles in final states with two or three leptons at $\sqrt{s} = 13\,TeV$ with the ATLAS detector. Eur. Phys. J. C **78**, 995 (2018). arXiv:1803.02762 [hep-ex]

26. CMS Collaboration, Searches for electroweak production of charginos, neutralinos, and sleptons decaying to leptons and W, Z, and Higgs bosons in pp collisions at 8 TeV. Eur. Phys. J. C **74**, 3036 (2014). arXiv:1405.7570 [hep-ex]

27. CMS Collaboration, Searches for electroweak neutralino and chargino production in channels with Higgs, Z, and W bosons in pp collisions at 8 TeV. Phys. Rev. D **90**, 092007 (2014). arXiv:1409.3168 [hep-ex]

28. CMS Collaboration, Search for electroweak production of charginos and neutralinos in multilepton final states in proton–proton collisions at $\sqrt{s} = 13\,TeV$. JHEP **03**, 166 (2018). arXiv:1709.05406 [hep-ex]

29. CMS Collaboration, Combined search for electroweak production of charginos and neutralinos in proton–proton collisions at $\sqrt{s} = 13$ TeV. JHEP **03**, 160 (2018). arXiv:1801.03957 [hep-ex]

30. CMS Collaboration, Search for supersymmetric partners of electrons and muons in proton–proton collisions at $\sqrt{s} = 13$ TeV. Phys. Lett. B **790**, 140 (2019). arXiv:1806.05264 [hep-ex]

31. CMS Collaboration, Searches for pair production of charginos and top squarks in final states with two oppositely charged leptons in proton-proton collisions at $\sqrt{s} = 13$ TeV. JHEP **11**, 079 (2018). arXiv:1807.07799 [hep-ex]

32. J. Alwall, P. Schuster, N. Toro, Simplified models for a first characterization of new physics at the LHC. Phys. Rev. D **79**, 075020 (2009). arXiv:0810.3921 [hep-ph]

33. ATLAS Collaboration, The ATLAS experiment at the CERN large hadron collider. JINST **3**, S08003 (2008)

34. ATLAS Collaboration, ATLAS insertable B-Layer Technical Design Report, ATLAS-TDR-19, 2010, https://cds.cern.ch/record/1291633, *ATLAS Insertable B-Layer Technical Design Report Addendum*, ATLAS-TDR-19-ADD-1, https://cds.cern.ch/record/1451888 (2012)

35. B. Abbott et al., Production and integration of the ATLAS insertable B-layer. JINST **13**, T05008 (2018). arXiv:1803.00844 [physics.ins-det]

36. ATLAS Collaboration, Performance of the ATLAS trigger system in 2015. Eur. Phys. J. C **77**, 317 (2017). arXiv:1611.09661 [hep-ex]

37. ATLAS Collaboration, Luminosity Determination in pp Collisions at $\sqrt{s} = 13$ TeV using the ATLAS detector at the LHC, ATLAS-CONF-2019-021 (2019). https://cds.cern.ch/record/2677054

38. G. Avoni et al., The new LUCID-2 detector for luminosity measurement and monitoring in ATLAS. JINST **13**, P07017 (2018)

39. ATLAS Collaboration, The ATLAS simulation infrastructure. Eur. Phys. J. C **70**, 823 (2010). arXiv:1005.4568 [physics.ins-det]

40. S. Agostinelli et al., GEANT4—a simulation toolkit. Nucl. Instrum. Methods A **506**, 250 (2003)

41. ATLAS Collaboration, Electron and photon performance measurements with the ATLAS detector using the 2015–2017 LHC proton–proton collision data. JINST. **14**, P12006 (2019). https://doi.org/10.1088/1748-0221/14/12/P12006

42. ATLAS Collaboration, Muon reconstruction performance of the ATLAS detector in proton–proton collision data at $\sqrt{s} = 13$ TeV. Eur. Phys. J. C **76**, 292 (2016). arXiv:1603.05598 [hep-ex]

43. ATLAS Collaboration, ATLAS b-jet identification performance and efficiency measurement with $t\bar{t}$ events in pp collisions at $\sqrt{s} = 13$ TeV. Eur. Phys. J. C **79**, 970 (2019). https://doi.org/10.1140/epjc/s10052-019-7450-8

44. ATLAS Collaboration, Improvements in $t\bar{t}$ modelling using NLO+PS Monte Carlo generators for Run 2, ATL-PHYS-PUB-2018-009 (2018). https://cds.cern.ch/record/2630327

45. ATLAS Collaboration, Simulation of top-quark production for the ATLAS experiment at $\sqrt{s} = 13$ TeV, ATL-PHYS-PUB-2016-004 (2016). https://cds.cern.ch/record/2120417

46. ATLAS Collaboration, Multi-boson simulation for 13 TeV ATLAS analyses, ATL-PHYS-PUB2017-005 (2017). https://cds.cern.ch/record/2261933

47. ATLAS Collaboration, ATLAS simulation of boson plus jets processes in Run 2, ATL-PHYS-PUB-2017-006 (2017). https://cds.cern.ch/record/2261937

48. J. Alwall et al., The automated computation of tree-level and next-to-leading order differential cross sections, and their matching to parton shower simulations. JHEP **07**, 079 (2014). arXiv:1405.0301 [hep-ph]

49. T. Sjöstrand, S. Mrenna, P.Z. Skands, A brief introduction to PYTHIA 8.1. Comput. Phys. Commun. **178**, 852 (2008). arXiv:0710.3820 [hep-ph]

50. ATLAS Collaboration, ATLAS Pythia 8 tunes to 7 TeV data, ATL-PHYS-PUB-2014-021 (2014). https://cds.cern.ch/record/1966419

51. R.D. Ball et al., Parton distributions with LHC data. Nucl. Phys. B **867**, 244 (2013). arXiv:1207.1303 [hep-ph]

52. L. Lönnblad, S. Prestel, Merging multi-leg NLO matrix elements with parton showers. JHEP **03**, 166 (2013). arXiv:1211.7278 [hep-ph]

53. J. Debove, B. Fuks, M. Klasen, Threshold resummation for gaugino pair production at hadron colliders. Nucl. Phys. B **842**, 51 (2011). arXiv:1005.2909 [hep-ph]

54. B. Fuks, M. Klasen, D.R. Lamprea, M. Rothering, Gaugino production in proton–proton collisions at a center-of-mass energy of 8 TeV. JHEP **10**, 081 (2012). arXiv:1207.2159 [hep-ph]

55. B. Fuks, M. Klasen, D.R. Lamprea, M. Rothering, Precision predictions for electroweak superpartner production at hadron colliders with RESUMMINO. Eur. Phys. J. C **73**, 2480 (2013). arXiv:1304.0790 [hep-ph]

56. J. Fiaschi, M. Klasen, Neutralino-chargino pair production at NLO+NLL with resummation-improved parton density functions for LHC Run II. Phys. Rev. D **98**, 055014 (2018). arXiv:1805.11322 [hep-ph]

57. G. Bozzi, B. Fuks, M. Klasen, Threshold resummation for slepton-pair production at hadron colliders. Nucl. Phys. B **777**, 157 (2007). arXiv:hep-ph/0701202 [hep-ph]

58. B. Fuks, M. Klasen, D.R. Lamprea, M. Rothering, Revisiting slepton pair production at the Large Hadron Collider. JHEP **01**, 168 (2014). arXiv:1310.2621 [hep-ph]

59. J. Fiaschi, M. Klasen, Slepton pair production at the LHC in NLO+NLL with resummation-improved parton densities. JHEP **03**, 094 (2018). arXiv:1801.10357 [hep-ph]

60. C. Borschensky et al., Squark and gluino production cross sections in pp collisions at $\sqrt{s} = 13, 14, 33$ and 100 TeV. Eur. Phys. J. C **74**, 3174 (2014). arXiv:1407.5066 [hep-ph]

61. D.J. Lange, The EvtGen particle decay simulation package. Nucl. Instrum. Methods A **462**, 152 (2001)

62. ATLAS Collaboration, The Pythia 8 A3 tune description of ATLAS minimum bias and inelastic measurements incorporating the Donnachie–Landshoff diffractive model, ATL-PHYS-PUB-2016-017 (2016). https://cds.cern.ch/record/2206965

63. S. Frixione, P. Nason, G. Ridolfi, A positive-weight next-to-leading-order Monte Carlo for heavy flavour hadroproduction. JHEP **09**, 126 (2007). arXiv:0707.3088 [hep-ph]

64. S. Frixione, P. Nason, C. Oleari, Matching NLO QCD computations with Parton Shower simulations: the POWHEG method. JHEP **11**, 070 (2007). arXiv:0709.2092 [hep-ph]

65. S. Alioli, P. Nason, C. Oleari, E. Re, A general framework for implementing NLO calculations in shower Monte Carlo programs: the POWHEG BOX. JHEP **06**, 043 (2010). arXiv:1002.2581 [hep-ph]

66. J.M. Campbell, R.K. Ellis, P. Nason, E. Re, Top-pair production and decay at NLO matched with parton showers. JHEP **04**, 114 (2015). arXiv:1412.1828 [hep-ph]

67. T. Sjöstrand et al., An introduction to PYTHIA 8.2. Comput. Phys. Commun. **191**, 159 (2015). arXiv:1410.3012 [hep-ph]

68. M. Czakon, A. Mitov, Top++: a program for the calculation of the top-pair cross-section at hadron colliders. Comput. Phys. Commun. **185**, 2930 (2014). arXiv:1112.5675 [hep-ph]

69. R.D. Ball et al., Parton distributions for the LHC run II. JHEP **04**, 040 (2015). arXiv:1410.8849 [hep-ph]

70. ATLAS Collaboration, Modelling of the $t\bar{t}H$ and $t\bar{t}V$ ($V = W, Z$) processes for $\sqrt{s} = 13\,TeV$ ATLAS analyses, ATL-PHYS-PUB-2016-005 (2016). https://cds.cern.ch/record/2120826

71. E. Re, Single-top Wt-channel production matched with parton showers using the POWHEG method. Eur. Phys. J. C **71**, 1547 (2011). arXiv:1009.2450 [hep-ph]

72. M. Aliev et al., HATHOR -HAdronic Top and Heavy quarks crOss section calculatoR. Comput. Phys. Commun. **182**, 1034 (2011). arXiv:1007.1327 [hep-ph]

73. P. Kant et al., HATHOR for single top-quark production: updated predictions and uncertainty estimates for single top-quark production in hadronic collisions. Comput. Phys. Commun. **191**, 74 (2015). arXiv:1406.4403 [hep-ph]

74. T. Gleisberg et al., Event generation with SHERPA 1.1. JHEP **02**, 007 (2009). arXiv:0811.4622 [hep-ph]

75. E. Bothmann et al., Event Generation with Sherpa 2.2 Sci. Post Phys. **7**, 034 (2019). https://doi.org/10.21468/SciPostPhys.7.3.034

76. ATLAS Collaboration, *Monte Carlo generators for the production of a W or Z/γ^* boson in association with jets at ATLAS in Run 2*, ATL-PHYS-PUB-2016-003 (2016). https://cds.cern.ch/record/2120133

77. R. Gavin, Y. Li, F. Petriello, S. Quackenbush, FEWZ 2.0: a code for hadronic Z production at next-to-next-to-leading order. Comput. Phys. Commun **182**, 2388 (2011). arXiv:1011.3540 [hep-ph]

78. T. Melia, P. Nason, R. Rontsch, G. Zanderighi, W^+W^-, WZ and ZZ production in the POWHEG BOX. JHEP **11**, 078 (2011). arXiv:1107.5051 [hep-ph]

79. P. Nason, G. Zanderighi, W^+W^-, WZ and ZZ production in the POWHEG-BOX-V2. Eur. Phys. J. C **74**, 2702 (2014). arXiv:1311.1365 [hep-ph]

80. ATLAS Collaboration, Measurement of the Z/γ^* boson transverse momentum distribution in pp collisions at $\sqrt{s} = 7$ TeV with the ATLAS detector. JHEP **09**, 145 (2014). arXiv:1406.3660 [hep-ex]

81. H.-L. Lai et al., New parton distributions for collider physics. Phys. Rev. D **82**, 074024 (2010). arXiv:1007.2241 [hep-ph]

82. J. Pumplin et al., New generation of parton distributions with uncertainties from global QCD analysis. JHEP **07**, 012 (2002). arXiv:hep-ph/0201195 [hep-ph]

83. S. Alioli, P. Nason, C. Oleari, E. Re, NLO Higgs boson production via gluon fusion matched with shower in POWHEG. JHEP **04**, 002 (2009). arXiv:0812.0578 [hep-ph]

84. P. Nason, C. Oleari, NLO Higgs boson production via vector-boson fusion matched with shower in POWHEG. JHEP **1002**, 037 (2010). arXiv: 0911.5299 [hep-ph]

85. K. Hamilton, P. Nason, E. Re, G. Zanderighi, NNLOPS simulation of Higgs boson production. JHEP **1310**, 222 (2013). arXiv:1309.0017 [hep-ph]

86. K. Hamilton, P. Nason, G. Zanderighi, Finite quark-mass effects in the NNLOPS POWHEG+MiNLO Higgs generator. JHEP **1505**, 140 (2015). arXiv:1501.04637 [hep-ph]

87. D. de Florian et al., Handbook of LHC Higgs cross sections: 4. Deciphering the nature of the Higgs sector, CERN-2017-002-M (2017). arXiv:1610.07922 [hep-ph]

88. ATLAS Collaboration, Topological cell clustering in the ATLAS calorimeters and its performance in LHC Run 1. Eur. Phys. J. C **77**, 490 (2017). arXiv:1603.02934 [hep-ex]

89. M. Cacciari, G.P. Salam, G. Soyez, The anti-k_t jet clustering algorithm. JHEP **04**, 063 (2008). arXiv:0802.1189 [hep-ph]

90. M. Cacciari, G.P. Salam, G. Soyez, FastJet user manual. Eur. Phys. J. C **72**, 1896 (2012). arXiv:1111.6097 [hep-ph]

91. ATLAS Collaboration, Jet energy scale measurements and their systematic uncertainties in proton–proton collisions at $\sqrt{s} = 13$ TeV with the ATLAS detector. Phys. Rev. D **96**, 072002 (2017). arXiv:1703.09665 [hep-ex]

92. ATLAS Collaboration, Tagging and suppression of pileup jets with the ATLAS detector, ATLAS-CONF-2014-018 (2014). https://cds.cern.ch/record/1700870

93. ATLAS Collaboration, Forward Jet Vertex Tagging: a new technique for the identification and rejection of forward pileup jets, ATL-PHYS-PUB-2015-034 (2015). https://cds.cern.ch/record/2042098

94. ATLAS Collaboration, Selection of jets produced in 13 TeV proton–proton collisions with the ATLAS detector, ATLAS-CONF-2015-029 (2015). https://cds.cern.ch/record/2037702

95. ATLAS Collaboration, Performance of pile-up mitigation techniques for jets in pp collisions at $\sqrt{s} = 8$ TeV using the ATLAS detector. Eur. Phys. J. C **76**, 581 (2016). arXiv:1510.03823 [hep-ex]

96. ATLAS Collaboration, Performance of missing transverse momentum reconstruction with the ATLAS detector using proton–proton collisions at $\sqrt{s} = 13$ TeV. Eur. Phys. J. C **78**, 903 (2018). arXiv:1802.08168 [hep-ex]

97. ATLAS Collaboration, Object-based missing transverse momentum significance in the ATLAS Detector, ATLAS-CONF-2018-038 (2018). https://cds.cern.ch/record/2630948

98. C.G. Lester, D.J. Summers, Measuring masses of semi-invisibly decaying particles pair produced at hadron colliders. Phys. Lett. B **463**, 99 (1999). arXiv:hep-ph/9906349

99. A. Barr, C.G. Lester, P. Stephens, A variable for measuring masses at hadron colliders when missing energy is expected; m_{T2}: the truth behind the glamour. J. Phys. G **29**, 2343 (2003). arXiv:hep-ph/0304226

100. ATLAS Collaboration, Measurement of the top quark-pair production cross section with ATLAS in pp collisions at $\sqrt{s} = 7$ TeV. Eur. Phys. J. C **71**, 1577 (2011). arXiv:1012.1792 [hep-ex]

101. M. Bähr et al., Herwig++ physics and manual. Eur. Phys. J. C **58**, 639 (2008). arXiv:0803.0883 [hep-ph]

102. J. Bellm et al., Herwig 7.0/Herwig++ 3.0 release note. Eur. Phys. J. C **76**, 196 (2016). arXiv:1512.01178 [hep-ph]

103. ATLAS Collaboration, Studies on top-quark Monte Carlo modelling for Top2016, ATL-PHYS-PUB-2016-020 (2016). https://cds.cern.ch/record/2216168

104. ATLAS Collaboration, Studies on top-quark Monte Carlo modelling with Sherpa and MG5_aMC@NLO, ATL-PHYS-PUB-2017-007 (2017). https://cds.cern.ch/record/2261938

105. M. Baak et al., HistFitter software framework for statistical data analysis. Eur. Phys. J. C **75**, 153 (2015). arXiv:1410.1280 [hep-ex]

106. R.D. Cousins, J.T. Linnemann, J. Tucker, Evaluation of three methods for calculating statistical significance when incorporating a systematic uncertainty into a test of the background-only hypothesis for a Poisson process. Nucl. Instrum. Methods A **595**, 480 (2008). arXiv:physics/0702156 [physics.data-an]

107. A.L. Read, Presentation of search results: the CL_S technique. J. Phys. G **28**, 2693 (2002)

108. ATLAS Collaboration, *ATLAS Computing Acknowledgements*, ATL-GEN-PUB-2016-002, url: https://cds.cern.ch/record/2202407

ATLAS Collaboration

G. Aad[101], B. Abbott[128], D. C. Abbott[102], O. Abdinov[13,*], A. Abed Abud[70a,70b], K. Abeling[53], D. K. Abhayasinghe[93], S. H. Abidi[167], O. S. AbouZeid[40], N. L. Abraham[156], H. Abramowicz[161], H. Abreu[160], Y. Abulaiti[6], B. S. Acharya[66a,66b,p], B. Achkar[53], S. Adachi[163], L. Adam[99], L. Adamczyk[83a], L. Adamek[167], J. Adelman[121], M. Adersberger[114], A. Adiguzel[12c,ak], S. Adorni[54], T. Adye[144], A. A. Affolder[146], Y. Afik[160], C. Agapopoulou[132], M. N. Agaras[38], A. Aggarwal[119], C. Agheorghiesei[27c], J. A. Aguilar-Saavedra[140a,140f,aj], F. Ahmadov[79], W. S. Ahmed[103], X. Ai[15a], G. Aielli[73a,73b], S. Akatsuka[85], T. P. A. Åkesson[96], E. Akilli[54], A. V. Akimov[110], K. Al Khoury[132], G. L. Alberghi[23a,23b], J. Albert[176], M. J. Alconada Verzini[88], S. Alderweireldt[36], M. Aleksa[36], I. N. Aleksandrov[79], C. Alexa[27b], D. Alexandre[19], T. Alexopoulos[10], A. Alfonsi[120], M. Alhroob[128], B. Ali[142], G. Alimonti[68a], J. Alison[37], S. P. Alkire[148], C. Allaire[132], B. M. M. Allbrooke[156], B. W. Allen[131], P. P. Allport[21], A. Aloisio[69a,69b], A. Alonso[40], F. Alonso[88], C. Alpigiani[148], A. A. Alshehri[57], M. Alvarez Estevez[98], D. Álvarez Piqueras[174], M. G. Alviggi[69a,69b], Y. Amaral Coutinho[80b], A. Ambler[103], L. Ambroz[135], C. Amelung[26], D. Amidei[105], S. P. Amor Dos Santos[140a], S. Amoroso[46], C. S. Amrouche[54], F. An[78], C. Anastopoulos[149], N. Andari[145], T. Andeen[11], C. F. Anders[61b], J. K. Anders[20], A. Andreazza[68a,68b], V. Andrei[61a], C. R. Anelli[176], S. Angelidakis[38], A. Angerami[39], A. V. Anisenkov[122a,122b], A. Annovi[71a], C. Antel[61a], M. T. Anthony[149], M. Antonelli[51], D. J. A. Antrim[171], M. Aoki[81], J. A. Aparisi Pozo[174], L. Aperio Bella[36], G. Arabidze[106], J. P. Araque[140a], V. Araujo Ferraz[80b], R. Araujo Pereira[80b], C. Arcangeletti[51], A. T. H. Arce[49], F. A. Arduh[88], J-F. Arguin[109], S. Argyropoulos[77], J.-H. Arling[46], A. J. Armbruster[36], A. Armstrong[171], O. Arnaez[167], H. Arnold[120], A. Artamonov[111,*], G. Artoni[135], S. Artz[99], S. Asai[163], N. Asbah[59], E. M. Asimakopoulou[172], L. Asquith[156], K. Assamagan[29], R. Astalos[28a], R. J. Atkin[33a], M. Atkinson[173], N. B. Atlay[151], H. Atmani[132], K. Augsten[142], G. Avolio[36], R. Avramidou[60a], M. K. Ayoub[15a], A. M. Azoulay[168b], G. Azuelos[109,ay], M. J. Baca[21], H. Bachacou[145], K. Bachas[67a,67b], M. Backes[135], F. Backman[45a,45b], P. Bagnaia[72a,72b], M. Bahmani[84], H. Bahrasemani[152], A. J. Bailey[174], V. R. Bailey[173], J. T. Baines[144], M. Bajic[40], C. Bakalis[10], O. K. Baker[183], P. J. Bakker[120], D. Bakshi Gupta[8], S. Balaji[157], E. M. Baldin[122a,122b], P. Balek[180], F. Balli[145], W. K. Balunas[135], J. Balz[99], E. Banas[84], A. Bandyopadhyay[24], S. Banerjee[181,k], A. A. E. Bannoura[182], L. Barak[161], W. M. Barbe[38], E. L. Barberio[104], D. Barberis[55a,55b], M. Barbero[101], T. Barillari[115], M-S. Barisits[36], J. Barkeloo[131], T. Barklow[153], R. Barnea[160], S. L. Barnes[60c], B. M. Barnett[144], R. M. Barnett[18], Z. Barnovska-Blenessy[60a], A. Baroncelli[60a], G. Barone[29], A. J. Barr[135], L. Barranco Navarro[45a,45b], F. Barreiro[98], J. Barreiro Guimarães da Costa[15a], S. Barsov[138], R. Bartoldus[153], G. Bartolini[101], A. E. Barton[89], P. Bartos[28a], A. Basalaev[46], A. Bassalat[132], R. L. Bates[57], S. J. Batista[167], S. Batlamous[35e], J. R. Batley[32], B. Batool[151], M. Battaglia[146], M. Bauce[72a,72b], F. Bauer[145], K. T. Bauer[171], H. S. Bawa[31,n], J. B. Beacham[126],

T. Beau[136], P. H. Beauchemin[170], F. Becherer[52], P. Bechtle[24], H. C. Beck[53], H. P. Beck[20,t], K. Becker[52], M. Becker[99], C. Becot[46], A. Beddall[12d], A. J. Beddall[12a], V. A. Bednyakov[79], M. Bedognetti[120], C. P. Bee[155], T. A. Beermann[76], M. Begalli[80b], M. Begel[29], A. Behera[155], J. K. Behr[46], F. Beisiegel[24], A. S. Bell[94], G. Bella[161], L. Bellagamba[23b], A. Bellerive[34], P. Bellos[9], K. Beloborodov[122a,122b], K. Belotskiy[112], N. L. Belyaev[112], D. Benchekroun[35a], N. Benekos[10], Y. Benhammou[161], D. P. Benjamin[6], M. Benoit[54], J. R. Bensinger[26], S. Bentvelsen[120], L. Beresford[135], M. Beretta[51], D. Berge[46], E. Bergeaas Kuutmann[172], N. Berger[5], B. Bergmann[142], L. J. Bergsten[26], J. Beringer[18], S. Berlendis[7], N. R. Bernard[102], G. Bernardi[136], C. Bernius[153], T. Berry[93], P. Berta[99], C. Bertella[15a], I. A. Bertram[89], G. J. Besjes[40], O. Bessidskaia Bylund[182], N. Besson[145], A. Bethani[100], S. Bethke[115], A. Betti[24], A. J. Bevan[92], J. Beyer[115], R. Bi[139], R. M. Bianchi[139], O. Biebel[114], D. Biedermann[19], R. Bielski[36], K. Bierwagen[99], N. V. Biesuz[71a,71b], M. Biglietti[74a], T. R. V. Billoud[109], M. Bindi[53], A. Bingul[12d], C. Bini[72a,72b], S. Biondi[23a,23b], M. Birman[180], T. Bisanz[53], J. P. Biswal[161], A. Bitadze[100], C. Bittrich[48], K. Bjørke[134], K. M. Black[25], T. Blazek[28a], I. Bloch[46], C. Blocker[26], A. Blue[57], U. Blumenschein[92], G. J. Bobbink[120], V. S. Bobrovnikov[122a,122b], S. S. Bocchetta[96], A. Bocci[49], D. Boerner[46], D. Bogavac[14], A. G. Bogdanchikov[122a,122b], C. Bohm[45a], V. Boisvert[93], P. Bokan[53,172], T. Bold[83a], A. S. Boldyrev[113], A. E. Bolz[61b], M. Bomben[136], M. Bona[92], J. S. Bonilla[131], M. Boonekamp[145], H. M. Borecka-Bielska[90], A. Borisov[123], G. Borissov[89], J. Bortfeldt[36], D. Bortoletto[135], V. Bortolotto[73a,73b], D. Boscherini[23b], M. Bosman[14], J. D. Bossio Sola[103], K. Bouaouda[35a], J. Boudreau[139], E. V. Bouhova-Thacker[89], D. Boumediene[38], C. Bourdarios[132], S. K. Boutle[57], A. Boveia[126], J. Boyd[36], D. Boye[33b,as], I. R. Boyko[79], A. J. Bozson[93], J. Bracinik[21], N. Brahimi[101], G. Brandt[182], O. Brandt[61a], F. Braren[46], U. Bratzler[164], B. Brau[102], J. E. Brau[131], W. D. Breaden Madden[57], K. Brendlinger[46], L. Brenner[46], R. Brenner[172], S. Bressler[180], B. Brickwedde[99], D. L. Briglin[21], D. Britton[57], D. Britzger[115], I. Brock[24], R. Brock[106], G. Brooijmans[39], W. K. Brooks[147b], E. Brost[121], J.H Broughton[21], P. A. Bruckman de Renstrom[84], D. Bruncko[28b], A. Bruni[23b], G. Bruni[23b], L. S. Bruni[120], S. Bruno[73a,73b], B. H. Brunt[32], M. Bruschi[23b], N. Bruscino[139], P. Bryant[37], L. Bryngemark[96], T. Buanes[17], Q. Buat[36], P. Buchholz[151], A. G. Buckley[57], I. A. Budagov[79], M. K. Bugge[134], F. Bührer[52], O. Bulekov[112], T. J. Burch[121], S. Burdin[90], C. D. Burgard[120], A. M. Burger[129], B. Burghgrave[8], K. Burka[84], J. T. P. Burr[46], V. Büscher[99], E. Buschmann[53], P. Bussey[57], J. M. Butler[25], C. M. Buttar[57], J. M. Butterworth[94], P. Butti[36], W. Buttinger[36], A. Buzatu[158], A. R. Buzykaev[122a,122b], G. Cabras[23a,23b], S. Cabrera Urbán[174], D. Caforio[56], H. Cai[173], V. M. M. Cairo[153], O. Cakir[4a], N. Calace[36], P. Calafiura[18], A. Calandri[101], G. Calderini[136], P. Calfayan[65], G. Callea[57], L. P. Caloba[80b], S. Calvente Lopez[98], D. Calvet[38], S. Calvet[38], T. P. Calvet[155], M. Calvetti[71a,71b], R. Camacho Toro[136], S. Camarda[36], D. Camarero Munoz[98], P. Camarri[73a,73b], D. Cameron[134], R. Caminal Armadans[102], C. Camincher[36], S. Campana[36], M. Campanelli[94], A. Camplani[40], A. Campoverde[151], V. Canale[69a,69b], A. Canesse[103], M. Cano Bret[60c], J. Cantero[129], T. Cao[161], Y. Cao[173], M. D. M. Capeans Garrido[36], M. Capua[41a,41b], R. Cardarelli[73a], F. C. Cardillo[149], I. Carli[143], T. Carli[36], G. Carlino[69a], B. T. Carlson[139], L. Carminati[68a,68b], R. M. D. Carney[45a,45b], S. Caron[119], E. Carquin[147b], S. Carrá[46], J. W. S. Carter[167], M. P. Casado[14,f], A. F. Casha[167], D. W. Casper[171], R. Castelijn[120], F. L. Castillo[174], V. Castillo Gimenez[174], N. F. Castro[140a,140e], A. Catinaccio[36], J. R. Catmore[134], A. Cattai[36], J. Caudron[24], V. Cavaliere[29], E. Cavallaro[14], M. Cavalli-Sforza[14], V. Cavasinni[71a,71b], E. Celebi[12b], L. Cerda Alberich[174], K. Cerny[130], A. S. Cerqueira[80a], A. Cerri[156], L. Cerrito[73a,73b], F. Cerutti[18], A. Cervelli[23a,23b], S. A. Cetin[12b], D. Chakraborty[121], S. K. Chan[59], W. S. Chan[120], W. Y. Chan[90], J. D. Chapman[32], B. Chargeishvili[159b], D. G. Charlton[21], T. P. Charman[92], C. C. Chau[34], S. Che[126], A. Chegwidden[106], S. Chekanov[6], S. V. Chekulaev[168a], G. A. Chelkov[79,ax], M. A. Chelstowska[36], B. Chen[78], C. Chen[60a], C. H. Chen[78], H. Chen[29], J. Chen[60a], J. Chen[39], S. Chen[137], S. J. Chen[15c], X. Chen[15b,aw], Y. Chen[82], Y-H. Chen[46], H. C. Cheng[63a], H. J. Cheng[15d], A. Cheplakov[79], E. Cheremushkina[123], R. Cherkaoui El Moursli[35e], E. Cheu[7], K. Cheung[64], T. J. A. Chevalérias[145], L. Chevalier[145], V. Chiarella[51], G. Chiarelli[71a], G. Chiodini[67a], A. S. Chisholm[36,21], A. Chitan[27b], I. Chiu[163], Y. H. Chiu[176], M. V. Chizhov[79], K. Choi[65], A. R. Chomont[72a,72b], S. Chouridou[162], Y. S. Chow[120], M. C. Chu[63a], X. Chu[15a], J. Chudoba[141], A. J. Chuinard[103], J. J. Chwastowski[84], L. Chytka[130], K. M. Ciesla[84], D. Cinca[47], V. Cindro[91], I. A. Cioară[27b], A. Ciocio[18], F. Cirotto[69a,69b], Z. H. Citron[180], M. Citterio[68a], D. A. Ciubotaru[27b], B. M. Ciungu[167], A. Clark[54], M. R. Clark[39], P. J. Clark[50], C. Clement[45a,45b], Y. Coadou[101], M. Cobal[66a,66c], A. Coccaro[55b], J. Cochran[78], H. Cohen[161], A. E. C. Coimbra[36], L. Colasurdo[119], B. Cole[39], A. P. Colijn[120], J. Collot[58], P. Conde Muiño[140a,g], E. Coniavitis[52], S. H. Connell[33b], I. A. Connelly[57], S. Constantinescu[27b], F. Conventi[69a,az], A. M. Cooper-Sarkar[135], F. Cormier[175], K. J. R. Cormier[167], L. D. Corpe[94], M. Corradi[72a,72b], E. E. Corrigan[96], F. Corriveau[103,af], A. Cortes-Gonzalez[36], M. J. Costa[174], F. Costanza[5], D. Costanzo[149], G. Cowan[93], J. W. Cowley[32], J. Crane[100], K. Cranmer[124], S. J. Crawley[57], R. A. Creager[137], S. Crépé-Renaudin[58], F. Crescioli[136], M. Cristinziani[24], V. Croft[120], G. Crosetti[41a,41b], A. Cueto[5], T. Cuhadar Donszelmann[149], A. R. Cukierman[153], S. Czekierda[84], P. Czodrowski[36], M. J. Da Cunha Sargedas De Sousa[60b], J. V. Da Fonseca Pinto[80b], C. Da Via[100], W. Dabrowski[83a], T. Dado[28a], S. Dahbi[35e], T. Dai[105], C. Dallapiccola[102], M. Dam[40], G. D'amen[23a,23b], V. D'Amico[74a,74b], J. Damp[99], J. R. Dandoy[137], M. F. Daneri[30], N. P. Dang[181], N. D. Dann[100], M. Danninger[175], V. Dao[36], G. Darbo[55b],

O. Dartsi[5], A. Dattagupta[131], T. Daubney[46], S. D'Auria[68a,68b], W. Davey[24], C. David[46], T. Davidek[143], D. R. Davis[49], I. Dawson[149], K. De[8], R. De Asmundis[69a], M. De Beurs[120], S. De Castro[23a,23b], S. De Cecco[72a,72b], N. De Groot[119], P. de Jong[120], H. De la Torre[106], A. De Maria[15c], D. De Pedis[72a], A. De Salvo[72a], U. De Sanctis[73a,73b], M. De Santis[73a,73b], A. De Santo[156], K. De Vasconcelos Corga[101], J. B. De Vivie De Regie[132], C. Debenedetti[146], D. V. Dedovich[79], A. M. Deiana[42], M. Del Gaudio[41a,41b], J. Del Peso[98], Y. Delabat Diaz[46], D. Delgove[132], F. Deliot[145,s], C. M. Delitzsch[7], M. Della Pietra[69a,69b], D. Della Volpe[54], A. Dell'Acqua[36], L. Dell'Asta[73a,73b], M. Delmastro[5], C. Delporte[132], P. A. Delsart[58], D. A. DeMarco[167], S. Demers[183], M. Demichev[79], G. Demontigny[109], S. P. Denisov[123], D. Denysiuk[120], L. D'Eramo[136], D. Derendarz[84], J. E. Derkaoui[35d], F. Derue[136], P. Dervan[90], K. Desch[24], C. Deterre[46], K. Dette[167], C. Deutsch[24], M. R. Devesa[30], P. O. Deviveiros[36], A. Dewhurst[144], S. Dhaliwal[26], F. A. Di Bello[54], A. Di Ciaccio[73a,73b], L. Di Ciaccio[5], W. K. Di Clemente[137], C. Di Donato[69a,69b], A. Di Girolamo[36], G. Di Gregorio[71a,71b], B. Di Micco[74a,74b], R. Di Nardo[102], K. F. Di Petrillo[59], R. Di Sipio[167], D. Di Valentino[34], C. Diaconu[101], F. A. Dias[40], T. Dias Do Vale[140a], M. A. Diaz[147a], J. Dickinson[18], E. B. Diehl[105], J. Dietrich[19], S. Díez Cornell[46], A. Dimitrievska[18], W. Ding[15b], J. Dingfelder[24], F. Dittus[36], F. Djama[101], T. Djobava[159b], J. I. Djuvsland[17], M. A. B. Do Vale[80c], M. Dobre[27b], D. Dodsworth[26], C. Doglioni[96], J. Dolejsi[143], Z. Dolezal[143], M. Donadelli[80d], J. Donini[38], A. D'onofrio[92], M. D'Onofrio[90], J. Dopke[144], A. Doria[69a], M. T. Dova[88], A. T. Doyle[57], E. Drechsler[152], E. Dreyer[152], T. Dreyer[53], A. S. Drobac[170], Y. Duan[60b], F. Dubinin[110], M. Dubovsky[28a], A. Dubreuil[54], E. Duchovni[180], G. Duckeck[114], A. Ducourthial[136], O. A. Ducu[109], D. Duda[115], A. Dudarev[36], A. C. Dudder[99], E. M. Duffield[18], L. Duflot[132], M. Dührssen[36], C. Dülsen[182], M. Dumancic[180], A. E. Dumitriu[27b], A. K. Duncan[57], M. Dunford[61a], A. Duperrin[101], H. Duran Yildiz[4a], M. Düren[56], A. Durglishvili[159b], D. Duschinger[48], B. Dutta[46], D. Duvnjak[1], G. Dyckes[137], M. Dyndal[36], S. Dysch[100], B. S. Dziedzic[84], K. M. Ecker[115], R. C. Edgar[105], T. Eifert[36], G. Eigen[17], K. Einsweiler[18], T. Ekelof[172], M. El Kacimi[35c], R. El Kosseifi[101], V. Ellajosyula[172], M. Ellert[172], F. Ellinghaus[182], A. A. Elliot[92], N. Ellis[36], J. Elmsheuser[29], M. Elsing[36], D. Emeliyanov[144], A. Emerman[39], Y. Enari[163], M. B. Epland[49], J. Erdmann[47], A. Ereditato[20], M. Errenst[36], M. Escalier[132], C. Escobar[174], O. Estrada Pastor[174], E. Etzion[161], H. Evans[65], A. Ezhilov[138], F. Fabbri[57], L. Fabbri[23a,23b], V. Fabiani[119], G. Facini[94], R. M. Faisca Rodrigues Pereira[140a], R. M. Fakhrutdinov[123], S. Falciano[72a], P. J. Falke[5], S. Falke[5], J. Faltova[143], Y. Fang[15a], Y. Fang[15a], G. Fanourakis[44], M. Fanti[68a,68b], A. Farbin[8], A. Farilla[74a], E. M. Farina[70a,70b], T. Farooque[106], S. Farrell[18], S. M. Farrington[178], P. Farthouat[36], F. Fassi[35e], P. Fassnacht[36], D. Fassouliotis[9], M. Faucci Giannelli[50], W. J. Fawcett[32], L. Fayard[132], O. L. Fedin[138,q], W. Fedorko[175], M. Feickert[42], S. Feigl[134], L. Feligioni[101], A. Fell[149], C. Feng[60b], E. J. Feng[36], M. Feng[49], M. J. Fenton[57], A. B. Fenyuk[123], J. Ferrando[46], A. Ferrante[173], A. Ferrari[172], P. Ferrari[120], R. Ferrari[70a], D. E. Ferreira de Lima[61b], A. Ferrer[174], D. Ferrere[54], C. Ferretti[105], F. Fiedler[99], A. Filipčič[91], F. Filthaut[119], K. D. Finelli[25], M. C. N. Fiolhais[140a,a], L. Fiorini[174], F. Fischer[114], W. C. Fisher[106], I. Fleck[151], P. Fleischmann[105], R. R. M. Fletcher[137], T. Flick[182], B. M. Flierl[114], L. M. Flores[137], L. R. Flores Castillo[63a], F. M. Follega[75a,75b], N. Fomin[17], J. H. Foo[167], G. T. Forcolin[75a,75b], A. Formica[145], F. A. Förster[14], A. C. Forti[100], A. G. Foster[21], M. G. Foti[135], D. Fournier[132], H. Fox[89], P. Francavilla[71a,71b], S. Francescato[72a,72b], M. Franchini[23a,23b], S. Franchino[61a], D. Francis[36], L. Franconi[20], M. Franklin[59], A. N. Fray[92], B. Freund[109], W. S. Freund[80b], E. M. Freundlich[47], D. C. Frizzell[128], D. Froidevaux[36], J. A. Frost[135], C. Fukunaga[164], E. Fullana Torregrosa[174], E. Fumagalli[55a,55b], T. Fusayasu[116], J. Fuster[174], A. Gabrielli[23a,23b], A. Gabrielli[18], G. P. Gach[83a], S. Gadatsch[54], P. Gadow[115], G. Gagliardi[55a,55b], L. G. Gagnon[109], C. Galea[27b], B. Galhardo[140a], G. E. Gallardo[135], E. J. Gallas[135], B. J. Gallop[144], G. Galster[40], R. Gamboa Goni[92], K. K. Gan[126], S. Ganguly[180], J. Gao[60a], Y. Gao[90], Y. S. Gao[31,n], C. García[174], J. E. García Navarro[174], J. A. García Pascual[15a], C. Garcia-Argos[52], M. Garcia-Sciveres[18], R. W. Gardner[37], N. Garelli[153], S. Gargiulo[52], V. Garonne[134], A. Gaudiello[55a,55b], G. Gaudio[70a], I. L. Gavrilenko[110], A. Gavrilyuk[111], C. Gay[175], G. Gaycken[24], E. N. Gazis[10], A. A. Geanta[27b], C. N. P. Gee[144], J. Geisen[53], M. Geisen[99], M. P. Geisler[61a], C. Gemme[55b], M. H. Genest[58], C. Geng[105], S. Gentile[72a,72b], S. George[93], T. Geralis[44], L. O. Gerlach[53], P. Gessinger-Befurt[99], G. Gessner[47], S. Ghasemi[151], M. Ghasemi Bostanabad[176], M. Ghneimat[24], A. Ghosh[132], A. Ghosh[77], B. Giacobbe[23b], S. Giagu[72a,72b], N. Giangiacomi[23a,23b], P. Giannetti[71a], A. Giannini[69a,69b], S. M. Gibson[93], M. Gignac[146], D. Gillberg[34], G. Gilles[182], D. M. Gingrich[3,ay], M. P. Giordani[66a,66c], F. M. Giorgi[23b], P. F. Giraud[145], G. Giugliarelli[66a,66c], D. Giugni[68a], F. Giuli[73a,73b], S. Gkaitatzis[162], I. Gkialas[9,i], E. L. Gkougkousis[14], P. Gkountoumis[10], L. K. Gladilin[113], C. Glasman[98], J. Glatzer[14], P. C. F. Glaysher[46], A. Glazov[46], M. Goblirsch-Kolb[26], S. Goldfarb[104], T. Golling[54], D. Golubkov[123], A. Gomes[140a,140b], R. Goncalves Gama[53], R. Gonçalo[140a,140b], G. Gonella[52], L. Gonella[21], A. Gongadze[79], F. Gonnella[21], J. L. Gonski[59], S. González de la Hoz[174], S. Gonzalez-Sevilla[54], G. R. Gonzalvo Rodriguez[174], L. Goossens[36], P. A. Gorbounov[111], H. A. Gordon[29], B. Gorini[36], E. Gorini[67a,67b], A. Gorišek[91], A. T. Goshaw[49], C. Gössling[47], M. I. Gostkin[79], C. A. Gottardo[24], M. Gouighri[35b], D. Goujdami[35c], A. G. Goussiou[148], N. Govender[33b,b], C. Goy[5], E. Gozani[160], I. Grabowska-Bold[83a], E. C. Graham[90], J. Gramling[171], E. Gramstad[134], S. Grancagnolo[19], M. Grandi[156], V. Gratchev[138], P. M. Gravila[27f], F. G. Gravili[67a,67b], C. Gray[57], H. M. Gray[18], C. Grefe[24], K. Gregersen[96], I. M. Gregor[46],

P. Grenier[153], K. Grevtsov[46], N. A. Grieser[128], J. Griffiths[8], A. A. Grillo[146], K. Grimm[31,m], S. Grinstein[14,z], J.-F. Grivaz[132], S. Groh[99], E. Gross[180], J. Grosse-Knetter[53], Z. J. Grout[94], C. Grud[105], A. Grummer[118], L. Guan[105], W. Guan[181], J. Guenther[36], A. Guerguichon[132], J. G. R. Guerrero Rojas[174], F. Guescini[115], D. Guest[171], R. Gugel[52], T. Guillemin[5], S. Guindon[36], U. Gul[57], J. Guo[60c], W. Guo[105], Y. Guo[60a,u], Z. Guo[101], R. Gupta[46], S. Gurbuz[12c], G. Gustavino[128], P. Gutierrez[128], C. Gutschow[94], C. Guyot[145], C. Gwenlan[135], C. B. Gwilliam[90], A. Haas[124], C. Haber[18], H. K. Hadavand[8], N. Haddad[35e], A. Hadef[60a], S. Hageböck[36], M. Hagihara[169], M. Haleem[177], J. Haley[129], G. Halladjian[106], G. D. Hallewell[101], K. Hamacher[182], P. Hamal[130], K. Hamano[176], H. Hamdaoui[35e], G. N. Hamity[149], K. Han[60a,am], L. Han[60a], S. Han[15d], K. Hanagaki[81,x], M. Hance[146], D. M. Handl[114], B. Haney[137], R. Hankache[136], P. Hanke[61a], E. Hansen[96], J. B. Hansen[40], J. D. Hansen[40], M. C. Hansen[24], P. H. Hansen[40], E. C. Hanson[100], K. Hara[169], A. S. Hard[181], T. Harenberg[182], S. Harkusha[107], P. F. Harrison[178], N. M. Hartmann[114], Y. Hasegawa[150], A. Hasib[50], S. Hassani[145], S. Haug[20], R. Hauser[106], L. B. Havener[39], M. Havranek[142], C. M. Hawkes[21], R. J. Hawkings[36], D. Hayden[106], C. Hayes[155], R. L. Hayes[175], C. P. Hays[135], J. M. Hays[92], H. S. Hayward[90], S. J. Haywood[144], F. He[60a], M. P. Heath[50], V. Hedberg[96], L. Heelan[8], S. Heer[24], K. K. Heidegger[52], J. Heilman[34], S. Heim[46], T. Heim[18], B. Heinemann[46,at], J. J. Heinrich[131], L. Heinrich[36], C. Heinz[56], J. Hejbal[141], L. Helary[61b], A. Held[175], S. Hellesund[134], C. M. Helling[146], S. Hellman[45a,45b], C. Helsens[36], R. C. W. Henderson[89], Y. Heng[181], S. Henkelmann[175], A. M. Henriques Correia[36], G. H. Herbert[19], H. Herde[26], V. Herget[177], Y. Hernández Jiménez[33c], H. Herr[99], M. G. Herrmann[114], T. Herrmann[48], G. Herten[52], R. Hertenberger[114], L. Hervas[36], T. C. Herwig[137], G. G. Hesketh[94], N. P. Hessey[168a], A. Higashida[163], S. Higashino[81], E. Higón-Rodriguez[174], K. Hildebrand[37], E. Hill[176], J. C. Hill[32], K. K. Hill[29], K. H. Hiller[46], S. J. Hillier[21], M. Hils[48], I. Hinchliffe[18], F. Hinterkeuser[24], M. Hirose[133], S. Hirose[52], D. Hirschbuehl[182], B. Hiti[91], O. Hladik[141], D. R. Hlaluku[33c], X. Hoad[50], J. Hobbs[155], N. Hod[180], M. C. Hodgkinson[149], A. Hoecker[36], F. Hoenig[114], D. Hohn[52], D. Hohov[132], T. R. Holmes[37], M. Holzbock[114], L.B.A.H Hommels[32], S. Honda[169], T. Honda[81], T. M. Hong[139], A. Hönle[115], B. H. Hooberman[173], W. H. Hopkins[6], Y. Horii[117], P. Horn[48], L. A. Horyn[37], A. Hostiuc[148], S. Hou[158], A. Hoummada[35a], J. Howarth[100], J. Hoya[88], M. Hrabovsky[130], J. Hrdinka[76], I. Hristova[19], J. Hrivnac[132], A. Hrynevich[108], T. Hryn'ova[5], P. J. Hsu[64], S.-C. Hsu[148], Q. Hu[29], S. Hu[60c], Y. Huang[15a], Z. Hubacek[142], F. Hubaut[101], M. Huebner[24], F. Huegging[24], T. B. Huffman[135], M. Huhtinen[36], R. F. H. Hunter[34], P. Huo[155], A. M. Hupe[34], N. Huseynov[79,ah], J. Huston[106], J. Huth[59], R. Hyneman[105], S. Hyrych[28a], G. Iacobucci[54], G. Iakovidis[29], I. Ibragimov[151], L. Iconomidou-Fayard[132], Z. Idrissi[35e], P. Iengo[36], R. Ignazzi[40], O. Igonkina[120,ab,*], R. Iguchi[163], T. Iizawa[54], Y. Ikegami[81], M. Ikeno[81], D. Iliadis[162], N. Ilic[119], F. Iltzsche[48], G. Introzzi[70a,70b], M. Iodice[74a], K. Iordanidou[168a], V. Ippolito[72a,72b], M. F. Isacson[172], M. Ishino[163], M. Ishitsuka[165], W. Islam[129], C. Issever[135], S. Istin[160], F. Ito[169], J. M. Iturbe Ponce[63a], R. Iuppa[75a,75b], A. Ivina[180], H. Iwasaki[81], J. M. Izen[43], V. Izzo[69a], P. Jacka[141], P. Jackson[1], R. M. Jacobs[24], B. P. Jaeger[152], V. Jain[2], G. Jäkel[182], K. B. Jakobi[99], K. Jakobs[52], S. Jakobsen[76], T. Jakoubek[141], J. Jamieson[57], K. W. Janas[83a], R. Jansky[54], J. Janssen[24], M. Janus[53], P. A. Janus[83a], G. Jarlskog[96], N. Javadov[79,ah], T. Javůrek[36], M. Javurkova[52], F. Jeanneau[145], L. Jeanty[131], J. Jejelava[159a,ai], A. Jelinskas[178], P. Jenni[52,c], J. Jeong[46], N. Jeong[46], S. Jézéquel[5], H. Ji[181], J. Jia[155], H. Jiang[78], Y. Jiang[60a], Z. Jiang[153,r], S. Jiggins[52], F. A. Jimenez Morales[38], J. Jimenez Pena[174], S. Jin[15c], A. Jinaru[27b], O. Jinnouchi[165], H. Jivan[33c], P. Johansson[149], K. A. Johns[7], C. A. Johnson[65], K. Jon-And[45a,45b], R. W. L. Jones[89], S. D. Jones[156], S. Jones[7], T. J. Jones[90], J. Jongmanns[61a], P. M. Jorge[140a], J. Jovicevic[36], X. Ju[18], J. J. Junggeburth[115], A. Juste Rozas[14,z], A. Kaczmarska[84], M. Kado[132], H. Kagan[126], M. Kagan[153], C. Kahra[99], T. Kaji[179], E. Kajomovitz[160], C. W. Kalderon[96], A. Kaluza[99], A. Kamenshchikov[123], L. Kanjir[91], Y. Kano[163], V. A. Kantserov[112], J. Kanzaki[81], L. S. Kaplan[181], D. Kar[33c], M. J. Kareem[168b], S. N. Karpov[79], Z. M. Karpova[79], V. Kartvelishvili[89], A. N. Karyukhin[123], L. Kashif[181], R. D. Kass[126], A. Kastanas[45a,45b], Y. Kataoka[163], C. Kato[60c,60d], J. Katzy[46], K. Kawade[82], K. Kawagoe[87], T. Kawaguchi[117], T. Kawamoto[163], G. Kawamura[53], E. F. Kay[176], V. F. Kazanin[122a,122b], R. Keeler[176], R. Kehoe[42], J. S. Keller[34], E. Kellermann[96], D. Kelsey[156], J. J. Kempster[21], J. Kendrick[21], O. Kepka[141], S. Kersten[182], B. P. Kerševan[91], S. Ketabchi Haghighat[167], M. Khader[173], F. Khalil-Zada[13], M. K. Khandoga[145], A. Khanov[129], A. G. Kharlamov[122a,122b], T. Kharlamova[122a,122b], E. E. Khoda[175], A. Khodinov[166], T. J. Khoo[54], E. Khramov[79], J. Khubua[159b], S. Kido[82], M. Kiehn[54], C. R. Kilby[93], Y. K. Kim[37], N. Kimura[66a,66c], O. M. Kind[19], B. T. King[90,*], D. Kirchmeier[48], J. Kirk[144], A. E. Kiryunin[115], T. Kishimoto[163], D. P. Kisliuk[167], V. Kitali[46], O. Kivernyk[5], E. Kladiva[28b,*], T. Klapdor-Kleingrothaus[52], M. Klassen[61a], M. H. Klein[105], M. Klein[90], U. Klein[90], K. Kleinknecht[99], P. Klimek[121], A. Klimentov[29], T. Klingl[24], T. Klioutchnikova[36], F. F. Klitzner[114], P. Kluit[120], S. Kluth[115], E. Kneringer[76], E. B. F. G. Knoops[101], A. Knue[52], D. Kobayashi[87], T. Kobayashi[163], M. Kobel[48], M. Kocian[153], P. Kodys[143], P. T. Koenig[24], T. Koffas[34], N. M. Köhler[36], T. Koi[153], M. Kolb[61b], I. Koletsou[5], T. Komarek[130], T. Kondo[81], N. Kondrashova[60c], K. Köneke[52], A. C. König[119], T. Kono[125], R. Konoplich[124,ap], V. Konstantinides[94], N. Konstantinidis[94], B. Konya[96], R. Kopeliansky[65], S. Koperny[83a], K. Korcyl[84], K. Kordas[162], G. Koren[161], A. Korn[94], I. Korolkov[14], E. V. Korolkova[149], N. Korotkova[113], O. Kortner[115], S. Kortner[115], T. Kosek[143], V. V. Kostyukhin[24], A. Kotwal[49], A. Koulouris[10], A. Kourkoumeli-Charalampidi[70a,70b],

C. Kourkoumelis[9], E. Kourlitis[149], V. Kouskoura[29], A. B. Kowalewska[84], R. Kowalewski[176], C. Kozakai[163], W. Kozanecki[145], A. S. Kozhin[123], V. A. Kramarenko[113], G. Kramberger[91], D. Krasnopevtsev[60a], M. W. Krasny[136], A. Krasznahorkay[36], D. Krauss[115], J. A. Kremer[83a], J. Kretzschmar[90], P. Krieger[167], F. Krieter[114], A. Krishnan[61b], K. Krizka[18], K. Kroeninger[47], H. Kroha[115], J. Kroll[141], J. Kroll[137], J. Krstic[16], U. Kruchonak[79], H. Krüger[24], N. Krumnack[78], M. C. Kruse[49], J. A. Krzysiak[84], T. Kubota[104], S. Kuday[4b], J. T. Kuechler[46], S. Kuehn[36], A. Kugel[61a], T. Kuhl[46], V. Kukhtin[79], R. Kukla[101], Y. Kulchitsky[107,al], S. Kuleshov[147b], Y. P. Kulinich[173], M. Kuna[58], T. Kunigo[85], A. Kupco[141], T. Kupfer[47], O. Kuprash[52], H. Kurashige[82], L. L. Kurchaninov[168a], Y. A. Kurochkin[107], A. Kurova[112], M. G. Kurth[15d], E. S. Kuwertz[36], M. Kuze[165], A. K. Kvam[148], J. Kvita[130], T. Kwan[103], A. La Rosa[115], L. La Rotonda[41a,41b], F. La Ruffa[41a,41b], C. Lacasta[174], F. Lacava[72a,72b], D. P. J. Lack[100], H. Lacker[19], D. Lacour[136], E. Ladygin[79], R. Lafaye[5], B. Laforge[136], T. Lagouri[33c], S. Lai[53], S. Lammers[65], W. Lampl[7], C. Lampoudis[162], E. Lançon[29], U. Landgraf[52], M. P. J. Landon[92], M. C. Lanfermann[54], V. S. Lang[46], J. C. Lange[53], R. J. Langenberg[36], A. J. Lankford[171], F. Lanni[29], K. Lantzsch[24], A. Lanza[70a], A. Lapertosa[55a,55b], S. Laplace[136], J. F. Laporte[145], T. Lari[68a], F. Lasagni Manghi[23a,23b], M. Lassnig[36], T. S. Lau[63a], A. Laudrain[132], A. Laurier[34], M. Lavorgna[69a,69b], M. Lazzaroni[68a,68b], B. Le[104], O. Le Dortz[136], E. Le Guirriec[101], M. LeBlanc[7], T. LeCompte[6], F. Ledroit-Guillon[58], C. A. Lee[29], G. R. Lee[17], L. Lee[59], S. C. Lee[158], S. J. Lee[34], B. Lefebvre[168a], M. Lefebvre[176], F. Legger[114], C. Leggett[18], K. Lehmann[152], N. Lehmann[182], G. Lehmann Miotto[36], W. A. Leight[46], A. Leisos[162,y], M. A. L. Leite[80d], R. Leitner[143], D. Lellouch[180,*], K. J. C. Leney[42], T. Lenz[24], B. Lenzi[36], R. Leone[7], S. Leone[71a], C. Leonidopoulos[50], A. Leopold[136], G. Lerner[156], C. Leroy[109], R. Les[167], C. G. Lester[32], M. Levchenko[138], J. Levêque[5], D. Levin[105], L. J. Levinson[180], D. J. Lewis[21], B. Li[15b], B. Li[105], C-Q. Li[60a], F. Li[60c], H. Li[60a], H. Li[60b], J. Li[60c], K. Li[153], L. Li[60c], M. Li[15a], Q. Li[15d], Q. Y. Li[60a], S. Li[60c,60d], X. Li[46], Y. Li[46], Z. Li[60b], Z. Liang[15a], B. Liberti[73a], A. Liblong[167], K. Lie[63c], S. Liem[120], C. Y. Lin[32], K. Lin[106], T. H. Lin[99], R. A. Linck[65], J. H. Lindon[21], A. L. Lionti[54], E. Lipeles[137], A. Lipniacka[17], M. Lisovyi[61b], T. M. Liss[173,av], A. Lister[175], A. M. Litke[146], J. D. Little[8], B. Liu[78,ae], B.L Liu[6], H. B. Liu[29], H. Liu[105], J. B. Liu[60a], J. K. K. Liu[135], K. Liu[136], M. Liu[60a], P. Liu[18], Y. Liu[15d], Y. L. Liu[105], Y. W. Liu[60a], M. Livan[70a,70b], A. Lleres[58], J. Llorente Merino[15a], S. L. Lloyd[92], C. Y. Lo[63b], F. Lo Sterzo[42], E. M. Lobodzinska[46], P. Loch[7], S. Loffredo[73a,73b], T. Lohse[19], K. Lohwasser[149], M. Lokajicek[141], J. D. Long[173], R. E. Long[89], L. Longo[36], K. A. Looper[126], J. A. Lopez[147b], I. Lopez Paz[100], A. Lopez Solis[149], J. Lorenz[114], N. Lorenzo Martinez[5], M. Losada[22], P. J. Lösel[114], A. Lösle[52], X. Lou[46], X. Lou[15a], A. Lounis[132], J. Love[6], P. A. Love[89], J. J. Lozano Bahilo[174], M. Lu[60a], Y. J. Lu[64], H. J. Lubatti[148], C. Luci[72a,72b], A. Lucotte[58], C. Luedtke[52], F. Luehring[65], I. Luise[136], L. Luminari[72a], B. Lund-Jensen[154], M. S. Lutz[102], D. Lynn[29], R. Lysak[141], E. Lytken[96], F. Lyu[15a], V. Lyubushkin[79], T. Lyubushkina[79], H. Ma[29], L. L. Ma[60b], Y. Ma[60b], G. Maccarrone[51], A. Macchiolo[115], C. M. Macdonald[149], J. Machado Miguens[137], D. Madaffari[174], R. Madar[38], W. F. Mader[48], N. Madysa[48], J. Maeda[82], K. Maekawa[163], S. Maeland[17], T. Maeno[29], M. Maerker[48], A. S. Maevskiy[113], V. Magerl[52], N. Magini[78], D. J. Mahon[39], C. Maidantchik[80b], T. Maier[114], A. Maio[140a,140b,140d], O. Majersky[28a], S. Majewski[131], Y. Makida[81], N. Makovec[132], B. Malaescu[136], Pa. Malecki[84], V. P. Maleev[138], F. Malek[58], U. Mallik[77], D. Malon[6], C. Malone[32], S. Maltezos[10], S. Malyukov[36], J. Mamuzic[174], G. Mancini[51], I. Mandić[91], L. Manhaes de Andrade Filho[80a], I. M. Maniatis[162], J. Manjarres Ramos[48], K. H. Mankinen[96], A. Mann[114], A. Manousos[76], B. Mansoulie[145], I. Manthos[162], S. Manzoni[120], A. Marantis[162], G. Marceca[30], L. Marchese[135], G. Marchiori[136], M. Marcisovsky[141], C. Marcon[96], C. A. Marin Tobon[36], M. Marjanovic[38], F. Marroquim[80b], Z. Marshall[18], M.U.F Martensson[172], S. Marti-Garcia[174], C. B. Martin[126], T. A. Martin[178], V. J. Martin[50], B. Martin dit Latour[17], L. Martinelli[74a,74b], M. Martinez[14,z], V. I. Martinez Outschoorn[102], S. Martin-Haugh[144], V. S. Martoiu[27b], A. C. Martyniuk[94], A. Marzin[36], S. R. Maschek[115], L. Masetti[99], T. Mashimo[163], R. Mashinistov[110], J. Masik[100], A. L. Maslennikov[122a,122b], L. H. Mason[104], L. Massa[73a,73b], P. Massarotti[69a,69b], P. Mastrandrea[71a,71b], A. Mastroberardino[41a,41b], T. Masubuchi[163], D. Matakias[10], A. Matic[114], P. Mättig[24], J. Maurer[27b], B. Maček[91], S. J. Maxfield[90], D. A. Maximov[122a,122b], R. Mazini[158], I. Maznas[162], S. M. Mazza[146], S. P. Mc Kee[105], T. G. McCarthy[115], L. I. McClymont[94], W. P. McCormack[18], E. F. McDonald[104], J. A. Mcfayden[36], G. Mchedlidze[53], M. A. McKay[42], K. D. McLean[176], S. J. McMahon[144], P. C. McNamara[104], C. J. McNicol[178], R. A. McPherson[176,af], J. E. Mdhluli[33c], Z. A. Meadows[102], S. Meehan[148], T. Megy[52], S. Mehlhase[114], A. Mehta[90], T. Meideck[58], B. Meirose[43], D. Melini[174], B. R. Mellado Garcia[33c], J. D. Mellenthin[53], M. Melo[28a], F. Meloni[46], A. Melzer[24], S. B. Menary[100], E. D. Mendes Gouveia[140a,140e], L. Meng[36], X. T. Meng[105], S. Menke[115], E. Meoni[41a,41b], S. Mergelmeyer[19], S. A. M. Merkt[139], C. Merlassino[20], P. Mermod[54], L. Merola[69a,69b], C. Meroni[68a], O. Meshkov[110,113], J. K. R. Meshreki[151], A. Messina[72a,72b], J. Metcalfe[6], A. S. Mete[171], C. Meyer[65], J. Meyer[160], J-P. Meyer[145], H. Meyer Zu Theenhausen[61a], F. Miano[156], M. Michetti[19], R. P. Middleton[144], L. Mijović[50], G. Mikenberg[180], M. Mikestikova[141], M. Mikuž[91], H. Mildner[149], M. Milesi[104], A. Milic[167], D. A. Millar[92], D. W. Miller[37], A. Milov[180], D. A. Milstead[45a,45b], R. A. Mina[153,r], A. A. Minaenko[123], M. Miñano Moya[174], I. A. Minashvili[159b], A. I. Mincer[124], B. Mindur[83a], M. Mineev[79], Y. Minegishi[163], Y. Ming[181], L. M. Mir[14], A. Mirto[67a,67b], K. P. Mistry[137], T. Mitani[179],

J. Mitrevski[114], V. A. Mitsou[174], M. Mittal[60c], A. Miucci[20], P. S. Miyagawa[149], A. Mizukami[81], J. U. Mjörnmark[96], T. Mkrtchyan[184], M. Mlynarikova[143], T. Moa[45a,45b], K. Mochizuki[109], P. Mogg[52], S. Mohapatra[39], R. Moles-Valls[24], M. C. Mondragon[106], K. Mönig[46], J. Monk[40], E. Monnier[101], A. Montalbano[152], J. Montejo Berlingen[36], M. Montella[94], F. Monticelli[88], S. Monzani[68a], N. Morange[132], D. Moreno[22], M. Moreno Llácer[36], C. Moreno Martinez[14], P. Morettini[55b], M. Morgenstern[120], S. Morgenstern[48], D. Mori[152], M. Morii[59], M. Morinaga[179], V. Morisbak[134], A. K. Morley[36], G. Mornacchi[36], A. P. Morris[94], L. Morvaj[155], P. Moschovakos[36], B. Moser[120], M. Mosidze[159b], T. Moskalets[145], H. J. Moss[149], J. Moss[31,o], K. Motohashi[165], E. Mountricha[36], E. J. W. Moyse[102], S. Muanza[101], J. Mueller[139], R. S. P. Mueller[114], D. Muenstermann[89], G. A. Mullier[96], J. L. Munoz Martinez[14], F. J. Munoz Sanchez[100], P. Murin[28b], W. J. Murray[178,144], A. Murrone[68a,68b], M. Muškinja[18], C. Mwewa[33a], A. G. Myagkov[123,aq], J. Myers[131], M. Myska[142], B. P. Nachman[18], O. Nackenhorst[47], A.Nag Nag[48], K. Nagai[135], K. Nagano[81], Y. Nagasaka[62], M. Nagel[52], E. Nagy[101], A. M. Nairz[36], Y. Nakahama[117], K. Nakamura[81], T. Nakamura[163], I. Nakano[127], H. Nanjo[133], F. Napolitano[61a], R. F. Naranjo Garcia[46], R. Narayan[42], I. Naryshkin[138], T. Naumann[46], G. Navarro[22], H. A. Neal[105,*], P. Y. Nechaeva[110], F. Nechansky[46], T. J. Neep[21], A. Negri[70a,70b], M. Negrini[23b], C. Nellist[53], M. E. Nelson[135], S. Nemecek[141], P. Nemethy[124], M. Nessi[36,e], M. S. Neubauer[173], M. Neumann[182], P. R. Newman[21], Y. S. Ng[19], Y. W. Y. Ng[171], H. D. N. Nguyen[101], T. Nguyen Manh[109], E. Nibigira[38], R. B. Nickerson[135], R. Nicolaidou[145], D. S. Nielsen[40], J. Nielsen[146], N. Nikiforou[11], V. Nikolaenko[123,aq], I. Nikolic-Audit[136], K. Nikolopoulos[21], P. Nilsson[29], H. R. Nindhito[54], Y. Ninomiya[81], A. Nisati[72a], N. Nishu[60c], R. Nisius[115], I. Nitsche[47], T. Nitta[179], T. Nobe[163], Y. Noguchi[85], I. Nomidis[136], M. A. Nomura[29], M. Nordberg[36], N. Norjoharuddeen[135], T. Novak[91], O. Novgorodova[48], R. Novotny[142], L. Nozka[130], K. Ntekas[171], E. Nurse[94], F. G. Oakham[34,ay], H. Oberlack[115], J. Ocariz[136], A. Ochi[82], I. Ochoa[39], J. P. Ochoa-Ricoux[147a], K. O'Connor[26], S. Oda[87], S. Odaka[81], S. Oerdek[53], A. Ogrodnik[83a], A. Oh[100], S. H. Oh[49], C. C. Ohm[154], H. Oide[55a,55b], M. L. Ojeda[167], H. Okawa[169], Y. Okazaki[85], Y. Okumura[163], T. Okuyama[81], A. Olariu[27b], L. F. Oleiro Seabra[140a], S. A. Olivares Pino[147a], D. Oliveira Damazio[29], J. L. Oliver[1], M. J. R. Olsson[171], A. Olszewski[84], J. Olszowska[84], D. C. O'Neil[152], A. Onofre[140a,140e], K. Onogi[117], P. U. E. Onyisi[11], H. Oppen[134], M. J. Oreglia[37], G. E. Orellana[88], Y. Oren[161], D. Orestano[74a,74b], N. Orlando[14], R. S. Orr[167], V. O'Shea[57], R. Ospanov[60a], G. Otero y Garzon[30], H. Otono[87], P. S. Ott[61a], M. Ouchrif[35d], J. Ouellette[29], F. Ould-Saada[134], A. Ouraou[145], Q. Ouyang[15a], M. Owen[57], R. E. Owen[21], V. E. Ozcan[12c], N. Ozturk[8], J. Pacalt[130], H. A. Pacey[32], K. Pachal[49], A. Pacheco Pages[14], C. Padilla Aranda[14], S. Pagan Griso[18], M. Paganini[183], G. Palacino[65], S. Palazzo[50], S. Palestini[36], M. Palka[83b], D. Pallin[38], I. Panagoulias[10], C. E. Pandini[36], J. G. Panduro Vazquez[93], P. Pani[46], G. Panizzo[66a,66c], L. Paolozzi[54], C. Papadatos[109], K. Papageorgiou[9,i], A. Paramonov[6], D. Paredes Hernandez[63b], S. R. Paredes Saenz[135], B. Parida[166], T. H. Park[167], A. J. Parker[89], M. A. Parker[32], F. Parodi[55a,55b], E. W. P. Parrish[121], J. A. Parsons[39], U. Parzefall[52], L. Pascual Dominguez[136], V. R. Pascuzzi[167], J. M. P. Pasner[146], E. Pasqualucci[72a], S. Passaggio[55b], F. Pastore[93], P. Pasuwan[45a,45b], S. Pataraia[99], J. R. Pater[100], A. Pathak[181,k], T. Pauly[36], B. Pearson[115], M. Pedersen[134], L. Pedraza Diaz[119], R. Pedro[140a], T. Peiffer[53], S. V. Peleganchuk[122a,122b], O. Penc[141], H. Peng[60a], B. S. Peralva[80a], M. M. Perego[132], A. P. Pereira Peixoto[140a], D. V. Perepelitsa[29], F. Peri[19], L. Perini[68a,68b], H. Pernegger[36], S. Perrella[69a,69b], K. Peters[46], R. F. Y. Peters[100], B. A. Petersen[36], T. C. Petersen[40], E. Petit[58], A. Petridis[1], C. Petridou[162], P. Petroff[132], M. Petrov[135], F. Petrucci[74a,74b], M. Pettee[183], N. E. Pettersson[102], K. Petukhova[143], A. Peyaud[145], R. Pezoa[147b], L. Pezzotti[70a,70b], T. Pham[104], F. H. Phillips[106], P. W. Phillips[144], M. W. Phipps[173], G. Piacquadio[155], E. Pianori[18], A. Picazio[102], R. H. Pickles[100], R. Piegaia[30], D. Pietreanu[27b], J. E. Pilcher[37], A. D. Pilkington[100], M. Pinamonti[73a,73b], J. L. Pinfold[3], M. Pitt[180], L. Pizzimento[73a,73b], M.-A. Pleier[29], V. Pleskot[143], E. Plotnikova[79], P. Podberezko[122a,122b], R. Poettgen[96], R. Poggi[54], L. Poggioli[132], I. Pogrebnyak[106], D. Pohl[24], I. Pokharel[53], G. Polesello[70a], A. Poley[18], A. Policicchio[72a,72b], R. Polifka[143], A. Polini[23b], C. S. Pollard[46], V. Polychronakos[29], D. Ponomarenko[112], L. Pontecorvo[36], S. Popa[27a], G. A. Popeneciu[27d], D. M. Portillo Quintero[58], S. Pospisil[142], K. Potamianos[46], I. N. Potrap[79], C. J. Potter[32], H. Potti[11], T. Poulsen[96], J. Poveda[36], T. D. Powell[149], G. Pownall[46], M. E. Pozo Astigarraga[36], P. Pralavorio[101], S. Prell[78], D. Price[100], M. Primavera[67a], S. Prince[103], M. L. Proffitt[148], N. Proklova[112], K. Prokofiev[63c], F. Prokoshin[147b], S. Protopopescu[29], J. Proudfoot[6], M. Przybycien[83a], D. Pudzha[138], A. Puri[173], P. Puzo[132], J. Qian[105], Y. Qin[100], A. Quadt[53], M. Queitsch-Maitland[46], A. Qureshi[1], P. Rados[104], F. Ragusa[68a,68b], G. Rahal[97], J. A. Raine[54], S. Rajagopalan[29], A. Ramirez Morales[92], K. Ran[15d], T. Rashid[132], S. Raspopov[5], D. M. Rauch[46], F. Rauscher[114], S. Rave[99], B. Ravina[149], I. Ravinovich[180], J. H. Rawling[100], M. Raymond[36], A. L. Read[134], N. P. Readioff[58], M. Reale[67a,67b], D. M. Rebuzzi[70a,70b], A. Redelbach[177], G. Redlinger[29], K. Reeves[43], L. Rehnisch[19], J. Reichert[137], D. Reikher[161], A. Reiss[99], A. Rej[151], C. Rembser[36], M. Renda[27b], M. Rescigno[72a], S. Resconi[68a], E. D. Resseguie[137], S. Rettie[175], E. Reynolds[21], O. L. Rezanova[122a,122b], P. Reznicek[143], E. Ricci[75a,75b], R. Richter[115], S. Richter[46], E. Richter-Was[83b], O. Ricken[24], M. Ridel[136], P. Rieck[115], C. J. Riegel[182], O. Rifki[46], M. Rijssenbeek[155], A. Rimoldi[70a,70b], M. Rimoldi[46], L. Rinaldi[23b], G. Ripellino[154], B. Ristić[89], I. Riu[14], J. C. Rivera Vergara[176], F. Rizatdinova[129],

E. Rizvi[92], C. Rizzi[36], R. T. Roberts[100], S. H. Robertson[103,af], M. Robin[46], D. Robinson[32], J. E. M. Robinson[46], C. M. Robles Gajardo[147b], A. Robson[57], E. Rocco[99], C. Roda[71a,71b], S. Rodriguez Bosca[174], A. Rodriguez Perez[14], D. Rodriguez Rodriguez[174], A. M. Rodríguez Vera[168b], S. Roe[36], O. Røhne[134], R. Röhrig[115], C. P. A. Roland[65], J. Roloff[59], A. Romaniouk[112], M. Romano[23a,23b], N. Rompotis[90], M. Ronzani[124], L. Roos[136], S. Rosati[72a], K. Rosbach[52], G. Rosin[102], B. J. Rosser[137], E. Rossi[46], E. Rossi[74a,74b], E. Rossi[69a,69b], L. P. Rossi[55b], L. Rossini[68a,68b], R. Rosten[14], M. Rotaru[27b], J. Rothberg[148], D. Rousseau[132], G. Rovelli[70a,70b], D. Roy[33c], A. Rozanov[101], Y. Rozen[160], X. Ruan[33c], F. Rubbo[153], F. Rühr[52], A. Ruiz-Martinez[174], A. Rummler[36], Z. Rurikova[52], N. A. Rusakovich[79], H. L. Russell[103], L. Rustige[38,47], J. P. Rutherfoord[7], E. M. Rüttinger[46,l], Y. F. Ryabov[138], M. Rybar[39], G. Rybkin[132], A. Ryzhov[123], G. F. Rzehorz[53], P. Sabatini[53], G. Sabato[120], S. Sacerdoti[132], H.F-W. Sadrozinski[146], R. Sadykov[79], F. Safai Tehrani[72a], B. Safarzadeh Samani[156], P. Saha[121], S. Saha[103], M. Sahinsoy[61a], A. Sahu[182], M. Saimpert[46], M. Saito[163], T. Saito[163], H. Sakamoto[163], A. Sakharov[124,ap], D. Salamani[54], G. Salamanna[74a,74b], J. E. Salazar Loyola[147b], P. H. Sales De Bruin[172], A. Salnikov[153], J. Salt[174], D. Salvatore[41a,41b], F. Salvatore[156], A. Salvucci[63a,63b,63c], A. Salzburger[36], J. Samarati[36], D. Sammel[52], D. Sampsonidis[162], D. Sampsonidou[162], J. Sánchez[174], A. Sanchez Pineda[66a,66c], H. Sandaker[134], C. O. Sander[46], I. G. Sanderswood[89], M. Sandhoff[182], C. Sandoval[22], D. P. C. Sankey[144], M. Sannino[55a,55b], Y. Sano[117], A. Sansoni[51], C. Santoni[38], H. Santos[140a,140b], S. N. Santpur[18], A. Santra[174], A. Sapronov[79], J. G. Saraiva[140a,140d], O. Sasaki[81], K. Sato[169], E. Sauvan[5], P. Savard[167,ay], N. Savic[115], R. Sawada[163], C. Sawyer[144], L. Sawyer[95,an], C. Sbarra[23b], A. Sbrizzi[23a], T. Scanlon[94], J. Schaarschmidt[148], P. Schacht[115], B. M. Schachtner[114], D. Schaefer[37], L. Schaefer[137], J. Schaeffer[99], S. Schaepe[36], U. Schäfer[99], A. C. Schaffer[132], D. Schaile[114], R. D. Schamberger[155], N. Scharmberg[100], V. A. Schegelsky[138], D. Scheirich[143], F. Schenck[19], M. Schernau[171], C. Schiavi[55a,55b], S. Schier[146], L. K. Schildgen[24], Z. M. Schillaci[26], E. J. Schioppa[36], M. Schioppa[41a,41b], K. E. Schleicher[52], S. Schlenker[36], K. R. Schmidt-Sommerfeld[115], K. Schmieden[36], C. Schmitt[99], S. Schmitt[46], S. Schmitz[99], J. C. Schmoeckel[46], U. Schnoor[52], L. Schoeffel[145], A. Schoening[61b], P. G. Scholer[52], E. Schopf[135], M. Schott[99], J. F. P. Schouwenberg[119], J. Schovancova[36], S. Schramm[54], F. Schroeder[182], A. Schulte[99], H-C. Schultz-Coulon[61a], M. Schumacher[52], B. A. Schumm[146], Ph. Schune[145], A. Schwartzman[153], T. A. Schwarz[105], Ph. Schwemling[145], R. Schwienhorst[106], A. Sciandra[146], G. Sciolla[26], M. Scodeggio[46], M. Scornajenghi[41a,41b], F. Scuri[71a], F. Scutti[104], L. M. Scyboz[115], C. D. Sebastiani[72a,72b], P. Seema[19], S. C. Seidel[118], A. Seiden[146], T. Seiss[37], J. M. Seixas[80b], G. Sekhniaidze[69a], K. Sekhon[105], S. J. Sekula[42], N. Semprini-Cesari[23a,23b], S. Sen[49], S. Senkin[38], C. Serfon[76], L. Serin[132], L. Serkin[66a,66b], M. Sessa[60a], H. Severini[128], F. Sforza[170], A. Sfyrla[54], E. Shabalina[53], J. D. Shahinian[146], N. W. Shaikh[45a,45b], D. Shaked Renous[180], L. Y. Shan[15a], R. Shang[173], J. T. Shank[25], M. Shapiro[18], A. S. Sharma[1], A. Sharma[135], P. B. Shatalov[111], K. Shaw[156], S. M. Shaw[100], A. Shcherbakova[138], Y. Shen[128], N. Sherafati[34], A. D. Sherman[25], P. Sherwood[94], L. Shi[158,au], S. Shimizu[81], C. O. Shimmin[183], Y. Shimogama[179], M. Shimojima[116], I. P. J. Shipsey[135], S. Shirabe[87], M. Shiyakova[79,ac], J. Shlomi[180], A. Shmeleva[110], M. J. Shochet[37], S. Shojaii[104], D. R. Shope[128], S. Shrestha[126], E. Shulga[112], P. Sicho[141], A. M. Sickles[173], P. E. Sidebo[154], E. Sideras Haddad[33c], O. Sidiropoulou[36], A. Sidoti[23a,23b], F. Siegert[48], Dj. Sijacki[16], M. Silva Jr.[181], M. V. Silva Oliveira[80a], S. B. Silverstein[45a], S. Simion[132], E. Simioni[99], R. Simoniello[99], P. Sinervo[167], V. Sinetckii[110,113], N. B. Sinev[131], M. Sioli[23a,23b], I. Siral[105], S. Yu. Sivoklokov[113], J. Sjölin[45a,45b], E. Skorda[96], P. Skubic[128], M. Slawinska[84], K. Sliwa[170], R. Slovak[143], V. Smakhtin[180], B. H. Smart[144], J. Smiesko[28a], N. Smirnov[112], S. Yu. Smirnov[112], Y. Smirnov[112], L. N. Smirnova[113,v], O. Smirnova[96], J. W. Smith[53], M. Smizanska[89], K. Smolek[142], A. Smykiewicz[84], A. A. Snesarev[110], H. L. Snoek[120], I. M. Snyder[131], S. Snyder[29], R. Sobie[176,af], A. M. Soffa[171], A. Soffer[161], A. Søgaard[50], F. Sohns[53], C. A. Solans Sanchez[36], E. Yu. Soldatov[112], U. Soldevila[174], A. A. Solodkov[123], A. Soloshenko[79], O. V. Solovyanov[123], V. Solovyev[138], P. Sommer[149], H. Son[170], W. Song[144], W. Y. Song[168b], A. Sopczak[142], F. Sopkova[28b], C. L. Sotiropoulou[71a,71b], S. Sottocornola[70a,70b], R. Soualah[66a,66c,h], A. M. Soukharev[122a,122b], D. South[46], S. Spagnolo[67a,67b], M. Spalla[115], M. Spangenberg[178], F. Spanò[93], D. Sperlich[52], T. M. Spieker[61a], R. Spighi[23b], G. Spigo[36], M. Spina[156], D. P. Spiteri[57], M. Spousta[143], A. Stabile[68a,68b], B. L. Stamas[121], R. Stamen[61a], M. Stamenkovic[120], E. Stanecka[84], R. W. Stanek[6], B. Stanislaus[135], M. M. Stanitzki[46], M. Stankaityte[135], B. Stapf[120], E. A. Starchenko[123], G. H. Stark[146], J. Stark[58], S. H. Stark[40], P. Staroba[141], P. Starovoitov[61a], S. Stärz[103], R. Staszewski[84], G. Stavropoulos[44], M. Stegler[46], P. Steinberg[29], A. L. Steinhebel[131], B. Stelzer[152], H. J. Stelzer[139], O. Stelzer-Chilton[168a], H. Stenzel[56], T. J. Stevenson[156], G. A. Stewart[36], M. C. Stockton[36], G. Stoicea[27b], M. Stolarski[140a], P. Stolte[53], S. Stonjek[115], A. Straessner[48], J. Strandberg[154], S. Strandberg[45a,45b], M. Strauss[128], P. Strizenec[28b], R. Ströhmer[177], D. M. Strom[131], R. Stroynowski[42], A. Strubig[50], S. A. Stucci[29], B. Stugu[17], J. Stupak[128], N. A. Styles[46], D. Su[153], S. Suchek[61a], V. V. Sulin[110], M. J. Sullivan[90], D. M. S. Sultan[54], S. Sultansoy[4c], T. Sumida[85], S. Sun[105], X. Sun[3], K. Suruliz[156], C. J. E. Suster[157], M. R. Sutton[156], S. Suzuki[81], M. Svatos[141], M. Swiatlowski[37], S. P. Swift[2], T. Swirski[177], A. Sydorenko[99], I. Sykora[28a], M. Sykora[143], T. Sykora[143], D. Ta[99], K. Tackmann[46,aa], J. Taenzer[161], A. Taffard[171], R. Tafirout[168a], H. Takai[29], R. Takashima[86], K. Takeda[82], T. Takeshita[150], E. P. Takeva[50], Y. Takubo[81],

M. Talby[101], A. A. Talyshev[122a,122b], N. M. Tamir[161], J. Tanaka[163], M. Tanaka[165], R. Tanaka[132], S. Tapia Araya[173], S. Tapprogge[99], A. Tarek Abouelfadl Mohamed[136], S. Tarem[160], G. Tarna[27b,d], G. F. Tartarelli[68a], P. Tas[143], M. Tasevsky[141], T. Tashiro[85], E. Tassi[41a,41b], A. Tavares Delgado[140a,140b], Y. Tayalati[35e], A. J. Taylor[50], G. N. Taylor[104], W. Taylor[168b], A. S. Tee[89], R. Teixeira De Lima[153], P. Teixeira-Dias[93], H. Ten Kate[36], J. J. Teoh[120], S. Terada[81], K. Terashi[163], J. Terron[98], S. Terzo[14], M. Testa[51], R. J. Teuscher[167,af], S. J. Thais[183], T. Theveneaux-Pelzer[46], F. Thiele[40], D. W. Thomas[93], J. O. Thomas[42], J. P. Thomas[21], A. S. Thompson[57], P. D. Thompson[21], L. A. Thomsen[183], E. Thomson[137], Y. Tian[39], R. E. Ticse Torres[53], V. O. Tikhomirov[110,ar], Yu. A. Tikhonov[122a,122b], S. Timoshenko[112], P. Tipton[183], S. Tisserant[101], K. Todome[23a,23b], S. Todorova-Nova[5], S. Todt[48], J. Tojo[87], S. Tokár[28a], K. Tokushuku[81], E. Tolley[126], K. G. Tomiwa[33c], M. Tomoto[117], L. Tompkins[153,r], K. Toms[118], B. Tong[59], P. Tornambe[102], E. Torrence[131], H. Torres[48], E. Torró Pastor[148], C. Tosciri[135], J. Toth[101,ad], D. R. Tovey[149], A. Traet[17], C. J. Treado[124], T. Trefzger[177], F. Tresoldi[156], A. Tricoli[29], I. M. Trigger[168a], S. Trincaz-Duvoid[136], W. Trischuk[167], B. Trocmé[58], A. Trofymov[132], C. Troncon[68a], M. Trovatelli[176], F. Trovato[156], L. Truong[33b], M. Trzebinski[84], A. Trzupek[84], F. Tsai[46], J.C-L. Tseng[135], P. V. Tsiareshka[107,al], A. Tsirigotis[162], N. Tsirintanis[9], V. Tsiskaridze[155], E. G. Tskhadadze[159a], M. Tsopoulou[162], I. I. Tsukerman[111], V. Tsulaia[18], S. Tsuno[81], D. Tsybychev[155], Y. Tu[63b], A. Tudorache[27b], V. Tudorache[27b], T. T. Tulbure[27a], A. N. Tuna[59], S. Turchikhin[79], D. Turgeman[180], I. Turk Cakir[4b,w], R. J. Turner[21], R. T. Turra[68a], P. M. Tuts[39], S. Tzamarias[162], E. Tzovara[99], G. Ucchielli[47], K. Uchida[163], I. Ueda[81], M. Ughetto[45a,45b], F. Ukegawa[169], G. Unal[36], A. Undrus[29], G. Unel[171], F. C. Ungaro[104], Y. Unno[81], K. Uno[163], J. Urban[28b], P. Urquijo[104], G. Usai[8], J. Usui[81], L. Vacavant[101], V. Vacek[142], B. Vachon[103], K. O. H. Vadla[134], A. Vaidya[94], C. Valderanis[114], E. Valdes Santurio[45a,45b], M. Valente[54], S. Valentinetti[23a,23b], A. Valero[174], L. Valéry[46], R. A. Vallance[21], A. Vallier[36], J. A. Valls Ferrer[174], T. R. Van Daalen[14], P. Van Gemmeren[6], I. Van Vulpen[120], M. Vanadia[73a,73b], W. Vandelli[36], A. Vaniachine[166], D. Vannicola[72a,72b], R. Vari[72a], E. W. Varnes[7], C. Varni[55a,55b], T. Varol[42], D. Varouchas[132], K. E. Varvell[157], M. E. Vasile[27b], G. A. Vasquez[176], J. G. Vasquez[183], F. Vazeille[38], D. Vazquez Furelos[14], T. Vazquez Schroeder[36], J. Veatch[53], V. Vecchio[74a,74b], M. J. Veen[120], L. M. Veloce[167], F. Veloso[140a,140c], S. Veneziano[72a], A. Ventura[67a,67b], N. Venturi[36], A. Verbytskyi[115], V. Vercesi[70a], M. Verducci[74a,74b], C. M. Vergel Infante[78], C. Vergis[24], W. Verkerke[120], A. T. Vermeulen[120], J. C. Vermeulen[120], M. C. Vetterli[152,ay], N. Viaux Maira[147b], M. Vicente Barreto Pinto[54], T. Vickey[149], O. E. Vickey Boeriu[149], G. H. A. Viehhauser[135], L. Vigani[135], M. Villa[23a,23b], M. Villaplana Perez[68a,68b], E. Vilucchi[51], M. G. Vincter[34], V. B. Vinogradov[79], A. Vishwakarma[46], C. Vittori[23a,23b], I. Vivarelli[156], M. Vogel[182], P. Vokac[142], S. E. von Buddenbrock[33c], E. Von Toerne[24], V. Vorobel[143], K. Vorobev[112], M. Vos[174], J. H. Vossebeld[90], M. Vozak[100], N. Vranjes[16], M. Vranjes Milosavljevic[16], V. Vrba[142], M. Vreeswijk[120], T. Šfiligoj[91], R. Vuillermet[36], I. Vukotic[37], T. Ženiš[28a], L. Živković[16], P. Wagner[24], W. Wagner[182], J. Wagner-Kuhr[114], H. Wahlberg[88], K. Wakamiya[82], V. M. Walbrecht[115], J. Walder[89], R. Walker[114], S. D. Walker[93], W. Walkowiak[151], V. Wallangen[45a,45b], A. M. Wang[59], C. Wang[60b], F. Wang[181], H. Wang[18], H. Wang[3], J. Wang[157], J. Wang[61b], P. Wang[42], Q. Wang[128], R.-J. Wang[99], R. Wang[60a], R. Wang[6], S. M. Wang[158], W. T. Wang[60a], W. Wang[15c,ag], W. X. Wang[60a,ag], Y. Wang[60a,ao], Z. Wang[60c], C. Wanotayaroj[46], A. Warburton[103], C. P. Ward[32], D. R. Wardrope[94], N. Warrack[57], A. Washbrook[50], A. T. Watson[21], M. F. Watson[21], G. Watts[148], B. M. Waugh[94], A. F. Webb[11], S. Webb[99], C. Weber[183], M. S. Weber[20], S. A. Weber[34], S. M. Weber[61a], A. R. Weidberg[135], J. Weingarten[47], M. Weirich[99], C. Weiser[52], P. S. Wells[36], T. Wenaus[29], T. Wengler[36], S. Wenig[36], N. Wermes[24], M. D. Werner[78], M. Wessels[61a], T. D. Weston[20], K. Whalen[131], N. L. Whallon[148], A. M. Wharton[89], A. S. White[105], A. White[8], M. J. White[1], D. Whiteson[171], B. W. Whitmore[89], W. Wiedenmann[181], M. Wielers[144], N. Wieseotte[99], C. Wiglesworth[40], L. A. M. Wiik-Fuchs[52], F. Wilk[100], H. G. Wilkens[36], L. J. Wilkins[93], H. H. Williams[137], S. Williams[32], C. Willis[106], S. Willocq[102], J. A. Wilson[21], I. Wingerter-Seez[5], E. Winkels[156], F. Winklmeier[131], O. J. Winston[156], B. T. Winter[52], M. Wittgen[153], M. Wobisch[95], A. Wolf[99], T. M. H. Wolf[120], R. Wolff[101], R. W. Wölker[135], J. Wollrath[52], M. W. Wolter[84], H. Wolters[140a,140c], V. W. S. Wong[175], N. L. Woods[146], S. D. Worm[21], B. K. Wosiek[84], K. W. Woźniak[84], K. Wraight[57], S. L. Wu[181], X. Wu[54], Y. Wu[60a], T. R. Wyatt[100], B. M. Wynne[50], S. Xella[40], Z. Xi[105], L. Xia[178], D. Xu[15a], H. Xu[60a,d], L. Xu[29], T. Xu[145], W. Xu[105], Z. Xu[60b], Z. Xu[153], B. Yabsley[157], S. Yacoob[33a], K. Yajima[133], D. P. Yallup[94], D. Yamaguchi[165], Y. Yamaguchi[165], A. Yamamoto[81], F. Yamane[82], M. Yamatani[163], T. Yamazaki[163], Y. Yamazaki[82], Z. Yan[25], H. J. Yang[60c,60d], H. T. Yang[18], S. Yang[77], X. Yang[60b,58], Y. Yang[163], W-M. Yao[18], Y. C. Yap[46], Y. Yasu[81], E. Yatsenko[60c,60d], J. Ye[42], S. Ye[29], I. Yeletskikh[79], M. R. Yexley[89], E. Yigitbasi[25], K. Yorita[179], K. Yoshihara[137], C. J. S. Young[36], C. Young[153], J. Yu[78], R. Yuan[60b,j], X. Yue[61a], S. P. Y. Yuen[24], B. Zabinski[84], G. Zacharis[10], E. Zaffaroni[54], J. Zahreddine[136], A. M. Zaitsev[123,aq], T. Zakareishvili[159b], N. Zakharchuk[34], S. Zambito[59], D. Zanzi[36], D. R. Zaripovas[57], S. V. Zeißner[47], C. Zeitnitz[182], G. Zemaityte[135], J. C. Zeng[173], O. Zenin[123], D. Zerwas[132], M. Zgubič[135], D. F. Zhang[15b], F. Zhang[181], G. Zhang[15b], H. Zhang[15c], J. Zhang[6], L. Zhang[15c], L. Zhang[60a], M. Zhang[173], R. Zhang[24], X. Zhang[60b], Y. Zhang[15d], Z. Zhang[63a], Z. Zhang[132], P. Zhao[49], Y. Zhao[60b], Z. Zhao[60a], A. Zhemchugov[79], Z. Zheng[105], D. Zhong[173], B. Zhou[105], C. Zhou[181], M. S. Zhou[15d], M. Zhou[155], N. Zhou[60c], Y. Zhou[7], C. G. Zhu[60b], H. L. Zhu[60a], H. Zhu[15a],

J. Zhu[105], Y. Zhu[60a], X. Zhuang[15a], K. Zhukov[110], V. Zhulanov[122a,122b], D. Zieminska[65], N. I. Zimine[79], S. Zimmermann[52], Z. Zinonos[115], M. Ziolkowski[151], G. Zobernig[181], A. Zoccoli[23a,23b], K. Zoch[53], T. G. Zorbas[149], R. Zou[37], L. Zwalinski[36]

1. Department of Physics, University of Adelaide, Adelaide, Australia
2. Physics Department, SUNY Albany, Albany, NY, USA
3. Department of Physics, University of Alberta, Edmonton, AB, Canada
4. (a)Department of Physics, Ankara University, Ankara, Turkey; (b)Istanbul Aydin University, Istanbul, Turkey; (c)Division of Physics, TOBB University of Economics and Technology, Ankara, Turkey
5. LAPP, Université Grenoble Alpes, Université Savoie Mont Blanc, CNRS/IN2P3, Annecy, France
6. High Energy Physics Division, Argonne National Laboratory, Argonne, IL, USA
7. Department of Physics, University of Arizona, Tucson, AZ, USA
8. Department of Physics, University of Texas at Arlington, Arlington, TX, USA
9. Physics Department, National and Kapodistrian University of Athens, Athens, Greece
10. Physics Department, National Technical University of Athens, Zografou, Greece
11. Department of Physics, University of Texas at Austin, Austin, TX, USA
12. (a)Bahcesehir University, Faculty of Engineering and Natural Sciences, Istanbul, Turkey; (b)Istanbul Bilgi University, Faculty of Engineering and Natural Sciences, Istanbul, Turkey; (c)Department of Physics, Bogazici University, Istanbul, Turkey; (d)Department of Physics Engineering, Gaziantep University, Gaziantep, Turkey
13. Institute of Physics, Azerbaijan Academy of Sciences, Baku, Azerbaijan
14. Institut de Física d'Altes Energies (IFAE), Barcelona Institute of Science and Technology, Barcelona, Spain
15. (a)Institute of High Energy Physics, Chinese Academy of Sciences, Beijing, China; (b)Physics Department, Tsinghua University, Beijing, China; (c)Department of Physics, Nanjing University, Nanjing, China; (d)University of Chinese Academy of Science (UCAS), Beijing, China
16. Institute of Physics, University of Belgrade, Belgrade, Serbia
17. Department for Physics and Technology, University of Bergen, Bergen, Norway
18. Physics Division, Lawrence Berkeley National Laboratory and University of California, Berkeley, CA, USA
19. Institut für Physik, Humboldt Universität zu Berlin, Berlin, Germany
20. Albert Einstein Center for Fundamental Physics and Laboratory for High Energy Physics, University of Bern, Bern, Switzerland
21. School of Physics and Astronomy, University of Birmingham, Birmingham, UK
22. Facultad de Ciencias y Centro de Investigaciónes, Universidad Antonio Nariño, Bogota, Colombia
23. (a)Dipartimento di Fisica, INFN Bologna and Universita' di Bologna, Bologna, Italy; (b)INFN Sezione di Bologna, Bologna, Italy
24. Physikalisches Institut, Universität Bonn, Bonn, Germany
25. Department of Physics, Boston University, Boston, MA, USA
26. Department of Physics, Brandeis University, Waltham, MA, USA
27. (a)Transilvania University of Brasov, Brasov, Romania; (b)Horia Hulubei National Institute of Physics and Nuclear Engineering, Bucharest, Romania; (c)Department of Physics, Alexandru Ioan Cuza University of Iasi, Iasi, Romania; (d)Physics Department, National Institute for Research and Development of Isotopic and Molecular Technologies, Cluj-Napoca, Romania; (e)University Politehnica Bucharest, Bucharest, Romania; (f)West University in Timisoara, Timisoara, Romania
28. (a)Faculty of Mathematics, Physics and Informatics, Comenius University, Bratislava, Slovakia; (b)Department of Subnuclear Physics, Institute of Experimental Physics of the Slovak Academy of Sciences, Kosice, Slovak Republic
29. Physics Department, Brookhaven National Laboratory, Upton, NY, USA
30. Departamento de Física, Universidad de Buenos Aires, Buenos Aires, Argentina
31. California State University, CA, USA
32. Cavendish Laboratory, University of Cambridge, Cambridge, UK
33. (a)Department of Physics, University of Cape Town, Cape Town, South Africa; (b)Department of Mechanical Engineering Science, University of Johannesburg, Johannesburg, South Africa; (c)School of Physics, University of the Witwatersrand, Johannesburg, South Africa
34. Department of Physics, Carleton University, Ottawa, ON, Canada
35. (a)Faculté des Sciences Ain Chock, Réseau Universitaire de Physique des Hautes Energies - Université Hassan II, Casablanca, Morocco; (b)Faculté des Sciences, Université Ibn-Tofail, Kénitra, Morocco; (c)Faculté des Sciences

Semlalia, Université Cadi Ayyad, LPHEA-Marrakech, Morocco; [d]Faculté des Sciences, Université Mohamed Premier and LPTPM, Oujda, Morocco; [e]Faculté des sciences, Université Mohammed V, Rabat, Morocco

36 CERN, Geneva, Switzerland

37 Enrico Fermi Institute, University of Chicago, Chicago, IL, USA

38 LPC, Université Clermont Auvergne, CNRS/IN2P3, Clermont-Ferrand, France

39 Nevis Laboratory, Columbia University, Irvington, NY, USA

40 Niels Bohr Institute, University of Copenhagen, Copenhagen, Denmark

41 [a]Dipartimento di Fisica, Università della Calabria, Rende, Italy; [b]INFN Gruppo Collegato di Cosenza, Laboratori Nazionali di Frascati, Frascati, Italy

42 Physics Department, Southern Methodist University, Dallas, TX, USA

43 Physics Department, University of Texas at Dallas, Richardson, TX, USA

44 National Centre for Scientific Research "Demokritos", Agia Paraskevi, Greece

45 [a]Department of Physics, Stockholm University, Stockholm, Sweden; [b]Oskar Klein Centre, Stockholm, Sweden

46 Deutsches Elektronen-Synchrotron DESY, Hamburg and Zeuthen, Germany

47 Lehrstuhl für Experimentelle Physik IV, Technische Universität Dortmund, Dortmund, Germany

48 Institut für Kern- und Teilchenphysik, Technische Universität Dresden, Dresden, Germany

49 Department of Physics, Duke University, Durham, NC, USA

50 SUPA-School of Physics and Astronomy, University of Edinburgh, Edinburgh, UK

51 INFN e Laboratori Nazionali di Frascati, Frascati, Italy

52 Physikalisches Institut, Albert-Ludwigs-Universität Freiburg, Freiburg, Germany

53 II. Physikalisches Institut, Georg-August-Universität Göttingen, Göttingen, Germany

54 Département de Physique Nucléaire et Corpusculaire, Université de Genève, Geneva, Switzerland

55 [a]Dipartimento di Fisica, Università di Genova, Genoa, Italy; [b]INFN Sezione di Genova, Genoa, Italy

56 II. Physikalisches Institut, Justus-Liebig-Universität Giessen, Giessen, Germany

57 SUPA-School of Physics and Astronomy, University of Glasgow, Glasgow, UK

58 LPSC, Université Grenoble Alpes, CNRS/IN2P3, Grenoble INP, Grenoble, France

59 Laboratory for Particle Physics and Cosmology, Harvard University, Cambridge, MA, USA

60 [a]Department of Modern Physics and State Key Laboratory of Particle Detection and Electronics, University of Science and Technology of China, Hefei, China; [b]Institute of Frontier and Interdisciplinary Science and Key Laboratory of Particle Physics and Particle Irradiation (MOE), Shandong University, Qingdao, China; [c]School of Physics and Astronomy, Shanghai Jiao Tong University, KLPPAC-MoE, SKLPPC, Shanghai, China; [d]Tsung-Dao Lee Institute, Shanghai, China

61 [a]Kirchhoff-Institut für Physik, Ruprecht-Karls-Universität Heidelberg, Heidelberg, Germany; [b]Physikalisches Institut, Ruprecht-Karls-Universität Heidelberg, Heidelberg, Germany

62 Faculty of Applied Information Science, Hiroshima Institute of Technology, Hiroshima, Japan

63 [a]Department of Physics, Chinese University of Hong Kong, Shatin, N.T., Hong Kong, China; [b]Department of Physics, University of Hong Kong, Hong Kong, China; [c]Department of Physics and Institute for Advanced Study, Hong Kong University of Science and Technology, Clear Water Bay, Kowloon, Hong Kong, China

64 Department of Physics, National Tsing Hua University, Hsinchu, Taiwan

65 Department of Physics, Indiana University, Bloomington, IN, USA

66 [a]INFN Gruppo Collegato di Udine, Sezione di Trieste, Udine, Italy; [b]ICTP, Trieste, Italy; [c]Dipartimento Politecnico di Ingegneria e Architettura, Università di Udine, Udine, Italy

67 [a]INFN Sezione di Lecce, Lecce, Italy; [b]Dipartimento di Matematica e Fisica, Università del Salento, Lecce, Italy

68 [a]INFN Sezione di Milano, Milan, Italy; [b]Dipartimento di Fisica, Università di Milano, Milan, Italy

69 [a]INFN Sezione di Napoli, Naples, Italy; [b]Dipartimento di Fisica, Università di Napoli, Naples, Italy

70 [a]INFN Sezione di Pavia, Pavia, Italy; [b]Dipartimento di Fisica, Università di Pavia, Pavia, Italy

71 [a]INFN Sezione di Pisa, Pisa, Italy; [b]Dipartimento di Fisica E. Fermi, Università di Pisa, Pisa, Italy

72 [a]INFN Sezione di Roma, Rome, Italy; [b]Dipartimento di Fisica, Sapienza Università di Roma, Rome, Italy

73 [a]INFN Sezione di Roma Tor Vergata, Rome, Italy; [b]Dipartimento di Fisica, Università di Roma Tor Vergata, Rome, Italy

74 [a]INFN Sezione di Roma Tre, Rome, Italy; [b]Dipartimento di Matematica e Fisica, Università Roma Tre, Rome, Italy

75 [a]INFN-TIFPA, Povo, Italy; [b]Università degli Studi di Trento, Trento, Italy

76 Institut für Astro- und Teilchenphysik, Leopold-Franzens-Universität, Innsbruck, Austria

[77] University of Iowa, Iowa City, IA, USA

[78] Department of Physics and Astronomy, Iowa State University, Ames, IA, USA

[79] Joint Institute for Nuclear Research, Dubna, Russia

[80] (a)Departamento de Engenharia Elétrica, Universidade Federal de Juiz de Fora (UFJF), Juiz de Fora, Brazil; (b)Universidade Federal do Rio De Janeiro COPPE/EE/IF, Rio de Janeiro, Brazil; (c)Universidade Federal de São João del Rei (UFSJ), São João del Rei, Brazil; (d)Instituto de Física, Universidade de São Paulo, São Paulo, Brazil

[81] KEK, High Energy Accelerator Research Organization, Tsukuba, Japan

[82] Graduate School of Science, Kobe University, Kobe, Japan

[83] (a)AGH University of Science and Technology, Faculty of Physics and Applied Computer Science, Krakow, Poland; (b)Marian Smoluchowski Institute of Physics, Jagiellonian University, Krakow, Poland

[84] Institute of Nuclear Physics Polish Academy of Sciences, Krakow, Poland

[85] Faculty of Science, Kyoto University, Kyoto, Japan

[86] Kyoto University of Education, Kyoto, Japan

[87] Research Center for Advanced Particle Physics and Department of Physics, Kyushu University, Fukuoka , Japan

[88] Instituto de Física La Plata, Universidad Nacional de La Plata and CONICET, La Plata, Argentina

[89] Physics Department, Lancaster University, Lancaster, UK

[90] Oliver Lodge Laboratory, University of Liverpool, Liverpool, UK

[91] Department of Experimental Particle Physics, Jožef Stefan Institute and Department of Physics, University of Ljubljana, Ljubljana, Slovenia

[92] School of Physics and Astronomy, Queen Mary University of London, London, UK

[93] Department of Physics, Royal Holloway University of London, Egham, UK

[94] Department of Physics and Astronomy, University College London, London, UK

[95] Louisiana Tech University, Ruston, LA, USA

[96] Fysiska institutionen, Lunds universitet, Lund, Sweden

[97] Centre de Calcul de l'Institut National de Physique Nucléaire et de Physique des Particules (IN2P3), Villeurbanne, France

[98] Departamento de Física Teorica C-15 and CIAFF, Universidad Autónoma de Madrid, Madrid, Spain

[99] Institut für Physik, Universität Mainz, Mainz, Germany

[100] School of Physics and Astronomy, University of Manchester, Manchester, UK

[101] CPPM, Aix-Marseille Université, CNRS/IN2P3, Marseille, France

[102] Department of Physics, University of Massachusetts, Amherst, MA, USA

[103] Department of Physics, McGill University, Montreal, QC, Canada

[104] School of Physics, University of Melbourne, Melbourne, VIC, Australia

[105] Department of Physics, University of Michigan, Ann Arbor, MI, USA

[106] Department of Physics and Astronomy, Michigan State University, East Lansing, MI, USA

[107] B.I. Stepanov Institute of Physics, National Academy of Sciences of Belarus, Minsk, Belarus

[108] Research Institute for Nuclear Problems of Byelorussian State University, Minsk, Belarus

[109] Group of Particle Physics, University of Montreal, Montreal, QC, Canada

[110] P.N. Lebedev Physical Institute of the Russian Academy of Sciences, Moscow, Russia

[111] Institute for Theoretical and Experimental Physics of the National Research Centre Kurchatov Institute, Moscow, Russia

[112] National Research Nuclear University MEPhI, Moscow, Russia

[113] D.V. Skobeltsyn Institute of Nuclear Physics, M.V. Lomonosov Moscow State University, Moscow, Russia

[114] Fakultät für Physik, Ludwig-Maximilians-Universität München, Munich, Germany

[115] Max-Planck-Institut für Physik (Werner-Heisenberg-Institut), Munich, Germany

[116] Nagasaki Institute of Applied Science, Nagasaki, Japan

[117] Graduate School of Science and Kobayashi-Maskawa Institute, Nagoya University, Nagoya, Japan

[118] Department of Physics and Astronomy, University of New Mexico, Albuquerque, NM, USA

[119] Institute for Mathematics, Astrophysics and Particle Physics, Radboud University Nijmegen/Nikhef, Nijmegen, The Netherlands

[120] Nikhef National Institute for Subatomic Physics and University of Amsterdam, Amsterdam, The Netherlands

[121] Department of Physics, Northern Illinois University, DeKalb, IL, USA

[122] (a)Budker Institute of Nuclear Physics and NSU, SB RAS, Novosibirsk, Russia; (b)Novosibirsk State University, Novosibirsk, Russia

[123] Institute for High Energy Physics of the National Research Centre Kurchatov Institute, Protvino, Russia

[124] Department of Physics, New York University, New York, NY, USA

[125] Ochanomizu University, Otsuka, Bunkyo-ku, Tokyo, Japan

[126] Ohio State University, Columbus, OH, USA

[127] Faculty of Science, Okayama University, Okayama, Japan

[128] Homer L. Dodge Department of Physics and Astronomy, University of Oklahoma, Norman, OK, USA

[129] Department of Physics, Oklahoma State University, Stillwater, OK, USA

[130] Palacký University, RCPTM, Joint Laboratory of Optics, Olomouc, Czech Republic

[131] Center for High Energy Physics, University of Oregon, Eugene, OR, USA

[132] LAL, Université Paris-Sud, CNRS/IN2P3, Université Paris-Saclay, Orsay, France

[133] Graduate School of Science, Osaka University, Osaka, Japan

[134] Department of Physics, University of Oslo, Oslo, Norway

[135] Department of Physics, Oxford University, Oxford, UK

[136] LPNHE, Sorbonne Université, Paris Diderot Sorbonne Paris Cité, CNRS/IN2P3, Paris, France

[137] Department of Physics, University of Pennsylvania, Philadelphia, PA, USA

[138] Konstantinov Nuclear Physics Institute of National Research Centre "Kurchatov Institute", PNPI, St. Petersburg, Russia

[139] Department of Physics and Astronomy, University of Pittsburgh, Pittsburgh, PA, USA

[140] (a)Laboratório de Instrumentação e Física Experimental de Partículas-LIP, Lisbon, Portugal; (b)Departamento de Física, Faculdade de Ciências, Universidade de Lisboa, Lisbon, Portugal; (c)Departamento de Física, Universidade de Coimbra, Coimbra, Portugal; (d)Centro de Física Nuclear da Universidade de Lisboa, Lisbon, Portugal; (e)Departamento de Física, Universidade do Minho, Braga, Portugal; (f)Universidad de Granada, Granada, Spain; (g)Dep Física and CEFITEC of Faculdade de Ciências e Tecnologia, Universidade Nova de Lisboa, Caparica, Portugal

[141] Institute of Physics of the Czech Academy of Sciences, Prague, Czech Republic

[142] Czech Technical University in Prague, Prague, Czech Republic

[143] Charles University, Faculty of Mathematics and Physics, Prague, Czech Republic

[144] Particle Physics Department, Rutherford Appleton Laboratory, Didcot, UK

[145] IRFU, CEA, Université Paris-Saclay, Gif-sur-Yvette, France

[146] Santa Cruz Institute for Particle Physics, University of California Santa Cruz, Santa Cruz, CA, USA

[147] (a)Departamento de Física, Pontificia Universidad Católica de Chile, Santiago, Chile; (b)Departamento de Física, Universidad Técnica Federico Santa María, Valparaíso, Chile

[148] Department of Physics, University of Washington, Seattle, WA, USA

[149] Department of Physics and Astronomy, University of Sheffield, Sheffield, UK

[150] Department of Physics, Shinshu University, Nagano, Japan

[151] Department Physik, Universität Siegen, Siegen, Germany

[152] Department of Physics, Simon Fraser University, Burnaby, BC, Canada

[153] SLAC National Accelerator Laboratory, Stanford, CA, USA

[154] Physics Department, Royal Institute of Technology, Stockholm, Sweden

[155] Departments of Physics and Astronomy, Stony Brook University, Stony Brook, NY, USA

[156] Department of Physics and Astronomy, University of Sussex, Brighton, UK

[157] School of Physics, University of Sydney, Sydney, Australia

[158] Institute of Physics, Academia Sinica, Taipei, Taiwan

[159] (a)E. Andronikashvili Institute of Physics, Iv. Javakhishvili Tbilisi State University, Tbilisi, Georgia; (b)High Energy Physics Institute, Tbilisi State University, Tbilisi, Georgia

[160] Department of Physics, Technion, Israel Institute of Technology, Haifa, Israel

[161] Raymond and Beverly Sackler School of Physics and Astronomy, Tel Aviv University, Tel Aviv, Israel

[162] Department of Physics, Aristotle University of Thessaloniki, Thessaloniki, Greece

[163] International Center for Elementary Particle Physics and Department of Physics, University of Tokyo, Tokyo, Japan

[164] Graduate School of Science and Technology, Tokyo Metropolitan University, Tokyo, Japan

[165] Department of Physics, Tokyo Institute of Technology, Tokyo, Japan

[166] Tomsk State University, Tomsk, Russia

[167] Department of Physics, University of Toronto, Toronto, ON, Canada

[168] (a)TRIUMF, Vancouver, BC, Canada; (b)Department of Physics and Astronomy, York University, Toronto, ON, Canada

[169] Division of Physics and Tomonaga Center for the History of the Universe, Faculty of Pure and Applied Sciences, University of Tsukuba, Tsukuba, Japan

[170] Department of Physics and Astronomy, Tufts University, Medford, MA, USA

[171] Department of Physics and Astronomy, University of California Irvine, Irvine, CA, USA

[172] Department of Physics and Astronomy, University of Uppsala, Uppsala, Sweden

[173] Department of Physics, University of Illinois, Urbana, IL, USA

[174] Instituto de Física Corpuscular (IFIC), Centro Mixto Universidad de Valencia - CSIC, Valencia, Spain

[175] Department of Physics, University of British Columbia, Vancouver, BC, Canada

[176] Department of Physics and Astronomy, University of Victoria, Victoria, BC, Canada

[177] Fakultät für Physik und Astronomie, Julius-Maximilians-Universität Würzburg, Würzburg, Germany

[178] Department of Physics, University of Warwick, Coventry, UK

[179] Waseda University, Tokyo, Japan

[180] Department of Particle Physics, Weizmann Institute of Science, Rehovot, Israel

[181] Department of Physics, University of Wisconsin, Madison, WI, USA

[182] Fakultät für Mathematik und Naturwissenschaften, Fachgruppe Physik, Bergische Universität Wuppertal, Wuppertal, Germany

[183] Department of Physics, Yale University, New Haven, CT, USA

[184] Yerevan Physics Institute, Yerevan, Armenia

[a] Also at Borough of Manhattan Community College, City University of New York, New York, NY, USA

[b] Also at Centre for High Performance Computing, CSIR Campus, Rosebank, Cape Town, South Africa

[c] Also at CERN, Geneva, Switzerland

[d] Also at CPPM, Aix-Marseille Université, CNRS/IN2P3, Marseille, France

[e] Also at Département de Physique Nucléaire et Corpusculaire, Université de Genève, Geneva, Switzerland

[f] Also at Departament de Fisica de la Universitat Autonoma de Barcelona, Barcelona, Spain

[g] Also at Departamento de Física, Instituto Superior Técnico, Universidade de Lisboa, Lisbon, Portugal

[h] Also at Department of Applied Physics and Astronomy, University of Sharjah, Sharjah, UAE

[i] Also at Department of Financial and Management Engineering, University of the Aegean, Chios, Greece

[j] Also at Department of Physics and Astronomy, Michigan State University, East Lansing, MI, USA

[k] Also at Department of Physics and Astronomy, University of Louisville, Louisville, KY, USA

[l] Also at Department of Physics and Astronomy, University of Sheffield, Sheffield, UK

[m] Also at Department of Physics, California State University, East Bay, USA

[n] Also at Department of Physics, California State University, Fresno, USA

[o] Also at Department of Physics, California State University, Sacramento, USA

[p] Also at Department of Physics, King's College London, London, UK

[q] Also at Department of Physics, St. Petersburg State Polytechnical University, St. Petersburg, Russia

[r] Also at Department of Physics, Stanford University, Stanford, CA, USA

[s] Also at Department of Physics, University of Adelaide, Adelaide, Australia

[t] Also at Department of Physics, University of Fribourg, Fribourg, Switzerland

[u] Also at Department of Physics, University of Michigan, Ann Arbor, MI, USA

[v] Also at Faculty of Physics, M.V. Lomonosov Moscow State University, Moscow, Russia

[w] Also at Giresun University, Faculty of Engineering, Giresun, Turkey

[x] Also at Graduate School of Science, Osaka University, Osaka, Japan

[y] Also at Hellenic Open University, Patras, Greece

[z] Also at Institucio Catalana de Recerca i Estudis Avancats, ICREA, Barcelona, Spain

[aa] Also at Institut für Experimentalphysik, Universität Hamburg, Hamburg, Germany

[ab] Also at Institute for Mathematics, Astrophysics and Particle Physics, Radboud University Nijmegen/Nikhef, Nijmegen, The Netherlands

[ac] Also at Institute for Nuclear Research and Nuclear Energy (INRNE) of the Bulgarian Academy of Sciences, Sofia, Bulgaria

[ad] Also at Institute for Particle and Nuclear Physics, Wigner Research Centre for Physics, Budapest, Hungary

[ae] Also at Institute of High Energy Physics, Chinese Academy of Sciences, Beijing, China

[af] Also at Institute of Particle Physics (IPP), Toronto, Canada

[ag] Also at Institute of Physics, Academia Sinica, Taipei, Taiwan

[ah] Also at Institute of Physics, Azerbaijan Academy of Sciences, Baku, Azerbaijan

[ai] Also at Institute of Theoretical Physics, Ilia State University, Tbilisi, Georgia

[aj] Also at Instituto de Fisica Teorica, IFT-UAM/CSIC, Madrid, Spain

[ak] Also at Department of Physics, Istanbul University, Istanbul, Turkey

[al] Also at Joint Institute for Nuclear Research, Dubna, Russia

[am] Also at LAL, Université Paris-Sud, CNRS/IN2P3, Université Paris-Saclay, Orsay, France

[an] Also at Louisiana Tech University, Ruston, LA, USA

[ao] Also at LPNHE, Sorbonne Université, Paris Diderot Sorbonne Paris Cité, CNRS/IN2P3, Paris, France

[ap] Also at Manhattan College, New York, NY, USA

[aq] Also at Moscow Institute of Physics and Technology State University, Dolgoprudny, Russia

[ar] Also at National Research Nuclear University MEPhI, Moscow, Russia

[as] Also at Physics Dept, University of South Africa, Pretoria, South Africa

[at] Also at Physikalisches Institut, Albert-Ludwigs-Universität Freiburg, Freiburg, Germany

[au] Also at School of Physics, Sun Yat-sen University, Guangzhou, China

[av] Also at The City College of New York, New York, NY, USA

[aw] Also at The Collaborative Innovation Center of Quantum Matter (CICQM), Beijing, China

[ax] Also at Tomsk State University, Tomsk, and Moscow Institute of Physics and Technology State University, Dolgoprudny, Russia

[ay] Also at TRIUMF, Vancouver, BC, Canada

[az] Also at Universita di Napoli Parthenope, Naples, Italy

* Deceased